Mixture-Process Variable Design Experiments with Control and Noise Variables Within a Split-Plot Structure

by

Tae-Yeon Cho

A Dissertation Presented in Partial Fulfillment
of the Requirements for the Degree
Doctor of Philosophy

Approved August 2010 by the
Graduate Supervisory Committee:

Douglas C. Montgomery, Co-Chair
Connie M. Borror, Co-Chair
Dan L. Shunk
Esma S. Gel
Murat Kulahci

ARIZONA STATE UNIVERSITY

December 2010

ABSTRACT

In mixture-process variable experiments, it is common that the number of runs is greater than in mixture-only or process-variable experiments. These experiments have to estimate the parameters from the mixture components, process variables, and interactions of both variables. In some of these experiments there are variables that are hard to change or cannot be controlled under normal operating conditions. These situations often prohibit a complete randomization for the experimental runs due to practical and economical considerations. Furthermore, the process variables can be categorized into two types: variables that are controllable and directly affect the response, and variables that are uncontrollable and primarily affect the variability of the response. These uncontrollable variables are called noise factors and assumed controllable in a laboratory environment for the purpose of conducting experiments. The model containing both noise variables and control factors can be used to determine factor settings for the control factor that makes the response "robust" to the variability transmitted from the noise factors. These types of experiments can be analyzed in a model for the mean response and a model for the slope of the response within a split-plot structure. When considering the experimental designs, low prediction variances for the mean and slope model are desirable.

The methods for the mixture-process variable designs with noise variables considering a restricted randomization are demonstrated and some mixture-process variable designs that are robust to the coefficients of interaction with noise variables are evaluated using fraction design space plots with the respect to

the prediction variance properties. Finally, the G-optimal design that minimizes the maximum prediction variance over the entire design region is created using a genetic algorithm.

This dissertation is dedicated to my beloved family, my wife Hyunju Lee, my two children Ara and Ariene, my parents, and my parents-in-law.

ACKNOWLEDGMENTS

I am very grateful for the help, guidance and patience of my committee chairs, Dr. Douglas C. Montgomery and Dr. Connie M. Borror. I would like to acknowledge the contributions of my committee members, Dr. Dan Shunk, Dr. Esma Gel, and Dr. Murat Kulahci. Finally, I would like to acknowledge the support and assistance of my professors and fellow graduate students at ASU.

TABLE OF CONTENTS

CHAPTER Page

LIST OF TABLES

Table Page

LIST OF FIGURES

Figure Page

CHAPTER 1

INTRODUCTION

Research Idea and Objective

Mixture experiments are common problems in many fields, such as the chemical, food, pharmaceutical, and the process industries. Cornell (2002) defines that in mixture experiments, the response is assumed to depend only on the relative proportions of the mixture components and not on the amount of the mixture. In many industrial processes, however, the response depends not only on the proportion of the mixture components, but also on one or more process variables which can affect the blending properties of the mixture ingredients. See Cornell (2002) for more comprehensive details of mixture-process variable experiments. Goldfarb et al. (2003) addressed the mixture-process variable experiment with noise variables which are hard to control in practice.

In the mixture-process variable designs, the number of runs tends to be larger as the number of process variables increases. Also, some process variables, such as noise variables, can be hard-to-change due to practical and economical considerations. These constraints prohibit complete randomization of the experimental runs. In the situation where complete randomization is unrealistic, all combinations of the easy-to-change factors are run at a fixed level of the hard-to-change factors. Then a new level of the hard-to-change factors is selected and the combinations of other factors are run at that level. This design strategy, first developed by R.A Fisher in the early 1920's, is called a split-plot design. See Montgomery (2009) for more details on split-plot designs.

When the noise variables are treated as process variables in mixture-process variable designs, it is common to fix the level of the noise variables which are usually hard-to-change in practice and run all combinations of the other factors including the mixture components. This approach yields correlated observations within the fixed level of the noise variables and thus introduces a split-plot structure in the mixture-process variable designs. Accordingly, the first research objective is to extend the typical mixture-process variable designs to analyze two sources of errors that result from the SPD structure. Since the mixture-process variable designs in the SPD structure have two error types from the whole plot and subplot (say σ_δ^2 and σ_ε^2, respectively), restricted maximum likelihood (REML) is a popular method for estimating the variance component in SPDs. Fraction of design space (FDS) plots displaying mixture-process variable designs in a split-plot structure will be used to evaluate the designs. Fraction of design space plots for assessing mixture-process variable designs within a split-plot structure will be developed. Sliced FDS plots are implemented to evaluate the designs according to the specific level of noise variables (whole plot factors).

The second objective is to evaluate mixture-process variable designs within a split-plot structure in order to identify the most competitive designs in terms of prediction variance. Fraction of design space (FDS) plots, developed by Zahran, Anderson-Cook, and Myers (2003), and variance dispersion graphs (VDG), introduced by Giovannitti-Jensen and Myers (1989), are graphical tools to assess overall prediction capability of designs. In mixture-process variable designs, the conventional FDS and VDG have limitations in providing prediction

capability on the desired design spaces since these techniques show the prediction variance on the global design region. Goldfarb et al. (2004a) suggest three-dimensional VDGs which evaluate the prediction variance properties of a design through the combined mixture-process space.

The third objective is to develop and evaluate various designs by considering the mean and the variance of the response for mixture-process variable designs within a split-plot structure. In mixture-process variable designs, when some of process variables are noise variables, a robust design setting is needed to achieve robustness to inevitable changes in the noise variables. Noise variables, while uncontrollable under normal operating condition, are usually hard-to-control because they are only able to be managed in special experimental conditions. Goldfarb et al. (2003) developed models for robust mixture-process formulation problems to optimize the dual responses, mean and variance. In this research, the split-plot structure for the process robustness study is considered.

The last objective is to develop a genetic algorithm considering a split-plot structure to produce the optimal design that satisfies the joint optimization of the prediction variance of the mean model and slope model. The new generated design is compared against with the *D*-optimal design and *I*-optimal design using graphical tools, FDS plots of prediction variance, total predication variance, and prediction variance ratio of the mean model and the slope model.

Key Papers

Cornell (2002) presents comprehensive information about mixture experiments including mixture components and process variables. When the process variables are noise variables, Goldfarb et al. (2003) examined robust mixture-process designs considering the process mean and variance. Our research starts from this mixture-process variable design with noise variables and adapts the mixture-process variable designs within a split-plot structure. Thus, we place this article as our first key paper. Two more articles which are closely related to our research objective are selected.

The first key paper focuses on mixture-process variable designs with noise variables. In the paper, the authors developed a model containing mixture components, controllable process variables, and uncontrollable variables (noise variables). They also consider the models which allow correlations between the noise variables. Since the noise variables are uncontrollable in the normal process conditions, they use a process robustness study to find the variable levels that are robust to changes in the noise variables. In the robust study, they apply the delta method to find the mean and variance of response variable. This approach allows the experimenters to find the optimal combinations that yield a target value for the mean by minimizing the variance of process.

The second paper by Goldfarb et al. (2004b) presents fraction of design space (FDS) plots for mixture-process designs. Prediction variances over the design space are introduced by Giovannitti-Jensen and Myers (1989). They developed variance dispersion graphs (VDGs) which allow the practitioner to see

patterns of prediction variances throughout a design space. Zahran et al. (2003) introduced a fraction of design space (FDS) plot which is not a substitute for VDGs, but a complementary technique. It provides additional information on the distribution of the prediction variance over the design space. Goldfarb et al. (2004b) developed the approach to draw FDS plots for mixture designs and mixture-process variable designs. They showed that the random sampling method and shrunken region method by Piepel and Anderson (1992) yield equivalent results for FDS values and plots. For mixture-process variable designs, they introduced the global FDS plot and sliced FDS plot over different process space shrinkage value.

The last paper by Liang, Anderson-Cook, and Robinson (2006) discusses FDS plots for split-plot designs. When the design is completely randomized, the scaled prediction variance (SPV) is dependent upon the experimental design and assumed model. In considering the split-plot design, SPV becomes more complex because the covariance of the response consists of the whole-plot variance and the subplot variance. In the paper, the authors implemented FDS plots using a variance component ratio to study the relationship between the whole plot errors and subplot errors. They also use sliced FDS plots for various whole plot levels to study prediction capability throughout the subplot region in the design space. Furthermore, they consider the impact of the variance ratio on design performance.

Outline of Research

In chapter 2, a literature review that discusses mixture experiments, split-plot designs, graphical tools for design evaluation, and optimality theory is presented. First, the general concept of mixture experiments involving process variables and noise variables is reviewed. For design efficiency comparison, the design optimal criteria are introduced in this chapter. The graphical tools to evaluate the design are also studied: variance dispersion graphs (VDG) and fraction of design space (FDS) plots. It will also cover the genetic algorithm to construct the optimal designs and the desirability function.

Chapter 3 introduces mixture-process variable designs within a split-plot structure. The split-plot design is developed to solve the restricted randomization on the mixture-process variable designs. Fraction of design space (FDS) plots for a mixture-process variable design within a split-plot structure are developed and demonstrated. FDS plots are used to evaluate various designs according to the prediction capability.

In chapter 4, we consider statistical designs for experiments involving mixture variables, and noise variables with a restricted randomization for the experimental runs. We consider a split-plot design to solve this randomization restriction. We also consider noise factors in the process variables using robust parameter design. We construct *G*-optimal designs using a desirability function that simultaneously optimize both the prediction variance for the mean model and the slope model when there are process variables and noise variables in a split-plot structure.

Chapter 5 illustrates a specific case study for a diamond grinding wheel. In the evaluating of the grinding wheel manufacturing process, the mixture components interact with the process variables, resulting in a mixture-process variable experiment which requires a large number of runs to estimate the parameters. We consider a split-plot structure and robust parameter design for this grinding wheel manufacturing example with a tight mixture component design space. The effect of mixture component design space is compared using a graphical tool.

Chapter 6 concludes this dissertation, summarizing the main contribution and suggesting future research areas.

CHAPTER 2

LITERATURE REVIEW

Mixture-process variable experiments are commonly encountered in many industrial fields. Cornell (2002, Ch7) gives a full explanation of mixture-process variable experiment. Goldfarb et al. (2003) addressed the mixture-process variable experiment with noise variable which is hard to control in practice, but they did not consider randomization issues. In practice, when the process variables are added to the mixture experiment, the number of runs is radically increased and complete randomization is often impractical. The suggested method to deal with the restricted randomization is a split-plot design, according to Montgomery (2009).

In experiments, many designs are available for specific objectives. For example, in the view of cost analysis, the design which has smallest number of runs is preferred if it provides the enough information on the coefficients for the model. A second characteristic for selection of design is prediction capability. The suggested measure of prediction performance is the scaled prediction variance (SPV) which considers the total sample size to penalize large designs. When the size is not the major issue for cost, an alternative objective is unscaled prediction variance which compares directly the variance without penalizing the sample size. The design efficiency is a good choice for comparing and evaluating designs when we are interested in the prediction variance at the specific location. The design criteria, which focus on the prediction variance, are *G*-optimality, *V*-optimality, and *Q*-optimality.

To evaluate the prediction capability, the overall distribution of SPV throughout the design space should be considered instead of judging only a single point prediction estimate such as G and Q-efficiency since the prediction variances change at different points. Thus, the preferred design has relatively stable SPV over a whole design space. Box and Hunter (1957) suggested the concept of rotatability for the experimental design, which requires constant prediction variance at any two points that are the same distance from the design center. Giovannitti-Jensen and Myers (1989) introduced the variance dispersion graph (VDG), a graphical technique that displays the prediction variance properties of a design space for spherical design regions. The VDG technique is extended to the design with cuboidal regions by Rozum and Myers (1991). The VDGs for the mixture designs are discussed by Piepel and Anderson-Cook (1992) and Vining, Cornell, and Myers (1993). Goldfarb et al. (2003) introduce the three-dimensional VDGs for mixture-process experiments.

Zahran et al. (2003) introduce a supplementary technique to the VDG, called fraction of design space (FDS) plots. For the FDS plots, the SPV is calculated throughout the design space and then the fraction of the design space that is less than or equal to a given SPV value is determined. Goldfarb et al. (2004b) suggest the random sampling method for FDS plot for mixture design. Liang et al. (2006) adapted the FDS plot for split-plot designs. They used the proportional sizes of the sliced FDS curves for different whole plot shrinkage levels for a split-plot design over spherical region.

In next section, we discuss more specific concepts for our research. This review is organized as follow. First, the general concept of mixture experiments and mixture-process variables experiments is provided. Second, split-plot designs are presented and the expected mean square for a split-plot design is briefly mentioned. Lastly, the optimal design criteria are presented including the graphical tools to evaluate design.

Mixture-Process Variable Experiments

A mixture experiment or product formulation is a special type of experiment for chemical, food, pharmaceutical, and other consumer products industries. It is different from standard response surface experiments in that the factors are the components of mixture or ingredients and the response is a function of the proportion of mixture components. Assume that q components or ingredients are in the mixture and i^{th} component is represented by x_i, where

$$x_i \geq 0, \quad i = 1, 2, \cdots, q \tag{1}$$

and

$$\sum_{i=1}^{q} x_i = x_1 + x_2 + \cdots + x_q = 1 . \tag{2}$$

Equation (2) indicates that the sum of all components, which is all positive from Equation (1), is unity. Because of the requirement given in (2), the levels of components in the mixture experiments are not independent. This restriction makes mixture experiments different from usual response surface experiments.

The first-order model, when there are q variables for the usual response surface is

$$E(y) = \beta_0 + \sum_{i=1}^{q} \beta_i x_i \ . \tag{3}$$

In the mixture experiment, however, the parameters, β_i (i=0, 1, $\cdots$, q) are not unique due to the restriction given in Equation (2). The canonical or Scheffé form of this model is found by multiplying the intercept term by the identity, $x_1 + x_2 + \cdots + x_q = 1$ and simplifying the model, yielding

$$\begin{aligned} E(y) &= \beta_0 (x_1 + x_2 + \cdots + x_q) + \sum_{i=1}^{q} \beta_i x_i \\ &= \sum_{i=1}^{q} \beta_i^* x_i \end{aligned} \tag{4}$$

where, $\beta_i^* = \beta_0 + \beta_i$. This Scheffé form of mixture models can be expressed as a linear, quadratic, full cubic, or special cubic model. See Cornell (2002) and Myers et al. (2009) for more details.

In practice, the response for a mixture experiment may not only depend on the ingredients, but also on experimental conditions called process variables, such as temperature, speed, and time. They are not part of the mixture components, but can affect the mixture properties at the different variable levels. Piepel and Cornell (1985, 1987) address mixture problems where the amount of the mixture that is applied to the experimental unit is varied. Cornell (2002) gives a complete presentation of mixture-process variables experiments.

Split-Plot Designs

The split-plot design is used in order to solve the randomization problem in experiments when there are two different types of factors; hard-to-change factors and easy-to-change factors. In the split-plot design analysis, response surface methodology (RSM) is applied to find the optimum of these factors within the constraints. Recently, split-plot designs within a robust parameter design setting have been developed. Also, pure error estimates of the two variance components have been developed.

In designed experiments, randomization is an important requirement underlying the use of statistical methods. Properly randomized experiments satisfy the statistical requirement that the observations (or errors) are independently distributed random variables. When it is difficult or expensive to change the levels of some of the factors due to physical restrictions on the process, it is impractical to perform the experiments in a completely random order. In such cases, restrictions on the randomization of experimental runs are necessary resulting in a split-plot design structure, as described by Box and Jones (1992). In split-plot designs, the experiments are performed by fixing the levels of the hard-to-change factors and then running all or some of the combinations of the easy-to-change factor levels. Then, a new setting in the hard-to-change factors is selected and the process is repeated. The hard-to-change factors are called the whole plot factors or main treatments, and the easy-to-change factors are called the subplot factors or split-plots.

Within every split-plot design, there are two randomization requirements. The hard-to-change factors are randomly assigned to whole plots based on the whole plot design. Within each whole plot, the easy-to-change factors are randomly assigned to a subplot independent of each whole plot. With replication, this type of randomization leads to two error terms, one for the whole plot treatments and another for subplot treatments. Typically, the interaction between whole plot treatment and subplot treatment is a subplot effect as well.

TABLE 1. Expected Mean Squares for a Split-Plot Design

	Model Term	Expected Mean Square (EMS)
Whole plot	τ_i	$\sigma^2 + ab\sigma_\tau^2$
	β_j	$\sigma^2 + b\sigma_{\tau\beta}^2 + \frac{rb\sum \beta_j^2}{a-1}$
	$(\tau\beta)_{ij}$	$\sigma^2 + b\sigma_{\tau\beta}^2$
Subplot	γ_k	$\sigma^2 + a\sigma_{\tau\gamma}^2 + \frac{ra\sum \gamma_k^2}{b-1}$
	$(\tau\gamma)_{ik}$	$\sigma^2 + a\sigma_{\tau\gamma}^2$
	$(\beta\gamma)_{jk}$	$\sigma^2 + \sigma_{\tau\beta\gamma}^2 + \frac{r\sum\sum (\beta\gamma)_{jk}^2}{(a-1)(b-1)}$
	$(\tau\beta\gamma)_{ijk}$	$\sigma^2 + \sigma_{\tau\beta\gamma}^2$
	ε_{ijk}	σ^2 (not estimable)

Montgomery (2009) presents the linear model for the split-plot design for two factors as

$$y_{ijk} = \mu + \tau_i + \beta_j + (\tau\beta)_{ij} + \gamma_k + (\tau\gamma)_{ik} + (\beta\gamma)_{jk} + (\tau\beta\gamma)_{ijk} + \varepsilon_{ijk} \quad \begin{Bmatrix} i = 1,2,...,r \\ j = 1,2,...,a \\ k = 1,2,...,b \end{Bmatrix}$$

where τ_i, β_j, and $(\tau\beta)_{ij}$ make up the whole plot and represent respectively blocks (or replicates), main treatment (factor *A*), and whole plot error (replicates × *A*). The remaining terms γ_k, $(\tau\gamma)_{ik}$, $(\beta\gamma)_{jk}$, and $(\tau\beta\gamma)_{ijk}$ consist of the subplot and represent respectively the subplot treatment (factor *B*), the replicates × *B*, and *AB* interactions, and the subplot error (replicates × *AB*). The expected mean square for the split-plot design, with replicates or blocks random and main treatments and subplot treatments fixed, are shown in Montgomery (2009) and reproduced in Table 1.

Note that the main factor (*A*) in the whole plot is tested against the whole plot error, whereas the subplot treatment (*B*) is tested against the replicates × subplot treatment interaction. The *AB* interaction is tested against the subplot error. There are no tests for the replicate (or block) effect or the replicate × subplot treatment interaction. (see Montgomery (2009) for the further explanation).

Box and Jones (1992) show that a split-plot design is typically more efficient than a completely randomized design (CRD) because $\sigma^2_{sub} < \sigma^2_{CRD} < \sigma^2_{whole}$, where σ^2_{sub} is the subplot error variance and σ^2_{whole} is the whole plot error variance if there are two error terms. Lucas and Ju (1992) investigate the use of split-plot designs in industrial experiments where one factor is difficult to change. The results of their simulation study confirm that split-plot designs produce increased precision on the subplot factors while sacrificing precision on the whole plot

factors. Box (1996) states that completely randomized experiments are sometimes impractical in industry and split-plot experiments are good alternatives since they are very efficient and easy to run. Usually a split-plot design is also more cost effective than the CRD. The frequent level changes on hard-to-change factors induce higher costs than the changes on easy-to-change factors. In a split-plot design, whole plot factors are changed less often than in a CRD, which results in lower cost.

In the mixture-process variable experiments, the number of runs is likely to increase dramatically as the number of process variables increase. Furthermore, while noise variables are controllable in the laboratory environment, usually these variables are difficult to adjust and control. In designing experiments, randomization is an important requirement underlying the use of statistical methods. However, if it is difficult or expensive to change the levels of some factors, it is impractical to perform the experiments in a completely randomized order. In this situation, restrictions on the randomization of experimental runs are necessary resulting in a split-plot structure, as described by Box and Jones (1992). Cho et al. (2009) developed graphical evaluation techniques for the MPD within a split-plot structure; however, the authors did not consider robust parameter design for noise variables.

Robust Parameter Design

In the experimental design, the process variables can be categorized into two types: variables that are controllable and directly affect the response, and

variables that are uncontrollable and primarily affect the variability of the response. Myers et al. (2009) call these factors control factors and noise factors (or noise variables), respectively. We assumed that noise variables are controllable in a special laboratory environment for the purpose of conducting experiments. When production is moved from the laboratory to the manufacturing environment, noise factors are not necessarily controllable in the normal operation of the process. Consequently, it is important to consider noise variables at the design stage of the process. The model containing both noise variables and control factors can be used to determine factor settings for the control factor that makes the response "robust" to the variability transmitted from the noise factors. This type of study is called "robust parameter design". See Borror et al. (2002), Myers et al. (2009) and Montgomery (2009) for details and summaries. The mixture process variable designs with noise variables were developed by Steiner and Hamada (1997), Goldfarb et al. (2003), and Goldfarb et al. (2004c).

General Criteria for Comparing and Evaluating Designs

Design evaluation and comparison are often carried out using the design optimality, such as *D*-optimality, *G*-optimality, *V*-optimality, and *Q*-optimality. See Myers et al. (2009) for detailed discussion on design optimality. The most well known optimality criterion is *D*-optimality, which is based on the concept that the experimental design should be selected to maximize the determinant of the moment matrix; that is

$$\underset{\zeta}{\text{Max}}\left|\mathbf{M}(\zeta)\right|$$

$$\left|\mathbf{M}\right| = \frac{\left|\mathbf{X}'\mathbf{X}\right|}{N^p}$$

where p is the number of parameters in the model, $\mathbf{X}$ is the design space matrix, and Max implies that the maximum is determined over the entire designs ζ. Design criteria which focus on the prediction variance include *G*-optimality, *V*-optimality, and *Q*-optimality. The scaled prediction variance (SPV) is given by

$$v(\mathbf{x}) = \frac{N\ Var\left[\hat{y}(\mathbf{x})\right]}{\sigma^2} = N\ \mathbf{x}^{(m)'}\left(\mathbf{X}'\mathbf{X}\right)^{-1}\mathbf{x}^{(m)}$$

where $\mathbf{x}^{(m)}$ is a function of the location in the design variables at which one predicts and also expanded to the form of model being fit. SPV is not a single value but rather achieves different values depending on the location $\mathbf{x}^{(m)}$. *G*-optimality focuses on the design which provides the *minimum* value from the *maximum* $v(\mathbf{x})$ in the design space, given by

$$\underset{\zeta}{\text{Min}}\left[\underset{\mathbf{x}\in R}{\text{Max}}\, v(x)\right].$$

If the variance is scaled by N, 100% G-efficiency is equal to the number of parameters in the model. Another prediction variance-oriented optimality is *V*-optimality which considers the average prediction variance over the specific set of points of interest in the design space. Another important design optimality criterion is *Q*-optimality or *IV* (integrated variance) optimality, for which prediction variance $v(\mathbf{x})$ is averaged over the design region of interest R, given by

$$\underset{\zeta}{\text{Min}}\frac{1}{K}\int_R v(\mathbf{x})d\mathbf{x} = \underset{\zeta}{\text{Min}}\, Q(\zeta)$$

where K is the volume of design region R.

Variance Dispersion Graphs (VDGs)

Design efficiencies are not enough to evaluate the designs when we are looking for the designs with stable $v(\mathbf{x})$ over the design space, which involves multi-dimensionality. When $k = 2$, a two-dimensional plot of $v(\mathbf{x})$ can be easily constructed using a contour plot. For $k > 2$, however, the contour plots of $v(\mathbf{x})$ are insufficient to express the distribution of prediction variance over all variables.

Giovannitti-Jensen and Myers (1989) introduced the variance dispersion graph (VDG), a graphical technique that displays the prediction variance properties of a design space. The VDG plots three graphical components; these are

1. A plot of average $v(\mathbf{x})$ throughout the design space
2. A plot of the *maximum* $v(\mathbf{x})$ throughout the design space
3. A plot of the *minimum* $v(\mathbf{x})$ throughout the design space.

Myers, Vining, Giovannitti-Jensen, & Myers (1992), Vining (1993), Borkowski (1995), Trinca and Gilmour (1998), and Borror et al. (2002) use the VDGs to compare designs and show that D-optimality criterion can be misguiding if the researcher is interested in the prediction variance behavior. The design region is expanded from spherical to cuboidal regions by Rozum and Myers (1991), Myers et al. (2009), and Borror et al. (2002). Piepel and Anderson (1992) develop and demonstrate VDGs for mixture designs using a shrunken region approach. Vining,

Cornell, and Myers (1993) also develop VDGs for mixture designs by plotting the prediction variances along the Cox directions.

Fraction of Design Space (FDS) Plots

Zahran, Anderson-Cook, and Myers (2003) introduced fraction of design space (FDS) plots not to substitute, but to supplement the VDG. For the FDS plots, the SPV is calculated throughout the design space and then the fraction of the design space that is less than or equal to a given SPV value is determined. Let v be any given SPV value, k be the number of factors, and Ψ be the total volume of the design region. The FDS is defined as:

$$FDS = \frac{1}{\Psi}\int_{A}\cdots\int dx_k \cdots dx_1,$$

where $A = \{(x_1, \cdots, x_k): v(x) < v\}$. Goldfarb et al. (2004b) suggest a random sampling method for constructing the FDS plots for mixture designs. This method selects points completely at random that fit within the constraints of the region. Then, the scaled prediction variance (SPV) is calculated for each point. All SPV values at each point are sorted and plotted on the FDS plot. The minimum SPV value is located on the FDS of 0 and the maximum value is located on the FDS of 1. The FDS plot contains a single line that represents the pattern of SPV distribution throughout the design space, allowing evaluation of several designs on a single FDS plot. Liang et al. (2006) adapted the FDS plot for split-plot designs. They used the proportional sizes of the sliced FDS curves for different whole plot shrinkage level for a split-plot design in a spherical region. Rodriguez

et al. (2010) suggested variance ratio FDS (VRFDS) plot to compare several designs to a reference design.

Computer Algorithms for Design Creation

To construct optimal design, it is required to solve a large nonlinear mixed integer programming problem. As the feasible design space increases, the MIP solution is impossible to find exact optimal design. Approximation algorithms using random methods and greedy methods are suggested as an alternative for the exact solution. The typical methods using random algorithm is simulated annealing. In simulated annealing, an initial candidate set is generated and modified in random way. This candidate is accepted with a probability based on the special function. Simulated annealing is very successfully used in the area of combinatorial optimization such as the traveling salesman problem.

The point exchange algorism is a typical greedy algorithm for generating optimal designs. It used exhaustive search by adding new design points and removing existing design points to improve the objective function. Exchange algorithms are categorized into Rank-1 and Rank-2 based on how the point is changed in the current candidate design set:

Rank-1: Sequential exchange by adding new point and delete current point (Wynn, DETMAX).

Rank-2: Simultaneous exchange of new point and current point (Fedorov, Modified Fedorov, *k*-exchange, *kl*-exchange).

The coordinate exchange algorithm suggested by Meyer and Nachtsheim (1995) is an extension of the point exchange algorithm. They modified the *k*-exchange algorithm to make *kq* coordinate associated with k least critical point in the current design. It used the subset of new point to exchange. Firstly, choose *k* least critical points and examine each point for the best coordinate to exchange. Finally, make best coordinate exchange.

Goos and Vanderbroek (2001) suggested the use of optimal designs for the split-plot structure. They pointed out the difference between CRD and SPD to construct optimal designs. In particular, the covariance matrix **V** from whole-plot and subplot is included to compute the optimal criterion. Therefore, design matrix **X** and covariance matrix **V** are computed in same time. The other important aspect of optimal design for split-plot structure is the unknown variance component ratio, *d*. For the purpose of design construction, a reasonably accurate value of *d* is required.

The current exchange algorithms are able to be modified to construct the mixture-process experiment within split-plot structure. As shown in Goos and Vanderbroek (2001), the point-exchange algorithm provides a *D*-optimal split-plot design. Since the coordinate exchange algorithm is a modified version of *k*-exchange algorithms, coordinate exchange algorithms can be considered to generate optimal split-plot designs. However, we need to consider the whole-plot and subplot design space. Since the subplot is nested on the whole-plot, some restriction of coordinate subset may be required.

For other optimality criteria such as *G*-optimality and *Q*-optimality, there is no existing algorithm for split-plot structure. However, genetic algorithms can be considered to generate these optimal designs. Heredia-Langner et al. (2004) prove that a genetic algorithm method is efficient in computer generated design, especially experiments with mixture component and response surface experiment with constrained regions. They also suggest using genetic algorithms when the researcher cannot employ any of the traditional approach for design construction. Liang, Anderson-Cook, and Robinson (2006) also recommend a genetic algorithm for prediction variance based optimal design within split-plot structure. Goldfarb et al. (2005) and Chung et al. (2007) create *G*-optimal designs for mixture-process variable design with control and noise variables using a restricted form of a genetic algorithm (GA) (no mutation occurred). Rodriguez et al. (2009) generate *G*-optimal designs using a full GA, but no mixture variables are considered in the design.

CHAPTER 3

EVALUATION OF MIXTURE-PROCESS VARIABLE DESIGNS WITHIN A SPLIT-PLOT STRUCTURE

In this chapter, the analysis of mixture-process variable experiments within a split-plot structure is addressed. For a graphical evaluation, fraction of design space (FDS) plots for a mixture-process variable design within a split-plot structure are developed and demonstrated. FDS plots are used to evaluate the prediction capability of various designs. Sliced FDS plots are presented to show the influence of mixture variables and process variables on the prediction variance over the design space.

Introduction

Mixture experiments are used in a system where the response is affected by the proportion of ingredients. In mixture experiments, the response is a function of the ingredient or component proportion, and because the proportions must add to a constant, the variables are not independent. In many industrial processes, however, the response depends not only on the proportions of the mixture components, but also on other experimental factors which can be generally described as process variables. Although the mixture components cannot be controlled independently due to the constraints of mixture experiments, the process variables can be adjusted independently.

The practitioner has many design choices depending on the specific objectives of the experiments. For example, from the view of cost, the design

which has the smallest number of runs is preferred if it provides enough information to estimate the model coefficients. A second characteristic for selection of design is prediction capability. A widely-used measure of prediction performance is the scaled prediction variance (SPV) which takes into account the total sample size to penalize large designs. When the size of the design is not a major issue, an alternative objective is the unscaled prediction variance which directly compares the variance without penalizing for the sample size. Design efficiencies can also be good measures for comparing and evaluating designs in many situations. The design optimality criteria that focus on the prediction variance are *G*-optimality, *V*-optimality, and *I*-optimality. To fully evaluate the prediction capability, the overall distribution of SPV throughout the design space should be examined instead of relying on only a single number criterion, such as *G* and *I*-efficiency. The preferred design has relatively stable SPV over the entire design space.

Notation and Model Development

Assume that the mixture components are the subplot factors, x_i's, and the controllable process variables are also the subplot factors, w_p's. The hard-to-change process variables are the whole-plot factors, z_t's. Furthermore, we suppose that there are q mixture components (x_i, $i = 1, 2, \ldots, q$), c controllable variables (w_p, $p = 1, 2, \ldots, c$), and n hard-to-change variables (z_t, $t = 1, 2, \ldots, n$). The process variables are assumed to be continuous. Also suppose that there are m mixture terms, where m is a function of the number of the mixture components

and the degree of the model. A response can be represented as a function of *m* mixture terms in quadratic mixture model form, *n* continuous hard-to-change variables, and *c* continuous controllable variables. The model within a split-plot structure can be modeled as

$$y = f(\mathbf{x}, \mathbf{w}, \mathbf{z}) = f_w(\mathbf{z})'\beta_{wp} + \delta + f_s(\mathbf{x}, \mathbf{w}, \mathbf{z})'\beta_{sp} + \varepsilon, \tag{5}$$

where β_{wp} is a vector of coefficient terms from the whole-plot variables, β_{sp} is a vector of coefficient terms from the subplot variables, $\delta \sim N(0, \sigma_\delta^2)$ comes from the whole-plot (WP) randomization level and represents the random error term of the WP factors alone, and $\varepsilon \sim N(0, \sigma^2)$ comes from the subplot (SP) randomization level and represents the random error term from the subplot. The random components δ and ε are assumed to be independent. However, the WP terms, $f_w(\mathbf{z}_t)'\beta_{wp}$, can be removed since the hard-to-change variables only affect the response through interacting with the mixture components. Then, Equation (5) can be written as

$$\begin{aligned} y(\mathbf{x}, \mathbf{w}, \mathbf{z}) = & \sum_i \beta_i x_i + \sum_{i<j} \sum \beta_{ij} x_i x_j \\ & + \sum_i \sum_p \alpha_{ip} x_i w_p + \sum_{i<j} \sum_p \alpha_{ijp} x_i x_j w_p \\ & + \sum_i \sum_t \theta_{it} x_i z_t + \sum_{i<j} \sum_t \theta_{ijt} x_i x_j z_t \\ & + \sum_i \sum_p \sum_t \lambda_{ipt} x_i w_p z_t + \sum_{i<j} \sum_p \sum_t \lambda_{ijpt} x_i x_j w_p z_t + \delta + \varepsilon \end{aligned} \tag{6}$$

This model is exactly the same as in Goldfarb et al. (2003) except that it has two different sources of error, WP and SP errors. Equation (6) can be expressed in matrix form as

$$y(\mathbf{x},\mathbf{w},\mathbf{z}) = \mathbf{x}'\boldsymbol{\beta} + \mathbf{x}'\boldsymbol{\Lambda}\mathbf{w} + \mathbf{x}'\boldsymbol{\Theta}\mathbf{z} + \mathbf{x}'\boldsymbol{\Lambda}\mathbf{W}\mathbf{z} + \delta + \varepsilon ,$$

where **x** is the $m \times 1$ vectors which consist of all mixture model terms including higher order terms, **w** is the $c \times 1$ vector of controllable variables, and **z** is the $n \times 1$ vector of hard-to-change variables. **β** is the $m \times 1$ vectors coefficient matrix for mixture model terms, **A** is the $m \times c$ coefficient matrix for the mixture by controllable variable interactions and **Θ** is the $m \times n$ coefficient matrix for the mixture by hard-to-change variable interactions. **Λ** is the $m \times cn$ coefficient matrix for interactions, involving mixture components, controllable variables, and hard-to-change variables. Finally, **W** is a $cn \times n$ block-diagonal matrix whose columns contain the w elements and blocks of 0s. See Goldfarb et al. (2003) for additional discussion of all model terms.

We assume that $\delta + \varepsilon$ has mean 0 and variance–covariance matrix **V** which is a function of the WP variance σ_δ^2 and the SP variance σ_ε^2. The covariance matrix of the response is then given by

$$\mathbf{V} = \sigma_\delta^2\mathbf{J} + \sigma_\varepsilon^2\mathbf{I} = \sigma_\varepsilon^2[d\mathbf{J} + \mathbf{I}]$$

where

$$\mathbf{J} = \begin{bmatrix} \mathbf{1}_1\mathbf{1}_1' & 0 & \cdots & 0 \\ 0 & \mathbf{1}_2\mathbf{1}_2' & \cdots & 0 \\ \vdots & \vdots & \ddots & \vdots \\ 0 & 0 & \cdots & \mathbf{1}_a\mathbf{1}_a' \end{bmatrix} \text{ and } d = \frac{\sigma_\delta^2}{\sigma_\varepsilon^2} \text{ (the variance component ratio).}$$

The length of each $\mathbf{1}_i$ is n_i, the number of subplot runs within the whole-plot. Usually, the whole plot error variance is larger than the subplot error variance as shown by Box and Jones (1992). Vining et al. (2005) studied a split-

plot experiment and estimated the variances using pure error indicating larger whole plot error variance than subplot error variance ($d > 1$). If $d = 0$, the covariance matrix is $\mathbf{V} = \sigma^2\mathbf{I}$, which is equivalent to the completely randomized design. Restricted maximum likelihood (REML) is a recommended estimation method for the variance components.

The model parameters within the split-plot structure, $\boldsymbol{\beta}^*$, are estimated via generalized least squares, given by

$$\hat{\boldsymbol{\beta}}^* = \left(\mathbf{X}'\mathbf{V}^{-1}\mathbf{X}\right)^{-1}\mathbf{X}'\mathbf{V}^{-1}\mathbf{y},$$

with covariance matrix given by

$$\text{Var}(\boldsymbol{\beta}^*) = \left(\mathbf{X}'\mathbf{V}^{-1}\mathbf{X}\right)^{-1} = \sigma_\varepsilon^2\left[\mathbf{X}'\left(d\mathbf{J}+\mathbf{I}\right)^{-1}\mathbf{X}\right]^{-1}.$$

Example 1: Soap Manufacturing Process

Goldfarb et al. (2003) studied the amount of soap in pounds per hour that a manufacturing process yields. There are three ingredients in the process, soap(x_1), co-surfactant(x_2), and filler(x_3). The ingredients have the following constraints;

$$0.20 \le x_1 \le 0.80$$
$$0.15 \le x_2 \le 0.50$$
$$0.05 \le x_3 \le 0.30$$
$$x_1 + x_2 + x_3 = 1$$

Two process variables are also considered; the plodder temperature (z_1) and mixing time (w_1). The plodder temperature ranges from 15°C to 25°C while mixing time (w_1) ranges from 0.5 hour to 1 hour. The process variables are coded with low level and high level (-1, 1) in this example. The plodder temperature (z_1)

is treated as a noise variable and also hard-to-change in Goldfarb et al. (2003). In this experiment, however, we did not consider robust process design and assume that temperature is only hard-to-change. The mixing time (w_1) is a controllable variable which is easy-to-change. Since the plodder temperature (z_1) is the only hard-to-change factor, it is assigned to the whole-plot. The mixture variables and controllable variable are assigned to the subplot. Response data were simulated using the original model, but now including two different sources of errors, whole plot error and subplot error. Usually, the whole plot error variance is larger than the subplot error variance as shown by Box and Jones (1992). Vining et al. (2005) studied a split-plot experiment and estimated the variances using pure error indicating larger whole plot error variance than subplot error variance ($d > 1$). We generated data with $d = 5.0$ to examine the effect of whole plot error variance on the result of model fitting. As shown in Table 2, the usual CRD analysis gives results similar to Goldfarb et al. (2003) if the design is analyzed with the coded variables for the process variables. The final model with the CRD is

$$\begin{aligned}\hat{y}(\mathbf{x},\mathbf{w},\mathbf{z}) = {} & 464.37x_1 - 56.01x_2 + 613.03x_3 \\ & +8.86x_1w_1 + 65.22x_2w_1 - 50.64x_3w_1 \\ & +12.35x_2z_1 - 74.46x_3z_1 \\ & -4.26x_2w_1z_1 + 6.15x_3w_1z_1\end{aligned}$$

Note that the R-square and R-square adjusted values are greater than 0.999, indicating an adequate model. However, the SPD analysis, shown in Table 3, provides a slightly different result, indicating a significant difference between the SPD and CRD analysis. As proved by Vining et al. (2005), the coefficient estimates of model parameters are equivalent for CRD using OLS estimates and

SPD using GLS estimates, because the design is balanced and the subplot designs are orthogonal.

TABLE 2. JMP7.0 Fit Model of Soap Manufacturing Example Analyzed as a CRD

Response Y
Summary of Fit

RSquare	0.999515
RSquare Adj	0.999437
Root Mean Square Error	2.172708
Mean of Response	335.7587
Observations (or Sum Wgts)	80

Analysis of Variance

Source	DF	Sum of Squares	Mean Square	F Ratio
Model	11	662060.11	60187.3	12749.77
Error	68	321.00	4.7	Prob > F
C. Total	79	662381.11		<.0001

Tested against reduced model: Y=mean

Lack Of Fit

Source	DF	Sum of Squares	Mean Square	F Ratio
Lack Of Fit	4	5.42651	1.35663	0.2751
Pure Error	64	315.57823	4.93091	Prob > F
Total Error	68	321.00474		0.8930
				Max RSq
				0.9995

Parameter Estimates

Term	Estimate	Std Error	t Ratio	Prob>|t|
X1(Mixture)	464.3694	0.530811	874.83	<.0001
X2(Mixture)	-56.00925	1.137246	-49.25	<.0001
X3(Mixture)	613.03004	1.842157	332.78	<.0001
X1*z1	0.5521082	0.530811	1.04	0.3020
X1*w1	8.8568041	0.530811	16.69	<.0001
X2*z1	12.350042	1.137246	10.86	<.0001
X2*w1	65.215146	1.137246	57.34	<.0001
X3*z1	-74.45903	1.842157	-40.42	<.0001
X3*w1	-50.64127	1.842157	-27.49	<.0001
X1*z1*w1	-0.477407	0.530811	-0.90	0.3716
X2*z1*w1	-4.260443	1.137246	-3.75	0.0004
X3*z1*w1	6.1535929	1.842157	3.34	0.0014

The analysis with the SPD structure shows that the interaction $X_1w_1z_1$ is found to be statistically significant although it was not significant in the CRD structure. This result illustrates the role of whole-plot error and subplot error in SPD structure. Two different types of errors are used to calculate the test statistics for different factors. For example, the t-ratio for whole-plot factor (z_1) is calculated using the whole-plot error. Test statistics for other subplot factors and interactions with the subplot factors are calculated using the subplot error.

TABLE 3. JMP7.0 Fit Model of Soap Manufacturing Example Analyzed as a SPD

Response Y
Summary of Fit

RSquare	0.999924
RSquare Adj	0.999912
Root Mean Square Error	0.898223
Mean of Response	335.7587
Observations (or Sum Wgts)	80

Parameter Estimates

Term	Estimate	Std Error	DFDen	t Ratio	Prob>|t|
X1(Mixture)	464.3694	0.776285	6.833	598.19	<.0001
X2(Mixture)	-56.00925	0.880627	11.17	-63.60	<.0001
X3(Mixture)	613.03004	1.065106	22.05	575.56	<.0001
X1*z1	0.5521082	0.776285	6.833	0.71	0.5005
X1*w1	8.8568041	0.219443	62	40.36	<.0001
X2*z1	12.350042	0.880627	11.17	14.02	<.0001
X2*w1	65.215146	0.470151	62	138.71	<.0001
X3*z1	-74.45903	1.065106	22.05	-69.91	<.0001
X3*w1	-50.64127	0.761569	62	-66.50	<.0001
X1*z1*w1	-0.477407	0.219443	62	-2.18	0.0334
X2*z1*w1	-4.260443	0.470151	62	-9.06	<.0001
X3*z1*w1	6.1535929	0.761569	62	8.08	<.0001

REML Variance Component Estimates

Random Effect	Var Ratio	Var Component	Std Error	95% Lower	95% Upper	Pct of Total
Whole Plots	5.4978679	4.4357013	2.6075744	-0.675145	9.5465471	84.610
Residual		0.8068039	0.1449063	0.5840007	1.1874342	15.390
Total		5.2425052				100.000

-2 LogLikelihood = 224.09336357

As shown by Lucas and Ju (1992), in this example, the subplot factor ($X_1w_1z_1$) is precisely analyzed and determined to be significant in the model. Therefore, the suggested model is

$$\begin{aligned}\hat{y}(\mathbf{x},\mathbf{w},\mathbf{z}) = {} & 464.37x_1 - 56.01x_2 + 613.03x_3 \\ & +8.86x_1w_1 + 65.22x_2w_1 - 50.64x_3w_1 \\ & +12.35x_2z_1 - 74.46x_3z_1 \\ & -0.48x_1w_1z_1 - 4.26x_2w_1z_1 + 6.15x_3w_1z_1 .\end{aligned}$$

This example illustrated the problem with analyzing a split-plot design as if it was a completely randomized design. The estimates of the coefficients are identical, but the significance test can lead to erroneous results.

Prediction Variance for MPV Design within a SPD

The predicted mean response at any location $\mathbf{x}_0$ is given by

$$\hat{y}(\mathbf{x}_0) = \mathbf{x}_0'\hat{\boldsymbol{\beta}}^* ,$$

where $\mathbf{x}_0$ is the point of interest in the design space. The prediction variance at $\mathbf{x}_0$ is now given by

$$Var\left[\hat{y}(\mathbf{x}_0)\right] = \mathbf{x}_0'\left(\mathbf{X}'\mathbf{V}^{-1}\mathbf{X}\right)^{-1}\mathbf{x}_0 .$$

The covariance matrix $\mathbf{V} = \sigma^2\mathbf{I}$ can be used when the design is completely randomized and the optimal design for prediction variance depends only on the design space **X**. In the split-plot design, due to the different sources of error, the covariance matrix becomes more complex than the general form of **V**. The prediction variance of SPD is not only a function of the design space **X** but is also a function of the variance component ratio, *d*.

When considering prediction variance as an objective to evaluate the design, the prediction variance is scaled by the variance of observation error to make the quantity scale free and by design size to penalize larger designs. Liang et al. (2006) suggest determining the scaled prediction variance for split-plot design by multiplying the prediction variance by the total number of runs, *N*, and then dividing by the observational error variance ($\sigma_\delta^2 + \sigma^2$). The SPV for SPDs is given by

$$SPV = \frac{N\mathbf{x}_0'\left(\mathbf{X}'\mathbf{V}^{-1}\mathbf{X}\right)^{-1}\mathbf{x}_0}{\left(\sigma_\delta^2 + \sigma^2\right)} = N\mathbf{x}_0'\left(\mathbf{X}'\mathbf{R}^{-1}\mathbf{X}\right)^{-1}\mathbf{x}_0$$

where $\mathbf{R}$=diagonal $\{\mathbf{R}_1,\ldots, \mathbf{R}_a\}$ with $\mathbf{R}_i$ denoting the correlation matrix of observations within whole plot *i*. In SPDs, the size of the design is not closely related to the cost because the cost for the number of observation in SPDs is not the number of set-ups needed to collect the data. Then, we would model the variance of the estimated mean response divided by $\sigma_\delta^2 + \sigma^2$,

$PV = \mathbf{x}_0'\left(\mathbf{X}'\mathbf{V}^{-1}\mathbf{X}\right)^{-1}\mathbf{x}_0 \Big/ \left(\sigma_\delta^2 + \sigma^2\right) = \mathbf{x}_0'\left(\mathbf{X}'\mathbf{R}^{-1}\mathbf{X}\right)^{-1}\mathbf{x}_0$, directly. For the SPD case, this unscaled variance is a valid alternative to scaled prediction variance.

FDS Plots for MPV Designs within a SPD

Various methods involving prediction variance have been proposed to evaluate the prediction performance of a design. FDS plots were recommended by Zahran et al. (2003). To construct FDS plots, the SPV is calculated throughout the design space, and the fraction of the design space that is less than or equal to a

specific SPV value is determined. Goldfarb et al. (2004b) randomly generated design points within the constraints of the design region to construct FDS plots for mixture and mixture-process designs. The minimum of SPV is then plotted at an FDS of 0 and maximum is plotted at the fraction 1. A desirable design starts with small SPV and has a relatively flat slope across the FDS plot.

Sliced FDS Plot within a SPD

Sliced FDS plots can be developed to analyze the prediction variance distribution throughout the subplot space at specific whole-plot shrinkage levels. To construct the sliced FDS plot, random points are generated throughout the subplot space at each whole-plot shrinkage level from 0 to 1 (in steps of 0.1) depending on the variance ratio, *d*. The sliced FDS plots can also be constructed at different subplot shrinkage levels if one is interested in the trends in whole-plot space for a given subplot shrinkage level. The sliced FDS plots provide the *maximum* SPV value at a different shrinkage level for the whole-plot or subplot, which is used to construct sliced FDS. It is desirable to keep the SPV value small. These sliced FDS plots also provide information about the contribution of two spaces, whole-plot or subplot, to the change in SPV value. When we use the sliced FDS plots with different whole-plot shrinkage levels, and the FDS "slices" are far apart, it indicates that whole-plot location has a more significant effect on the SPV value than the subplot location. If the "slices" are close together, are increasing rapidly, or have similar patterns as the global FDS, then a change in the whole-plot location is not enough to significantly affect the SPV value, but the

subplot location has an impact on the SPV value. If the sliced FDS plots start from similar *minimum* SPV values, and are uniformly dispersed, then the contribution of two spaces is balanced to changes in the SPV values. In other words, the distance between FDS plots represents the effect of whole-plot space on the SPV values, and the slope of FDS plot explains the subplot space effect on the SPV values.

The other way to analyze the sliced FDS plot is to draw the FDS plot using different variance ratios, *d*, at the specific shrinkage level of desired plot. These sliced FDS plots show the trends of SPV by changing the variance component ratio at the specific shrinkage of whole-plot or subplot.

Example 2: Kowalski, Cornell, and Vining (KCV) Design for SPD

Kowalski et al. (2002) proposed a design for mixture-process variable experiments within a split-plot structure. They considered both the main-effects plus interaction model in the process variables and the second-order model containing $(n+1)(n+2)/2$ terms in the process variables which are crossed with the mixture components. They assume that the main effects of process variables are crossed only with the linear blending terms, and the combined model is

$$f(x,z) = \sum_{i=1}^{q} \beta_i x_i + \sum\sum_{i<j}^{q} \beta_{ij} x_i x_j + \sum\sum_{k<l}^{n} \alpha_{kl} z_k z_l + \sum_{i=1}^{q}\sum_{k=1}^{n} \gamma_{ik} x_i z_k + \delta + \varepsilon .$$

For a second-order model, the pure quadratic terms in the process variables are added to the main-effects plus interaction model, and the proposed combined second-order model is

$$f(x,z) = \sum_{i=1}^{q} \beta_i x_i + \sum\sum_{i<j}^{q} \beta_{ij} x_i x_j + \sum\sum_{k<l}^{n} \alpha_{kl} z_k z_l + \sum_{k=1}^{n} \alpha_{kk} z_k^2 + \sum_{i=1}^{q}\sum_{k=1}^{n} \gamma_{ik} x_i z_k + \delta + \varepsilon .$$

In the model, the process variables are assigned to the whole-plot and the mixture components are located in the subplot. Noise variables are not considered in the KCV design. For this example, we used the design with $q = 3$ mixture components and $n = 2$ process variables, which is given in Kowalski et al. (2002). Figures 1 and Figure 2 display the proposed design for the combined mixture-process variable models with the first-order process variables and the second-order process variables.

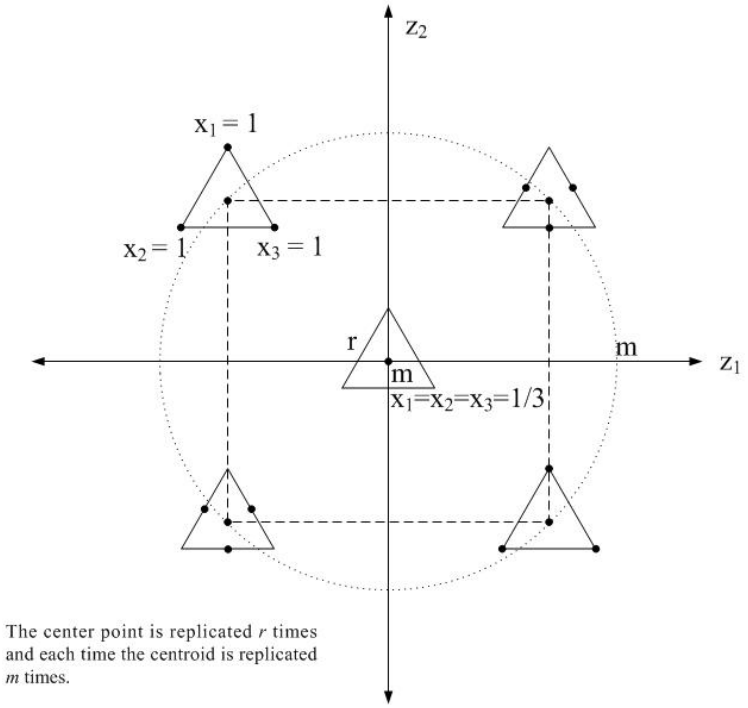

The figure was modified from Kowalski, Cornell, and Vining (2002)

FIGURE 1. Proposed Designs for a Split-Plot Structure to Support Fitting the Combined First-Order Mixture –Process Variable Model

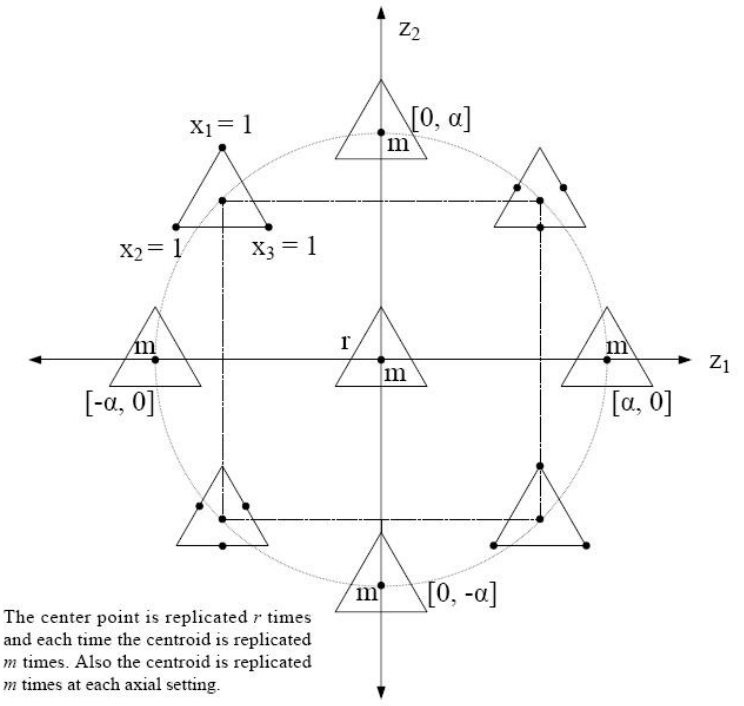

FIGURE 2. Proposed Designs for a Split-Plot Structure to Support Fitting the Combined Second-Order Mixture –Process Variable Model

In this example, we set $r = 2$ and then $r = 3$ to examine the effect of centroid replication and $m = 4$ to balance the number of runs in each subplot design for all cases, the first and second-order model in the process variables. The first-order process variable model is used to construct Figures 3, 4, and 5. Figure 3 shows FDS plots for the design with $m = 4$ resulting in a balanced design. As r increases from 2 to 3, the maximum SPV has increased, indicating the same pattern as seen previously for all levels of the variance component ratio, d. However, the increase in r does not result in a significant change in the FDS plots. Since the proposed design uses $m = 4$ to balance the number of runs in the

centroid portions, the number of centroid data points are already sufficient to compensate for the effect of *r* replications.

The centroid replication, however, is necessary to estimate the whole-plot errors. Thus, we suggest a small number of replicates at the centroid to reduce the prediction variance.

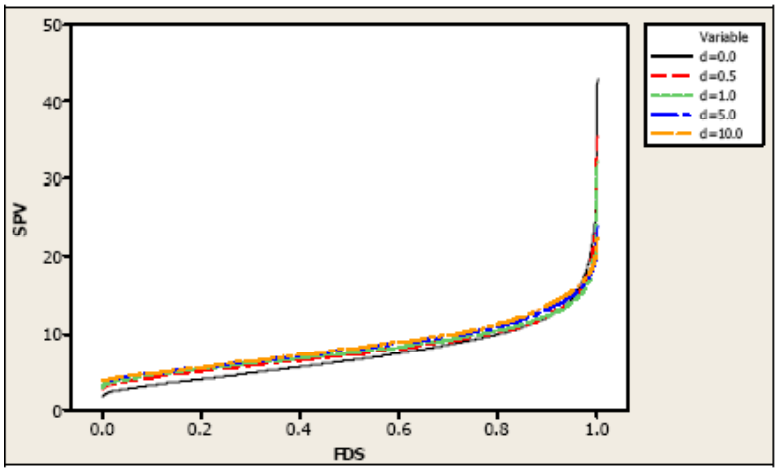

(a)

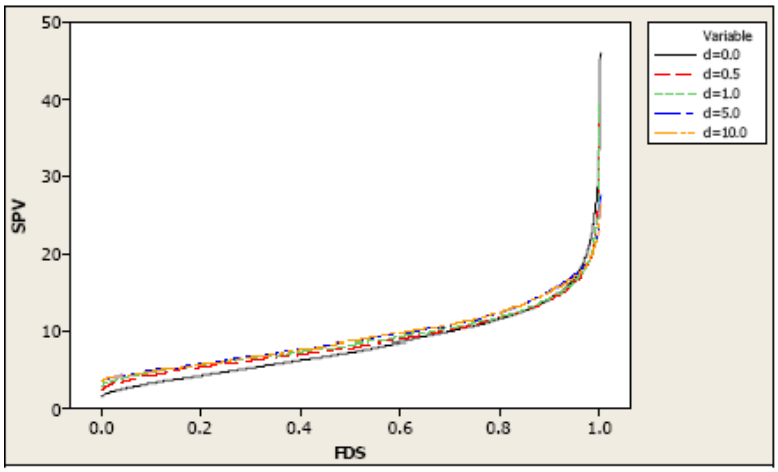

(b)

FIGURE 3. FDS for KCV Design using First-Order Process Variables with Centroid Replication, *r*

As seen in Figure 3 (a) and (b), the FDS plot slightly shifts upward, but the *maximum* SPV decreases as the variance component ratio, *d*, increases. The slopes are stable for large portions of fractions of design space, and are radically increased in small fractions. These increases are smaller as *d* increases. The whole-plot space does not significantly affect the behavior of SPV values and SPV values are highly dependent on the subplot design space. The sliced FDS plots are useful to see the specific effect of the whole-plot design space.

Figure 4 shows the sliced FDS plots at different variance component ratios. In each graph, sliced FDS plots with a whole-plot design space shrinkage level and a global FDS plot are displayed. As *d* increases, it is clear that the *maximum* SPVs within each shrinkage level are decreased and the minimum SPVs are increased, resulting in flatter slopes. In particular, when the whole-plot design points are from the outermost region (shrinkage = 1.0), we can see a significant change of *maximum* SPV, *minimum* SPV, and slope. Figure 5 confirms this analysis. FDS plots are only slightly affected by the variance component ratio while the whole-plot design space is small (or shrinkage level is low). Figures 4 and 5 show that the FDS plots are stable for high variance component ratio level ($d > 2.0$), while the shrinkage level of the whole-plot spaces are lower than 0.7.

Now the second-order process variable model is analyzed using the global FDS plot and sliced FDS plots. In this example, we can see the SPVs are not always increasing as the shrinkage level increases. The second-order terms in the process variables produces an SPV with a *minimum* value at middle of shrinkage level.

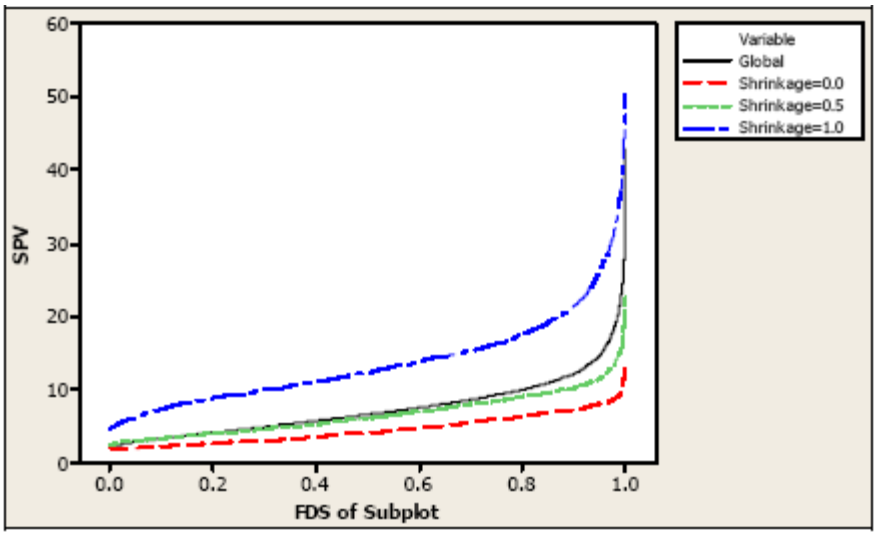

(a)

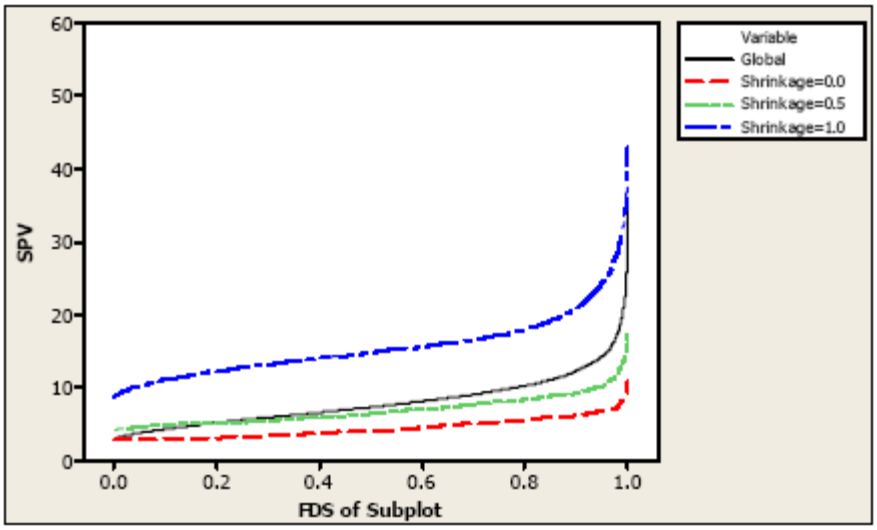

(b)

FIGURE 4. Sliced FDS for KCV Design using First-Order Process Variables with Different Shrinkage Levels

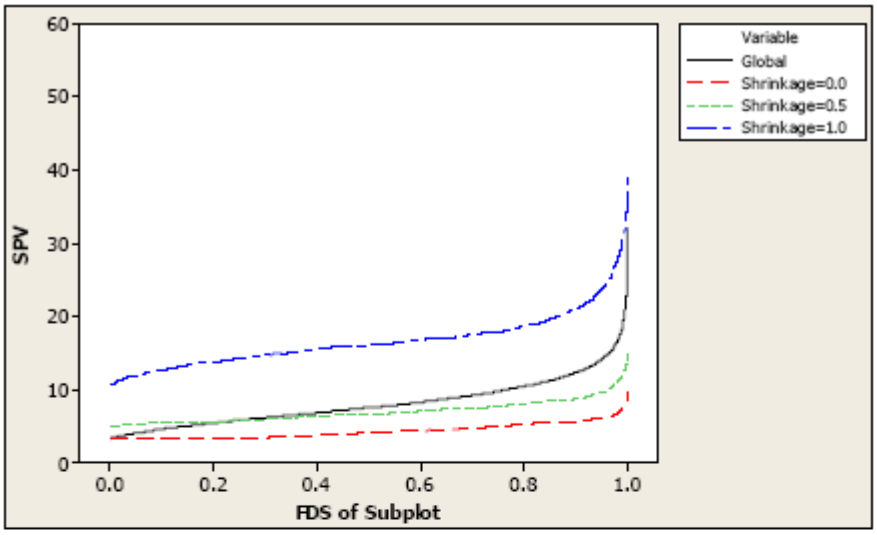

(c)

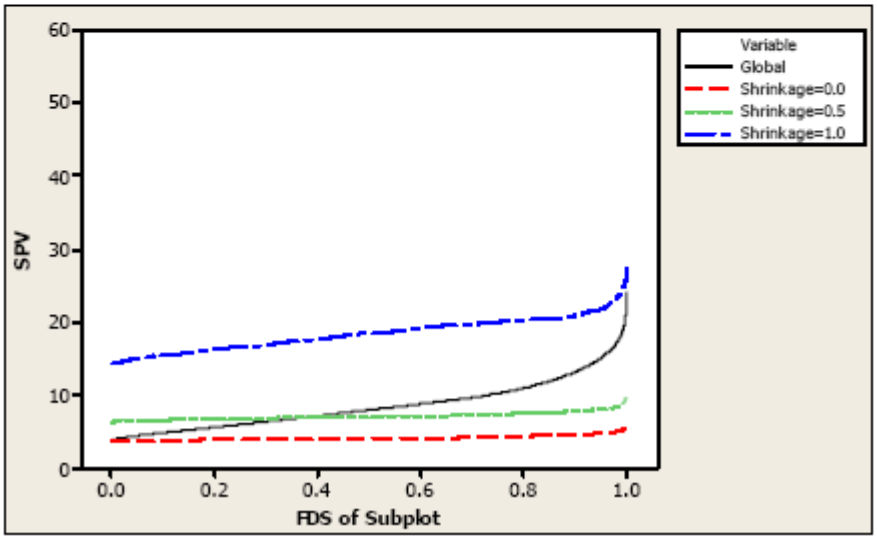

(d)

FIGURE 4. Sliced FDS for KCV Design using First-Order Process Variables with Different Shrinkage Levels (continued)

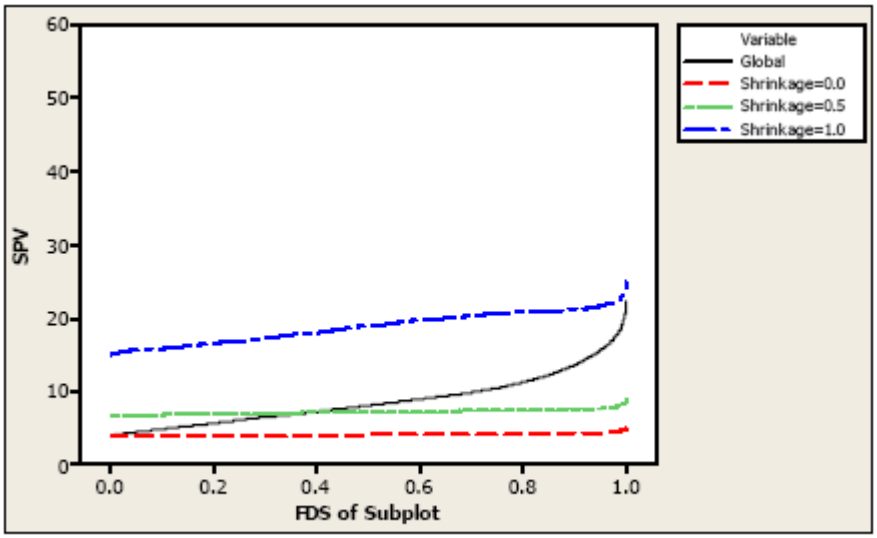

(e)

FIGURE 4. Sliced FDS for KCV Design using First-Order Process Variables with Different Shrinkage Levels (continued)

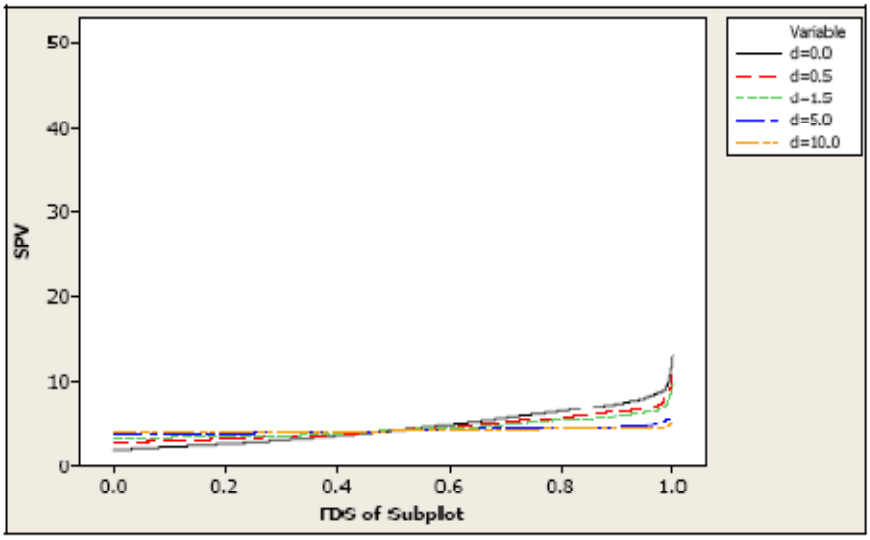

(a)

FIGURE 5. Sliced FDS for KCV Design using First-Order Process Variables with Variance Component Ratio, *d*

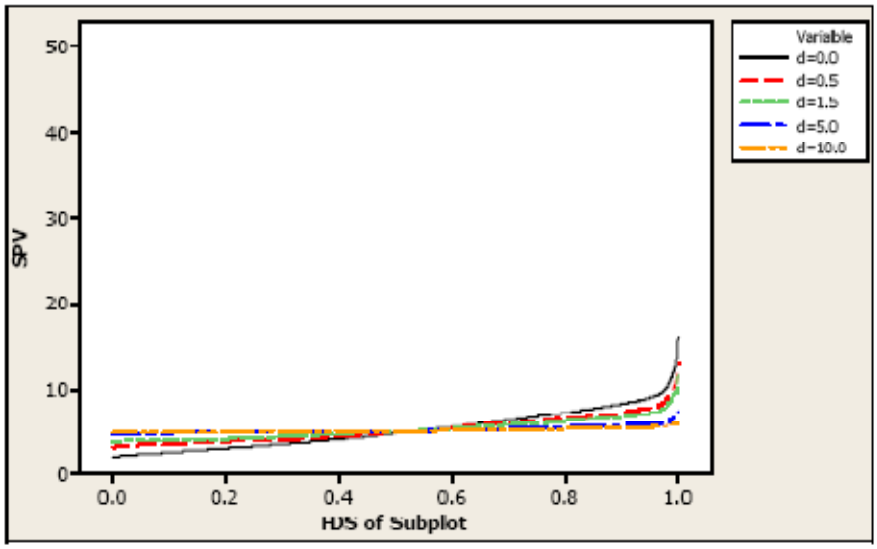

(b)

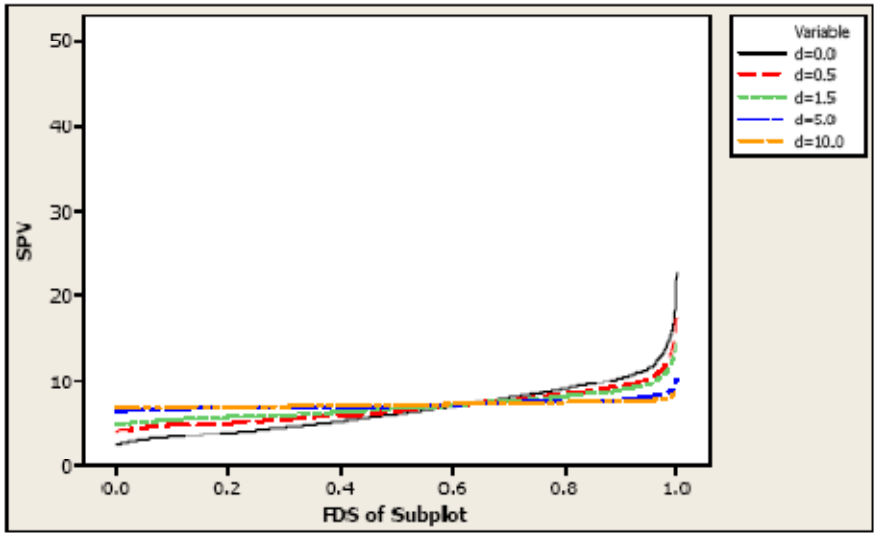

(c)

FIGURE 5. Sliced FDS for KCV Design using First-Order Process Variables with Variance Component Ratio, *d* (continued)

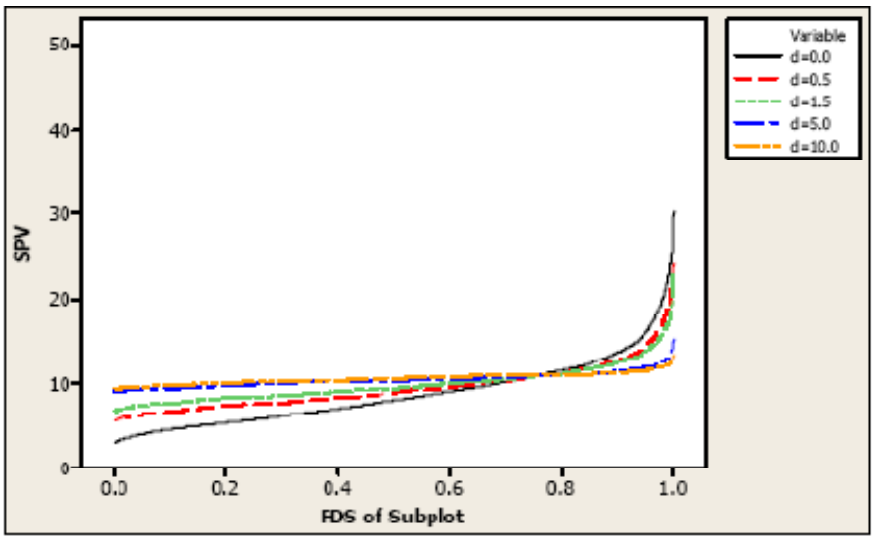

(d)

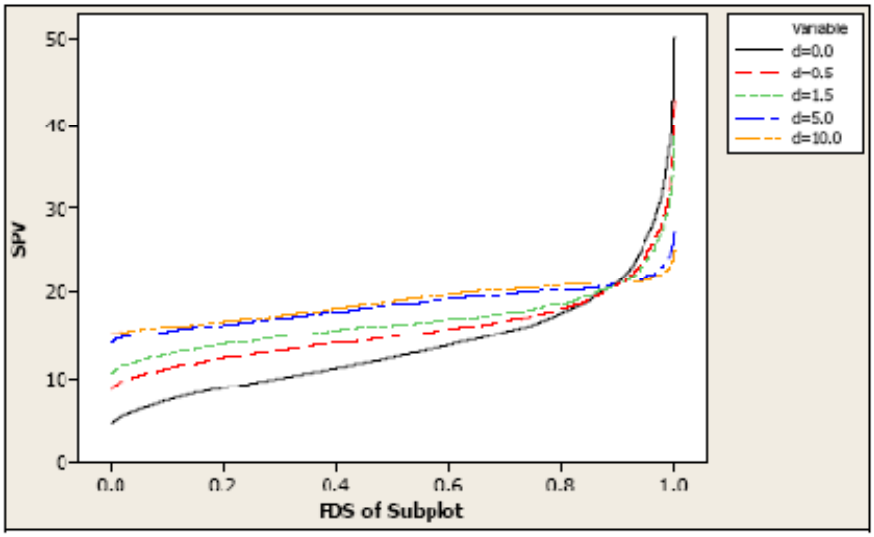

(e)

FIGURE 5. Sliced FDS for KCV Design using First-Order Process Variables with Variance Component Ratio, *d* (continued)

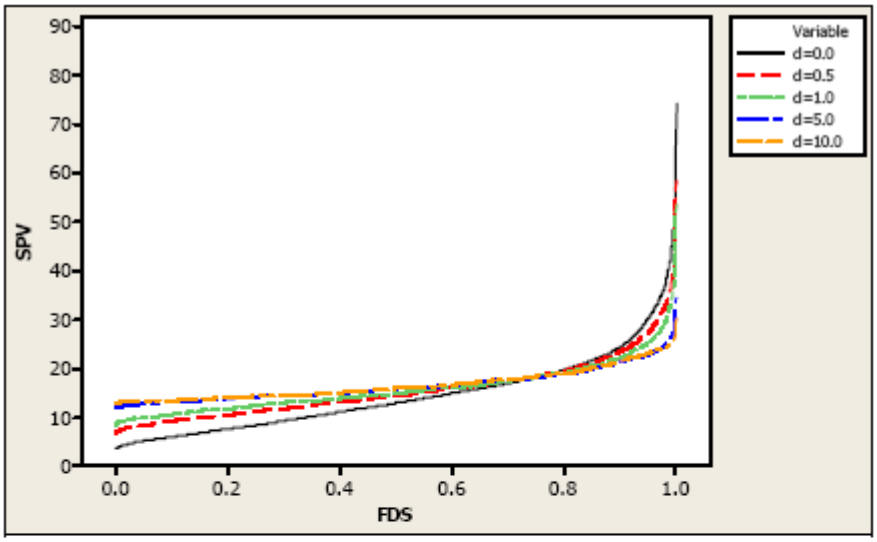

(a)

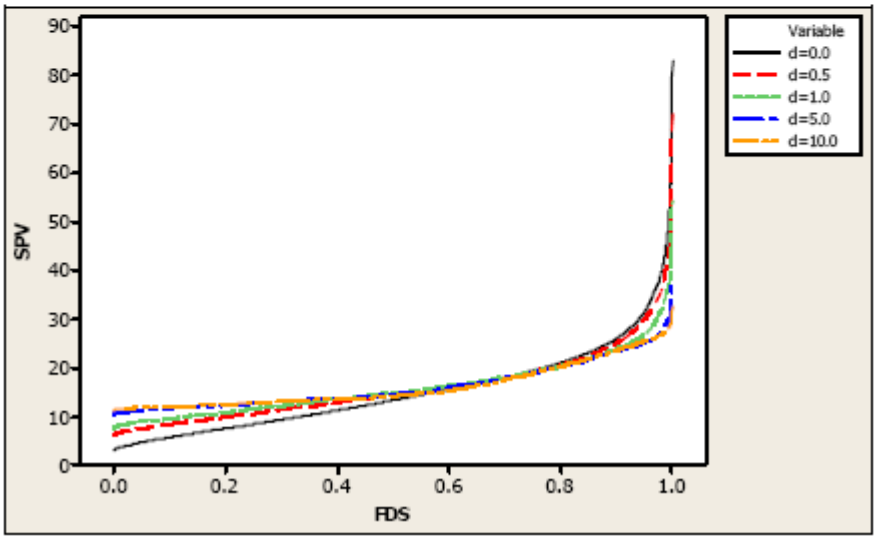

(b)

FIGURE 6. FDS for KCV Design using Second-Order Process Variables with Centroid Replication, *r*

The second-order process variable model is used to construct Figures 6, 7, and 8. As shown in Figure 6, the minimum SPV decreased slightly while the maximum SPV has increased, indicating the same pattern as seen previously for all levels of the variance component ratio, *d*, as *r* increased from 2 to 3. However,

the increase of r did not result in significant changes in the FDS plots. As seen in Figure 6 (a) and (b), it is clear that the FDS plot is going to be flat as the variance component ratio, d, increases. The *minimum* SPV increases while the *maximum* SPV decreases as d increases. If the whole-plot error is larger than the subplot error ($d > 1$), then the SPVs tend to be stable over the entire design space, which is preferable in most cases. Therefore, the split-plot structure for the mixture-process variable design problem results in stable prediction variance although it provides slightly higher SPVs for smaller fractions of the design space.

Since the number of centroid replicates does not significantly affect the prediction variance for the example, we examined sliced FDS plots with $r = 2$. The sliced FDS plots are shown in Figure 7 and Figure 8 and categorized by the shrinkage level and the variance component ratio, respectively. For the FDS plot with different shrinkage levels, it is obvious that the overall SPV values decrease as the shrinkage level increases up to 0.7, and then rapidly increases for all variance component ratios, d. This is due to the characteristic of a second-order model involving process variables. If we investigate the process variables without mixture components, SPV has its lowest value at a shrinkage level of approximately 0.7, high values in the small design space, and the highest value at the 1.0 shrinkage level, which is the outer region of whole-plot. Figure 7 illustrates that the whole-plot space has more effect on the SPV value as the variance component increases. This is evident because the FDS plots are flat and far apart from each other as d increases.

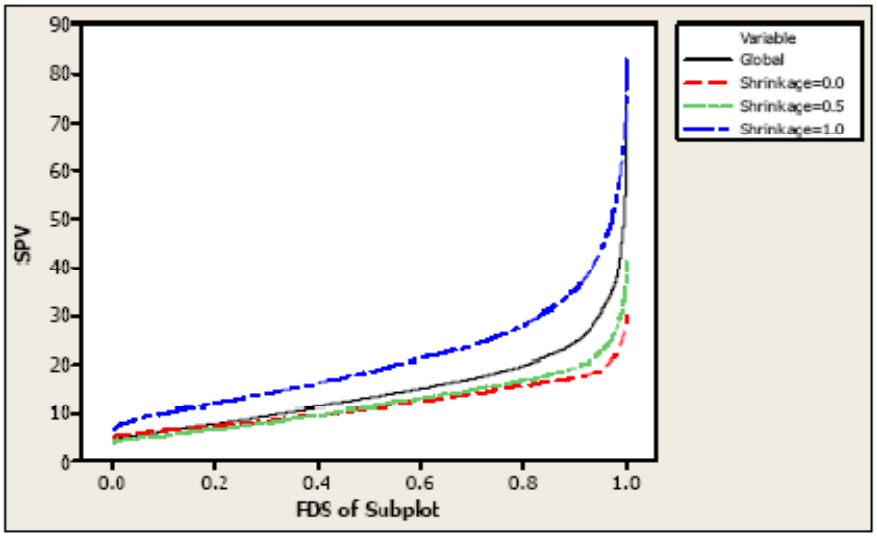

(a)

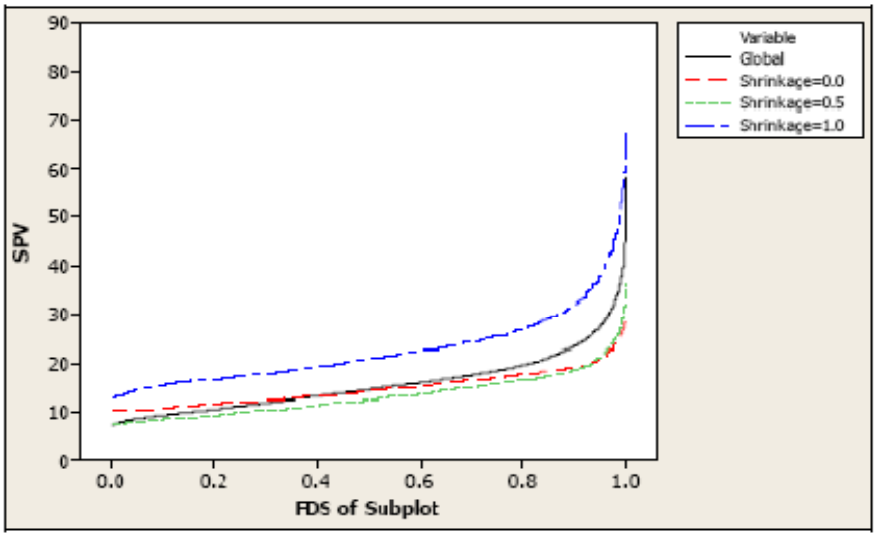

(b)

FIGURE 7. Sliced FDS for KCV Design using Second-Order Process Variables with Different Shrinkage Levels

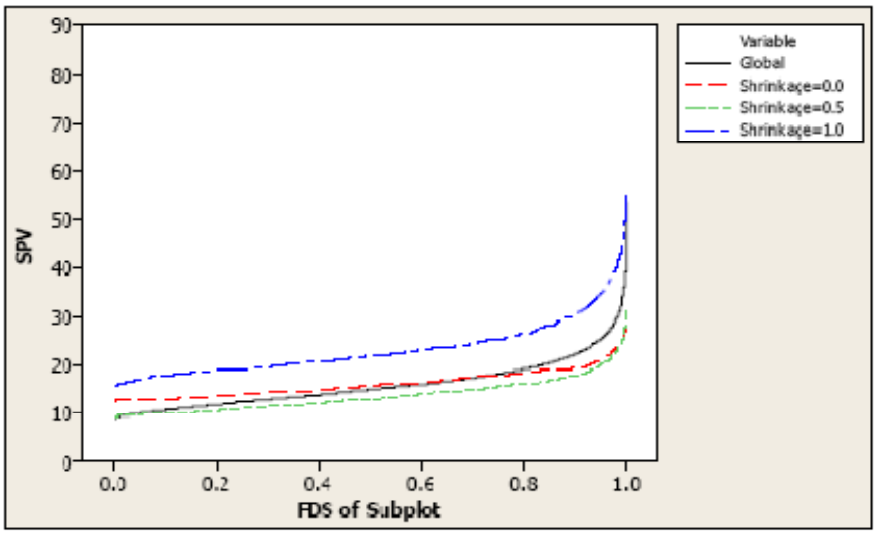

(c)

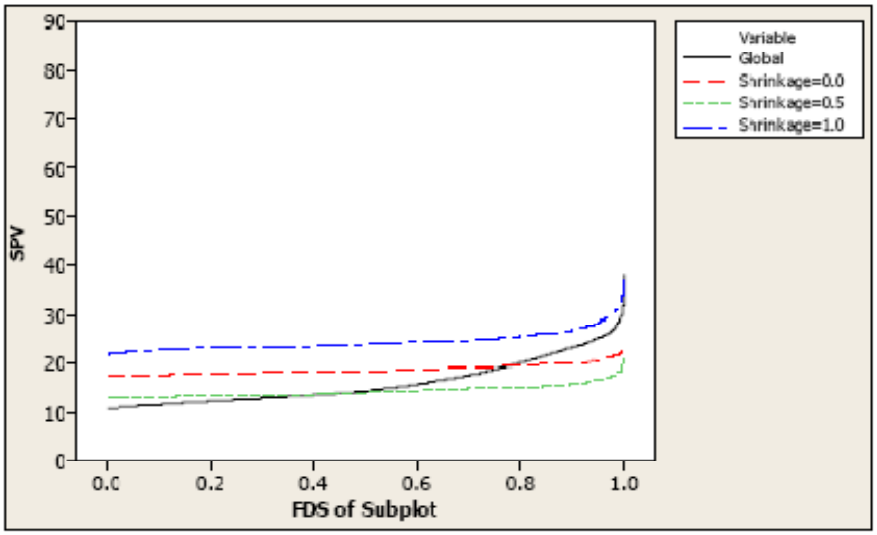

(d)

FIGURE 7. Sliced FDS for KCV Design using Second-Order Process Variables with Different Shrinkage Levels (continued)

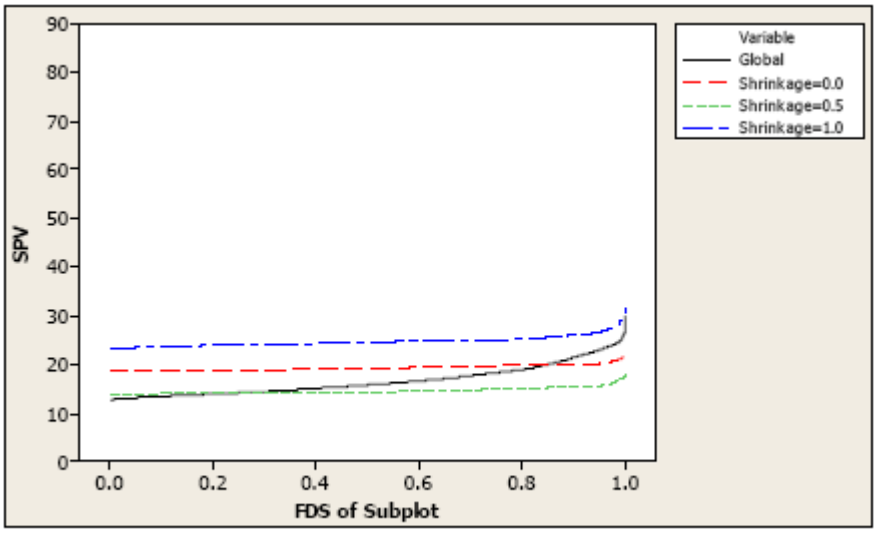

(e)

FIGURE 7. Sliced FDS for KCV Design using Second-Order Process Variables with Different Shrinkage Levels (continued)

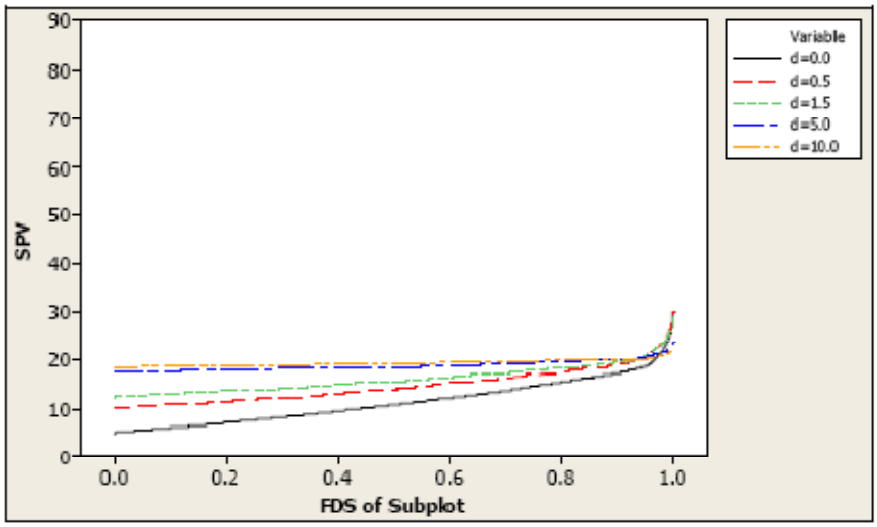

(a)

FIGURE 8. Sliced FDS for KCV Design using Second-Order Process Variables with Variance Component Ratio, *d*

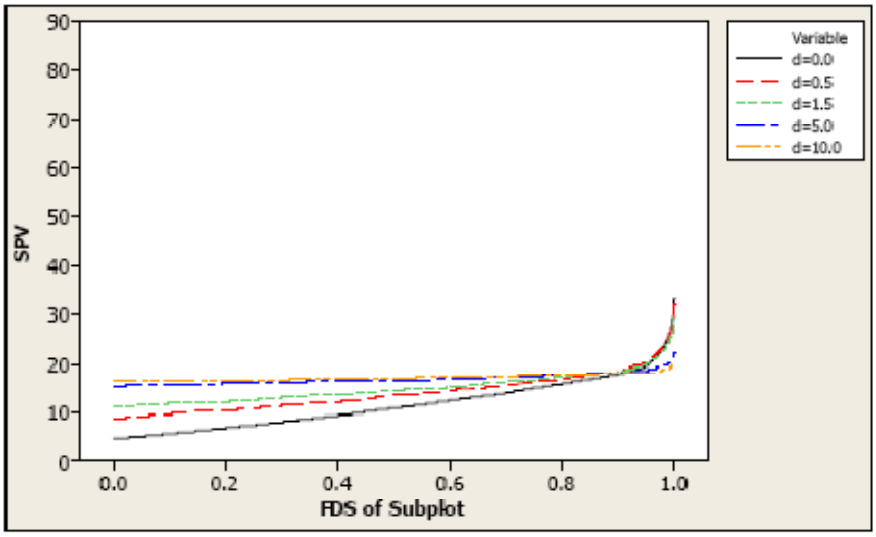

(b)

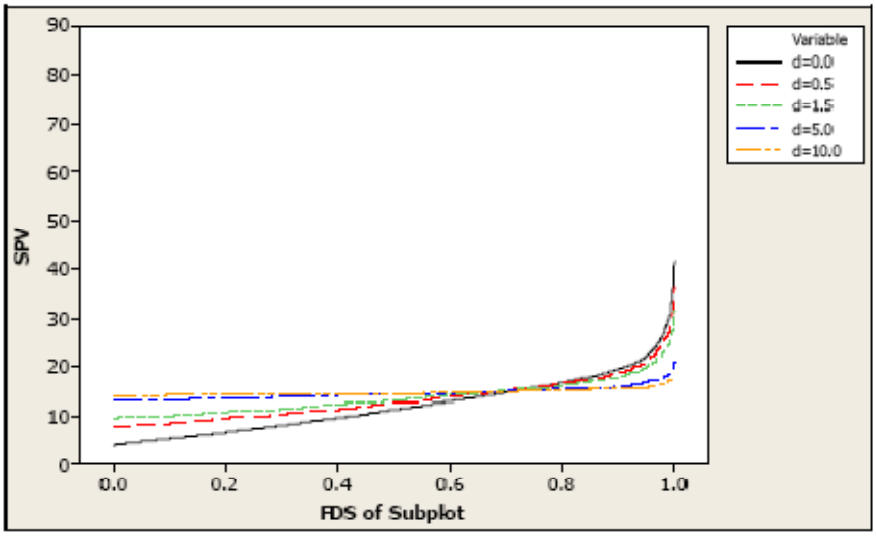

(c)

FIGURE 8. Sliced FDS for KCV Design using Second-Order Process Variables with Variance Component Ratio, *d* (continued)

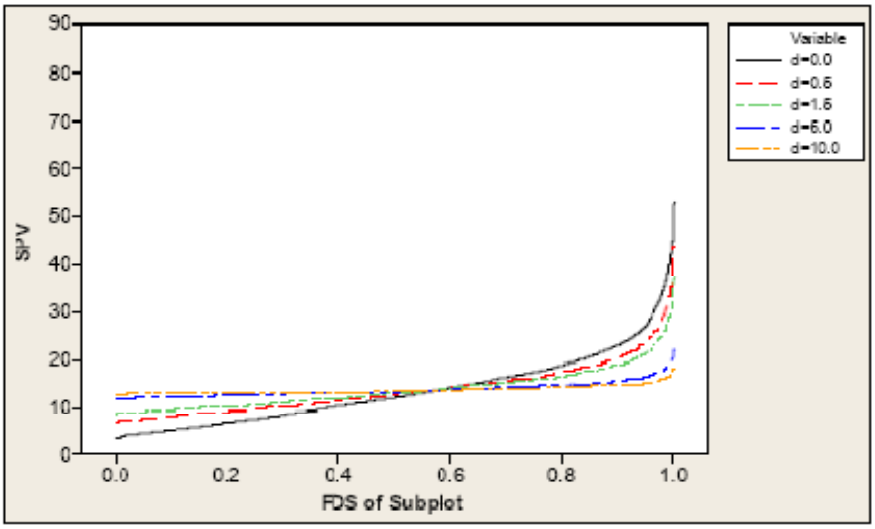

(d)

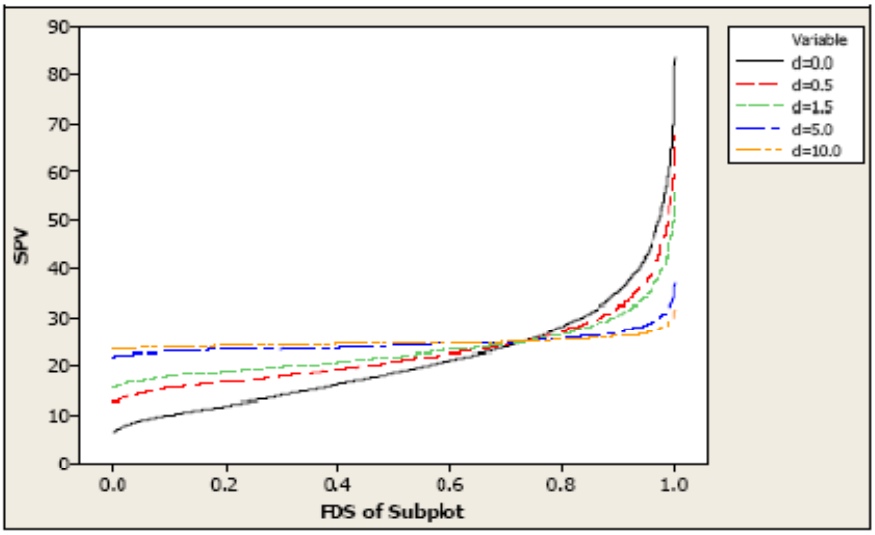

(e)

FIGURE 8. Sliced FDS for KCV Design using Second-Order Process Variables with Variance Component Ratio, *d* (continued)

The subplot space has an effect on the SPV value when there is no whole-plot error (i.e., $d = 0$). Therefore, if we did not consider a split-plot structure for this example and the whole-plot error exists, the prediction variance is poorly

estimated over a large range. Figure 8 displays the clear effect of whole-plot shrinkage levels. As seen in the sliced FDS plots, the small shrinkage level provides more stable and lower SPV values for all variance component ratios, *d*. The slopes of the FDS plot are going to be steeper as the shrinkage level increases yielding increased *maximum* of SPV value when *d* is less than 2.0. The FDS plots shift down and up as the shrinkage level increases while the slopes remain stable when *d* is greater than 2.0.

Example 3: Design Evaluation using the FDS Plot

Goos and Donev (2007) suggested tailor-made *D*-optimal split-plot designs for experiments with mixture and process variables. They used the point exchange algorithm with a specified set of candidate design points and a candidate set free algorithm with JMP 7.0 by SAS Institute Inc. (2007). They benchmarked their design with the design for the vinyl-thickness experiment proposed by Kowalski et al. (2002) and showed that *D*-optimal designs are superior to the benchmarked design in terms of optimal design criteria, such as *D-, A-, G-*, and *V*-efficiency. However, these optimality criteria are single number values and not entirely sufficient to explain all of the characteristics of prediction variance in the design space. In this example, we used FDS plots to evaluate the designs in terms of prediction variance over the entire design region. As shown in Figure 9, the *D*-optimal designs have relatively flat slopes in the FDS plot indicating a stable variance pattern over almost the entire design space for all levels of variance component ratio, *d*.

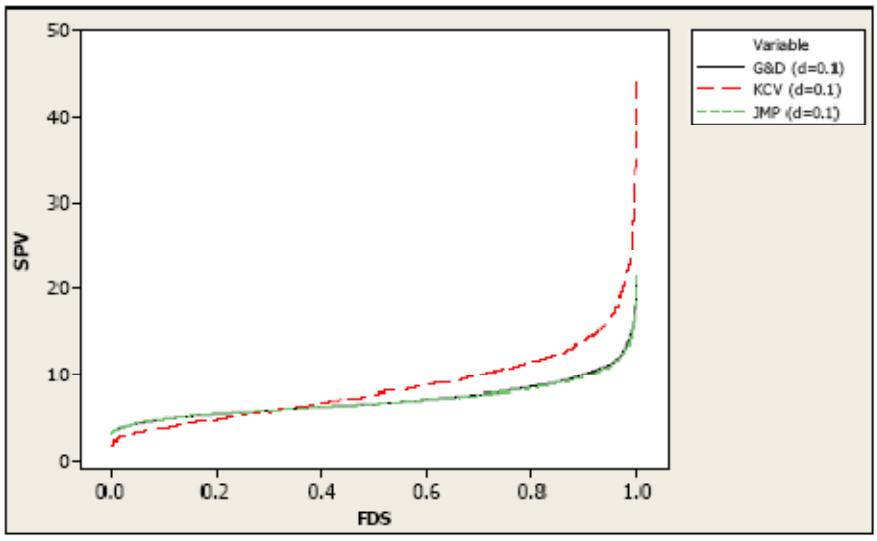

(a)

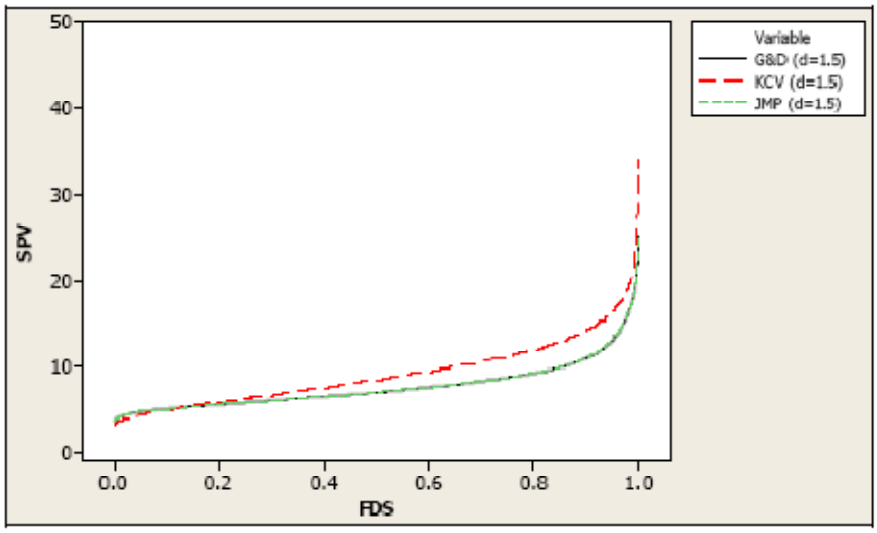

(b)

FIGURE 9. FDS Plots for Design Evaluation for Vinyl-Thickness Experiment

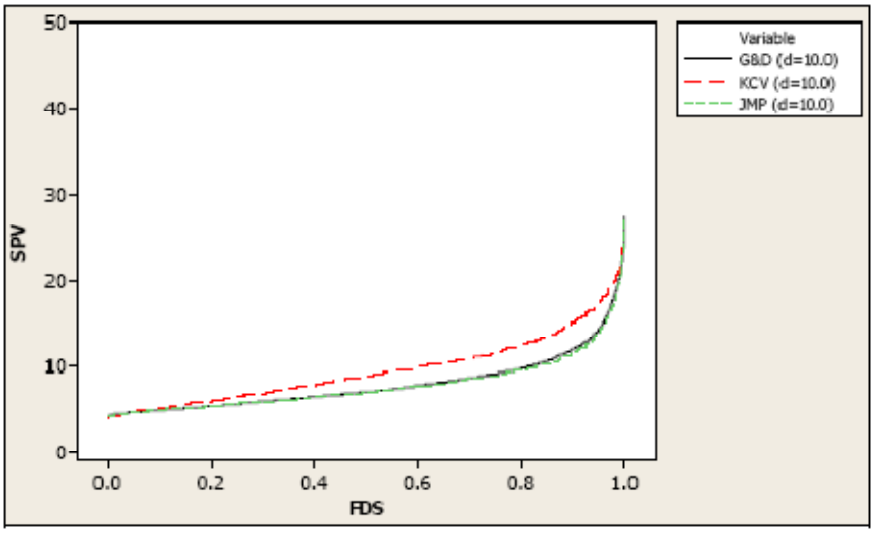

(c)

FIGURE 9. FDS Plots for Design Evaluation for Vinyl-Thickness Experiment (continued)

As shown in Figure 9 (a), however, the KCV design has small prediction variance values over 1/3 of the design space when *d* is small (0.1). However *G*-efficiency indicates that the D-optimal design is 153% more efficient than the KCV design. This shows that the KCV design has small prediction variance in some region of the design space when *d* is small (0.1). Also, these FDS plots show that the KCV design has stable prediction variance over 90% of the design space and only 10% of the design space has large prediction variance, which produces the poor *G*-efficiency. If the practitioner is interested in small prediction variance with some specified area in design space, then the KCV design is a good alternative. Furthermore, the FDS plots provide graphical support for the result of *G*-efficiency. Figure 9 (b) and (c) shows that there is little difference between *D*-optimal designs and the KCV design in the FDS plot slope, which is equivalent to

the optimality criteria result used in Goos and Donev (2007). Figure 9 illustrates that *D*-optimal designs by Goos and Donev (2007) and JMP have almost identical FDS plots for all variance component ratio levels. The *D*-optimal designs are not affected by the increase in *d* while the FDS plot of the KCV design is notably influenced. As *d* increases, the slope is flattened and the maximum of SPV is decreased. We conclude that the *D*-optimal designs suggested by Goos and Donev (2007) and JMP are robust for the extent of correlation within whole-plot from the viewpoint of prediction variance.

Conclusion

In this chapter, we have examined split-plot designs for mixture-process variable design problems and demonstrated the different results that can be obtained between completely randomized designs and split-plot designs using REML to estimate the whole-plot error and subplot error. In the example, we showed that the estimates of model parameter are equivalent if the design is balanced and the subplot designs are orthogonal. However, the statistics of the significant test for the factors are erroneous if restricted randomization problem is not considered in the analysis. We also implement the FDS plot to evaluate the mixture-process variable design within a split-plot structure. FDS plots provide visual information about the range of SPV values throughout the design space. We show the influence of the variance component ratio, *d*, on FDS plots. In the split-plot design, the prediction capability depends not only on the design and model, but also on the variance of the fitted model. If whole-plot effect on the

design is not considered in the analysis, the prediction variance from the fitted model cannot be precisely estimated. Sliced FDS plots are very useful to understand the distribution of SPV in the whole-plot and subplot spaces. They provide information regarding which of the two design space contributes more to the SPV values. The contribution on the SPV depends on the coefficient of each term in the model and the number of variables from each design space.

CHAPTER 4

MIXTURE-PROCESS VARIABLE EXPERIMENTS INCLUDING CONTROL AND NOISE VARIABLES WITHIN A SPLIT-PLOT STRUCTURE

In mixture-process variables experiments, it is common that the experimental runs are larger than the mixture-only design or basic experimental design to estimate the increased coefficient parameters due to the mixture components, process variable, and interaction between mixture and process variables, some of which are hard to change or cannot be controlled under normal operating condition. These situations often prohibit a complete randomization for the experimental runs due to the time or financial reason. These types of experiments can be analyzed in a model for the mean response and a model for the slope of the response within a split-plot structure. When considering the experimental designs, low prediction variances for the mean and slope model are desirable. We demonstrate the methods for the mixture-process variable designs with noise variables considering a restricted randomization and evaluate some mixture-process variable designs that are robust to the coefficients of interaction with noise variables using fraction design space plots with the respect to the prediction variance properties. Finally, we create the *G*-optimal design that minimizes the maximum prediction variance over the entire design region using a genetic algorithm.

Introduction

In mixture-process variable designs (MPDs), the process variables can be categorized into two types: variables that are controllable and directly affect the response, and variables that are uncontrollable and primarily affect the variability of the response. Myers et al. (2009) call these factors control factors and noise factors (or noise variables), respectively. We assumed that noise variables are controllable in a special laboratory environment for the purpose of conducting experiments. When production is moved from the laboratory to the manufacturing environment, noise factors are not necessarily controllable in the normal operation of the process. Consequently, it is important to consider noise variables at the design stage of the process. The model containing both noise variables and control factors can be used to determine factor settings for the control factor that makes the response "robust" to the variability transmitted from the noise factors. This type of study is called "robust parameter design". See Borror et al. (2002), Myers et al. (2009) and Montgomery (2009) for details and summaries. The MPDs with noise variables were developed by Steiner and Hamada (1997), Goldfarb et al. (2003), and Goldfarb et al. (2004c).

The number of runs for MPDs is likely to increase dramatically as the number of process variables increase. Furthermore, while noise variables are controllable in the laboratory environment, usually these variables are difficult to adjust and control. In designing experiments, randomization is an important requirement underlying the use of statistical methods. However, if it is difficult or expensive to change the levels of some factors, it is impractical to perform the

experiments in a completely randomized order. In this situation, restrictions on the randomization of experimental runs are necessary resulting in a split-plot structure, as described by Box and Jones (1992). Cho et al. (2009) developed graphical evaluation techniques for the MPD within a split-plot structure; however, the authors did not consider robust parameter design for noise variables. In this chapter, we considered robust parameter design for MPD with noise variables using a split-plot structure for the noise variables, which are assumed to be hard-to-change.

To evaluate the prediction capability of a design for MPD with noise variables within the split-plot structure, we considered scaled prediction variance (SPV) for the process mean and the variance of the slope of the response surface in the direction of each noise variable and used the covariance matrix which is a function of the whole-plot (WP) variance and sub-plot (SP) variance with respect to the variance component ratio, d. We evaluate the SPV values for the mean and slope models using fraction of design space (FDS) plots, introduced by Zahran et al. (2003).

Design generation and comparison are often carried out using the design optimality criteria, such as D-optimality, G-optimality, A-optimality, and I-optimality. See Myers et al. (2009) for detailed discussion on design optimality. When prediction variance is of primary interest, optimality criteria such as G-optimality and I-optimality are considered. Commercial statistical packages such as JMP or Design-Expert provide the I-optimality criteria for generating designs. There is no commercial software for constructing G-optimal designs. Goldfarb et

al. (2005) and Chung et al. (2007) create *G*-optimal designs for mixture-process variable design with control and noise variables using a restricted form of a genetic algorithm (GA) (no mutation occurred). Rodriguez et al. (2009) generate *G*-optimal designs using a full GA, but no mixture variables are considered in the design.

We develop the prediction variance models for the MPDs with noise variables within a split-plot structure and introduce simplified prediction capability to compare designs. We then demonstrate the use of modified FDS plots to evaluate various designs with examples. In generating the optimal design, we considered *G*-optimality for mixture-process variable designs with control and noise variables within a split-plot structure. We compare the new *G*-optimal design with other computer-generated optimal designs and G-optimal designs generated by Goldfarb et al. (2005) in terms of maximum prediction variance. Finally, we show a graphical analysis of the different designs using the VRFDS plot.

Notation and Model

Assume that the mixture components x_i and the controllable process variables w_p are the SP factors. The noise variables z_t are the WP factors. Furthermore, we suppose that there are p mixture components (x_i, $i = 1, 2, \ldots, q$), c controllable variables (w_j, $j = 1, 2, \ldots, c$), and q noise variables (z_t, $t = 1, 2, \ldots, n$). The process variables are assumed to be continuous. Also suppose that there are m mixture terms, where m is a function of the number of the mixture

components and the degree of the model. We will focus on the quadratic mixture model. A response can be represented as a function of *m* mixture terms in quadratic mixture model form, *q* continuous noise variables, and *c* continuous controllable variables. The model can be written as

$$y = f(\mathbf{x}, \mathbf{w}, \mathbf{z}) = f_w(\mathbf{z})'\beta_{wp} + \delta + f_s(\mathbf{x}, \mathbf{w}, \mathbf{z})'\beta_{sp} + \varepsilon, \quad (7)$$

where β_{wp} is a vector of coefficients from the WP variables, β_{sp} is a vector of coefficients from the SP variables, $\delta \sim N(0, \sigma_\delta^2)$ comes from the WP randomization level and represents the random error term of the WP factors alone, and $\varepsilon \sim N(0, \sigma^2)$ comes from the SP randomization level and represents the random error term from the SP. The random components δ and ε are assumed to be independent. However, the WP terms, $f_w(\mathbf{z}_t)'\beta_{wp}$, can be removed since the noise variables only affect the response through interacting with the mixture components. Then, Equation (7) can be written as

$$\begin{aligned} y(\mathbf{x}, \mathbf{w}, \mathbf{z}) = & \sum_i \beta_i x_i + \sum_{i<j} \sum \beta_{ij} x_i x_j \\ & + \sum_i \sum_p \alpha_{ip} x_i w_p + \sum_{i<j} \sum_p \sum \alpha_{ijp} x_i x_j w_p \\ & + \sum_i \sum_t \theta_{it} x_i z_t + \sum_{i<j} \sum_t \sum \theta_{ijt} x_i x_j z_t \\ & + \sum_i \sum_p \sum_t \lambda_{ipt} x_i w_p z_t + \sum_{i<j} \sum_p \sum_t \lambda_{ijpt} x_i x_j w_p z_t + \delta + \varepsilon \end{aligned} \quad (8)$$

This model is exactly the same as in Goldfarb et al. (2003) except that it has two different sources of error, WP and SP errors and we assume that all noise variables are in the WP. Equation (8) can be expressed in matrix form as

$$Y = f(\mathbf{x}, \mathbf{w}, \mathbf{z}) = \mathbf{x}'\boldsymbol{\beta} + \mathbf{x}'\mathbf{A}\mathbf{w} + \mathbf{x}'\boldsymbol{\Theta}\mathbf{z} + \mathbf{x}'\boldsymbol{\Lambda}\boldsymbol{\Xi}\mathbf{z} + \delta + \varepsilon \tag{9}$$

where

$$\mathbf{x}_{m\times 1} = \begin{bmatrix} x_1 \\ \vdots \\ x_m \end{bmatrix},\ \mathbf{w}_{c\times 1} = \begin{bmatrix} w_1 \\ \vdots \\ w_c \end{bmatrix},\ \mathbf{z}_{q\times 1} = \begin{bmatrix} z_1 \\ \vdots \\ z_n \end{bmatrix},\ ,\boldsymbol{\beta}_{m\times 1} = \begin{bmatrix} \beta_1 \\ \vdots \\ \beta_m \end{bmatrix},$$

$$\mathbf{A}_{m\times c} = \begin{bmatrix} \alpha_{11} & \cdots & \alpha_{1c} \\ \vdots & \ddots & \vdots \\ \alpha_{m1} & \cdots & \alpha_{mc} \end{bmatrix},$$

$$\boldsymbol{\Theta}_{m\times n} = \begin{bmatrix} \theta_{11} & \cdots & \theta_{1q} \\ \vdots & \ddots & \vdots \\ \theta_{m1} & \cdots & \theta_{mq} \end{bmatrix},\ \boldsymbol{\Lambda}_{m\times cn} = \begin{bmatrix} \lambda_{111}\cdots\lambda_{1c1} & \cdots & \lambda_{11n}\cdots\lambda_{1cn} \\ \vdots & \ddots & \vdots \\ \lambda_{m11}\cdots\lambda_{mc1} & \cdots & \lambda_{m1n}\cdots\lambda_{mcn} \end{bmatrix}, \text{ and}$$

$$\boldsymbol{\Xi}_{cn\times n} = \begin{bmatrix} w_1 & 0 & & 0 \\ \vdots & \vdots & \cdots & \vdots \\ w_c & 0 & & 0 \\ 0 & & & 0 \\ \vdots & & \ddots & \vdots \\ 0 & & & 0 \\ 0 & & 0 & w_1 \\ \vdots & \cdots & \vdots & \vdots \\ 0 & & 0 & w_c \end{bmatrix}.$$

x is the $m \times 1$ vector which consist of all mixture model terms including higher order terms, **w** is the $c \times 1$ vector of controllable variables, and **z** is the $n \times 1$ vector of noise variables. **β** is the $m \times 1$ vectors coefficient matrix for mixture model terms, **A** is the $m \times c$ coefficient matrix for the mixture by controllable variable interactions and **Θ** is the $m \times n$ coefficient matrix for the mixture by noise variable interactions. **Λ** is the $m \times cn$ coefficient matrix for interactions involving mixture components, controllable variables, and noise variables. Finally,

$\boldsymbol{\Xi}$ is a $cn \times n$ block-diagonal matrix whose columns contain the w elements and blocks of 0s. We assume that $\delta + \varepsilon$ has mean 0 and variance–covariance matrix $\mathbf{V}$ which is a function of the WP variance σ_δ^2 and the SP variance σ_ε^2 .The covariance matrix of the response is then given by

$$\mathbf{V} = \sigma_\delta^2 \mathbf{J} + \sigma_\varepsilon^2 \mathbf{I} = \sigma_\varepsilon^2 [d\mathbf{J} + \mathbf{I}], \tag{10}$$

where $\mathbf{J} = \begin{bmatrix} \mathbf{1}_{n_1}\mathbf{1}'_{n_1} & 0 & \cdots & 0 \\ 0 & \mathbf{1}_{n_2}\mathbf{1}'_{n_2} & \cdots & 0 \\ \vdots & \vdots & \ddots & \vdots \\ 0 & 0 & \cdots & \mathbf{1}_{n_{wp}}\mathbf{1}'_{n_{wp}} \end{bmatrix}$, $d = \dfrac{\sigma_\delta^2}{\sigma_\varepsilon^2}$ (the variance component ratio),

and $\mathbf{1}_{n_i}$ is the vector of 1s with length n_i (i=1, … ,wp), which is the number of SP runs within each WP. When the design is balanced (the number of sub-plots in each whole-plot is the same), the inverse of the covariance matrix $\mathbf{V}$ can be written as

$$\mathbf{V}^{-1} = \sigma_\varepsilon^{-2}\left(\mathbf{I} - \frac{d}{1+dk}\mathbf{J}\right)$$

where k is the number of sub-plots in each whole-plot and $\mathbf{JJ}=k\mathbf{J}$. We can prove this result by directly multiplying Equation (10) by this inverse matrix to obtain the identity matrix. This inverse matrix form reduces the computing time when we generate the optimal design using GA.

Robust Parameter Design for Noise Variables within a Split-Plot Structure

The expected value and variance of y can be found using the delta method, which utilizes a Taylor series expansion of the model around the mean of z.

Assume that the noise variables are uncorrelated, the model errors (δ and ε) are uncorrelated and independent, and the noise variables and the mixture components are uncorrelated with each other. Expanding $f(\mathbf{x},\mathbf{w},\mathbf{z})$ using a first-order Taylor series around z =0 yields

$$\mathbf{y} = f(\mathbf{x},\mathbf{w},\mathbf{0}) + (\mathbf{z}-\mathbf{0})' \left.\frac{\partial f(\mathbf{x},\mathbf{w},\mathbf{z})}{\partial \mathbf{z}}\right|_{\mathbf{z}=\mathbf{0}} + R + \delta + \varepsilon ,$$

where R is the remainder term comprised of higher order terms in the Taylor series expansion. Considering the model in two sub-models (the WP model and SP model), then equation (9) can be categorized into two sub models,

$$\begin{aligned} \mathbf{y}_{WP} &= f_w(\mathbf{z}) = \delta \\ \mathbf{y}_{SP} &= f_s(\mathbf{x},\mathbf{w},\mathbf{z}) = \mathbf{x}'\boldsymbol{\beta} + \mathbf{x}'\mathbf{A}\mathbf{w} + \mathbf{x}'\boldsymbol{\Theta}\mathbf{z} + \mathbf{x}'\boldsymbol{\Lambda}\boldsymbol{\Xi}\mathbf{z} + \varepsilon \end{aligned},$$

and a first-order Taylor series is given by

$$\begin{aligned} \mathbf{y}_{WP} &= \delta \\ \mathbf{y}_{SP} &= f_s(\mathbf{x},\mathbf{w},\mathbf{0}) + (\mathbf{z}-\mathbf{0})' \left.\frac{\partial f_s(\mathbf{x},\mathbf{w},\mathbf{z})}{\partial \mathbf{z}}\right|_{\mathbf{z}=\mathbf{0}} + R + \varepsilon \end{aligned}.$$

It follows that

$$\begin{aligned} E_z(\mathbf{y}) &\approx f_w(\mathbf{z}) + f_s(\mathbf{x},\mathbf{w},\mathbf{z}) \\ Var_z(\mathbf{y}) &\approx \left[\left.\frac{\partial f_w(\mathbf{z})}{\partial \mathbf{z}}\right|_{\mathbf{z}=\mathbf{0}}\right]' \sum_{\mathbf{z}} \left[\left.\frac{\partial f_w(\mathbf{z})}{\partial \mathbf{z}}\right|_{\mathbf{z}=\mathbf{0}}\right] + \sigma_\delta^2 \\ &\quad + \left[\left.\frac{\partial f_s(\mathbf{x},\mathbf{w},\mathbf{z})}{\partial \mathbf{z}}\right|_{\mathbf{z}=\mathbf{0}}\right]' \sum_{\mathbf{z}} \left[\left.\frac{\partial f_s(\mathbf{x},\mathbf{w},\mathbf{z})}{\partial \mathbf{z}}\right|_{\mathbf{z}=\mathbf{0}}\right] + \sigma_\varepsilon^2 \end{aligned},$$

where $\sum_{\mathbf{z}} = diag(\sigma_{z_1}^2, \sigma_{z_2}^2, \cdots, \sigma_{z_n}^2)$ is an $n \times n$ diagonal matrix with the variance of the noise variables on the diagonal and 0 elsewhere. Since the noise variables are coded by the low and high level at $\pm\sigma_{noise}$, we can obtain $\sigma_{z_i}^2 = 1$. $E_z(\mathbf{y})$ and $Var_z(\mathbf{y})$

are obtained by taking conditional expectation of y(**x,w,z**) with respect to the noise variables ***z*** and the random errors, δ and ε.

$$E_z(\mathbf{y}) = f_w(0) + f_s(\mathbf{x}, \mathbf{w}, 0) = \mathbf{x}'\boldsymbol{\beta} + \mathbf{x}'\mathbf{A}\mathbf{w} \tag{11}$$

$$\mathrm{Var}_z(\mathbf{y}) = \left[\boldsymbol{\Theta}'\mathbf{x} + \boldsymbol{\Xi}'\boldsymbol{\Lambda}'\mathbf{x}\right]' \sum_{\mathbf{z}} \left[\boldsymbol{\Theta}'\mathbf{x} + \boldsymbol{\Xi}'\boldsymbol{\Lambda}'\mathbf{x}\right] + \sigma_\delta^2 + \sigma_\varepsilon^2 \ , \tag{12}$$

since $\left.\frac{\partial f_w(\mathbf{z})}{\partial \mathbf{z}}\right|_{\mathbf{z}=\mathbf{0}} = \mathbf{0}$ and $\left.\frac{\partial f_s(\mathbf{x}, \mathbf{w}, \mathbf{z})}{\partial \mathbf{z}}\right|_{\mathbf{z}=\mathbf{0}} = \boldsymbol{\Theta}'\mathbf{x} + \boldsymbol{\Xi}'\boldsymbol{\Lambda}'\mathbf{x}$.

Borror et al. (2002) focused on the vector of partial derivatives of $f(\mathbf{x}, \mathbf{w}, \mathbf{z})$ with respect to the noise variables **z**. It is the slope of the response surface in the direction of the noise variables. Consequently, the response variance depends critically on the slope of the response model.

For the mean and variance model, the noise variables are treated as random effects for the purpose of deriving the mean and variance expressions. In the experimental environment, however, noise variables can be controlled, although they are uncontrollable in the normal operating environment. Therefore, they are commonly treated as fixed effects in robust parameter design and process robustness studies. Numerical optimization methods can be used to minimize the response variance while keeping the mean on a desired target. This provides the levels for the mixture and process variables that are robust to the noise variables in the operational setting.

Example 1: Soap Manufacturing

Recall the soap manufacturing process experiment from Goldfarb et al. (2003). In this example, there are three ingredients in the process, soap(x_1), co-surfactant(x_2), and filler(x_3). The ingredients have the following constraints;

$$0.20 \le x_1 \le 0.80$$
$$0.15 \le x_2 \le 0.50$$
$$0.05 \le x_3 \le 0.30$$
$$x_1 + x_2 + x_3 = 1 \quad .$$

Two process variables are also considered; the plodder temperature (z_1) and mixing time (w_1). The plodder temperature ranges from 15°C to 25°C while mixing time (w_1) ranges from 0.5 hour to 1 hour. The process variables are coded with low and high levels (-1, 1) in this example. The plodder temperature (z_1) is treated as a noise variable in Goldfarb et al. (2003). In this experiment, we also assume that temperature is hard-to-change. The mixing time (w_1) is a controllable variable that is easy-to-change. Since the plodder temperature (z_1) is the only hard-to-change factor, it is assigned to the WP. The mixture variables and the controllable variable are assigned to the SP. Response data were simulated using the original model, but now including two different sources of errors, whole plot error and subplot error. Usually, the whole plot error variance is larger than the subplot error variance as shown by Box and Jones (1992). Vining et al. (2005) studied a split-plot experiment and estimated the variances using pure error indicating larger whole plot error variance than subplot error variance ($d > 1$). We generated data with $d = 5.0$ to examine the effect of whole plot error variance on

the result of model fitting. The analysis with the split-plot structure shows that the suggested model is

$$\hat{y}(\mathbf{x},\mathbf{w},\mathbf{z}) = 464.37x_1 - 56.01x_2 + 613.03x_3 + 8.86x_1w_1 + 65.22x_2w_1 - 50.64x_3w_1 + 12.35x_2z_1 - 74.46x_3z_1 - 0.48x_1w_1z_1 - 4.26x_2w_1z_1 + 6.15x_3w_1z_1 .$$

Using Equations (11) and (12), the mean and variance response functions for the mixture-process variables with a noise variable (z_1) are estimated as

$$\widehat{E(Y)} = 464.37x_1 - 56.01x_2 + 613.03x_3 + 8.86x_1w_1 + 65.22x_2w_1 - 50.64x_3w_1$$

and

$$\widehat{\mathrm{Var}(Y)} = \hat{\sigma}^2_{z_1}(12.35x_2 - 74.46x_3 - 0.48x_1w_1 - 4.26x_2w_1 + 6.15x_3w_1)^2 + \hat{\sigma}^2_{\delta} + \hat{\sigma}^2_{\varepsilon},$$

where $\hat{\sigma}^2_{z_1}$ =1 since the noise variables are coded by the low and high level at $\pm\sigma_{noise}$, and the variance components, $\hat{\sigma}^2_{\delta}$ =4.44 and $\hat{\sigma}^2_{\varepsilon}$ =0.81, are estimated via the REML method.

In this process robust study, we need to minimize the value for the variance while concurrently maximizing the response for the mean. This dual optimization problem can be solved using the desirability function approach over the ranges of response for mean and variance model within the design. The suggested optimal levels are soap(x_1) = 0.8, co-surfactant(x_2) = 0.15, and filler(x_3) = 0.05 with mixing time (w_1) = 1 hour. The predicted mean output at this optimal level is 407.29 with a standard deviation of 3.26. When analyzed as a completely randomized design we find the same optimal setting for the design factors with the same predicted mean output and the same standard deviation because variances from whole-plot and sub-plot are added to the variance of total random

error. Also, we noticed the model coefficients using OLS are same as the values using GLS since the design satisfied the conditions for OLS-GLS equivalence developed by Vining et al. (2005).

Covariance Matrix of the Coefficients for the Model

The prediction variance for the mean model is suggested as the design evaluation criteria by Borror et al. (2002). This prediction variance includes the error in estimating the model parameters and the variability transmitted by the noise variables when the new value of y is observed. In the split-plot structure, the constant variance assumption is not valid and we consider generalized least squares to estimate the model coefficients $\boldsymbol{\beta}^*$. Then, the covariance matrix of the estimated coefficients $\boldsymbol{\beta}^*$, with the split-plot structure is given by

$$Var(\boldsymbol{\beta}^*) = \left(\mathbf{X}^{*'}\mathbf{V}^{-1}\mathbf{X}^*\right)^{-1} = \left(\sigma_\varepsilon^2 + \sigma_\delta^2\right)\left(\mathbf{X}^{*'}\mathbf{R}^{-1}\mathbf{X}^*\right)^{-1},$$

where the matrix $\mathbf{X}^*$ contains all columns representing the proposed model, the vector $\boldsymbol{\beta}^*$ contains the parameters in the fitted model, and $\mathbf{R}$ is the correlation matrix resulting from dividing the covariance matrix $\mathbf{V}$ by $\sigma_\varepsilon^2 + \sigma_\delta^2$. The correlation matrix $\mathbf{R}$ can be written using variance component ratio d, as

$$\mathbf{R} = \frac{\sigma_\varepsilon^2\left[d\mathbf{J} + \mathbf{I}\right]}{\sigma_\varepsilon^2 + \sigma_\delta^2} = \frac{\sigma_\varepsilon^2\left[d\mathbf{J} + \mathbf{I}\right]}{\sigma_\varepsilon^2\left(1+d\right)} = \frac{\left[d\mathbf{J} + \mathbf{I}\right]}{\left(1+d\right)}.$$

The variance-covariance matrix is important in estimating prediction variance for both the mean model and the slope model. Borror et al. (2002) defined the matrix $\mathbf{C}$, which is made of several sub-matrices for the variances of

each coefficient. Goldfarb et al. (2004c) extended this **C** matrix to include mixture components and process variables. For the split-plot structure, we modified this matrix including the correlation matrix given by

$$\mathbf{C} = \left[\mathbf{X}^{*\prime} \mathbf{R}^{-1} \mathbf{X}^{*} \right]^{-1} = \frac{1}{(1+d)} \left[\mathbf{X}^{*\prime} \left(\mathbf{I} - \frac{d}{1+dk} \mathbf{J} \right) \mathbf{X}^{*} \right]^{-1},$$

where the structure of **C** is exactly same as the **C** matrix defined by Goldfarb et al. (2004c) except that **C** includes the correlation matrix for the model. The order of the variables in the sub-matrices of **C** must be followed carefully. The ordering for the process and noise variables is shown in Figure 10.

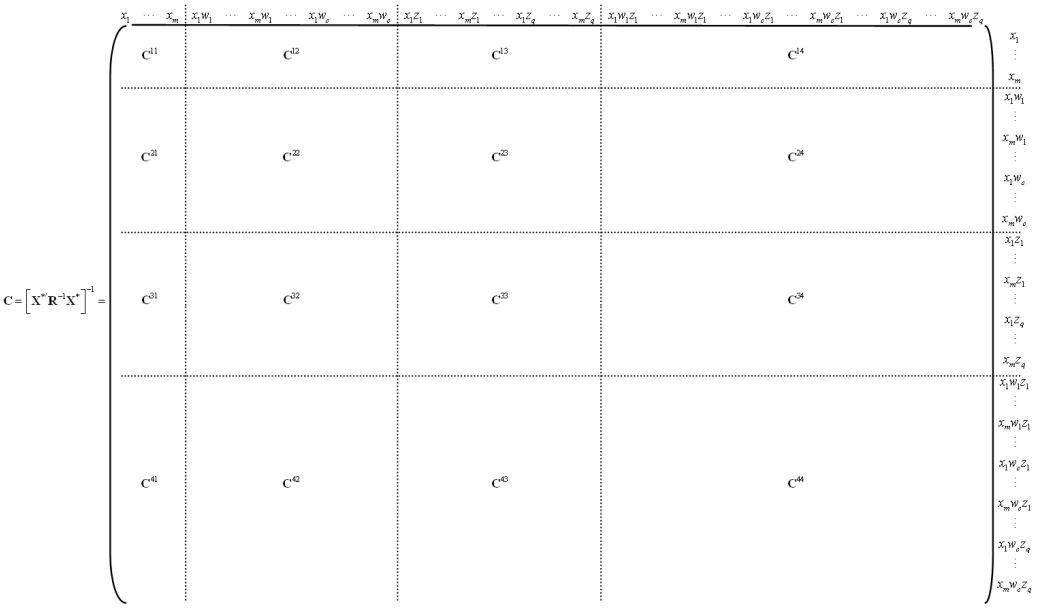

FIGURE 10. The Structure with Sub-Matrix of $\mathbf{C} = \left[\mathbf{X}^{*\prime} \mathbf{R}^{-1} \mathbf{X}^{*} \right]^{-1}$

Scaled Prediction Variance for the Mean Model

The prediction variance is an appropriate measure for evaluating a design with respect to the prediction capability. This prediction variance contains the variance in estimating the model parameters and the variance due to the noise variables when new observation, y, is estimated. The prediction variance of the fitted response model is given by

$$\begin{aligned}\underset{\mathbf{z},\varepsilon}{\mathrm{Var}}\left[\hat{y}(\mathbf{x},\mathbf{w},\mathbf{z})\right] &= \left(\sigma_\varepsilon^2+\sigma_\delta^2\right)\left[\mathbf{x}'\mathbf{C}^{11}\mathbf{x}+\left(\mathbf{xw}\right)'\mathbf{C}^{22}\left(\mathbf{xw}\right)\right]\\ &\quad+\sigma_z^2\left(\boldsymbol{\Theta}'\mathbf{x}+\boldsymbol{\Xi}'\boldsymbol{\Lambda}'\mathbf{x}\right)'\left(\boldsymbol{\Theta}'\mathbf{x}+\boldsymbol{\Xi}'\boldsymbol{\Lambda}'\mathbf{x}\right)\\ &= \left(\sigma_\varepsilon^2+\sigma_\delta^2\right)\left[\mathbf{x}'\mathbf{C}^{11}\mathbf{x}+\left(\mathbf{xw}\right)'\mathbf{C}^{22}\left(\mathbf{xw}\right)\right]\\ &\quad+\sigma_z^2\left(\mathbf{x}'\boldsymbol{\Theta}\boldsymbol{\Theta}'\mathbf{x}+2\mathbf{x}'\boldsymbol{\Lambda}\boldsymbol{\Xi}\boldsymbol{\Theta}'\mathbf{x}+\mathbf{x}'\boldsymbol{\Lambda}\boldsymbol{\Xi}\boldsymbol{\Xi}'\boldsymbol{\Lambda}'\mathbf{x}\right),\end{aligned} \tag{13}$$

where $\mathbf{xw}_{mc\times 1}=\left[x_1w_1 \quad \cdots \quad x_mw_1 \quad \cdots \quad x_1w_c \quad \cdots \quad x_mw_c\right]'$. Then the prediction variance can be written as

$$\begin{aligned}\underset{\mathbf{z},\varepsilon}{\mathrm{Var}}\left[\hat{y}(\mathbf{x},\mathbf{w},\mathbf{z})\right] &= \left(\sigma_\varepsilon^2+\sigma_\delta^2\right)\left[\mathbf{x}'\mathbf{C}^{11}\mathbf{x}+\left(\mathbf{xw}\right)'\mathbf{C}^{22}\left(\mathbf{xw}\right)\right]\\ &\quad+\sum_{i=1}^{m}\sum_{j=1}^{m}\sum_{p=1}^{n}x_ix_j\theta_{ip}\theta_{jp}\\ &\quad+\sum_{i=1}^{m}\sum_{j=1}^{m}\sum_{p=1}^{c}\sum_{r=1}^{n}x_ix_jw_p\theta_{ir}\lambda_{ipr}\\ &\quad+\sum_{i=1}^{m}\sum_{j=1}^{m}\sum_{p=1}^{c}\sum_{r=1}^{c}\sum_{s=1}^{n}x_ix_jw_pw_r\lambda_{ips}\lambda_{irs}\end{aligned}. \tag{14}$$

Borror et al. (2002) and Goldfarb et al. (2004c) suggested defining the element of the matrix of coefficients as multiples of the process standard deviation. In the split-plot design, we define these matrices as multiples of the subplot standard

deviation. (i.e., $\theta_{ij} = k_{ij}\sigma_\varepsilon$ and $\lambda_{ijk} = k_{ijk}\sigma_\varepsilon$). Equation (14) can be written in the form

$$\begin{aligned}\underset{\mathbf{z},\varepsilon}{\mathrm{Var}}\left[\hat{y}(\mathbf{x},\mathbf{w},\mathbf{z})\right] = \left(\sigma_\varepsilon^2 + \sigma_\delta^2\right)\left[\mathbf{x}'\mathbf{C}^{11}\mathbf{x} + \left(\mathbf{xw}\right)'\mathbf{C}^{22}\left(\mathbf{xw}\right)\right] \\ +\sigma_\varepsilon^2\sum_{i=1}^{m}\sum_{j=1}^{m}\sum_{p=1}^{n}x_i x_j k_{ip}k_{jp} \\ +\sigma_\varepsilon^2\sum_{i=1}^{m}\sum_{j=1}^{m}\sum_{p=1}^{c}\sum_{r=1}^{n}x_i x_j w_p k_{ir}k_{ipr} \\ +\sigma_\varepsilon^2\sum_{i=1}^{m}\sum_{j=1}^{m}\sum_{p=1}^{c}\sum_{r=1}^{c}\sum_{s=1}^{n}x_i x_j w_p w_r k_{ips}k_{irs}\end{aligned} . \quad (15)$$

If we assume that the noise variables equally influence the response, then $k_{ij} = k_{2a}$ and $k_{ijk} = k_{2b}$ as denoted by Goldfarb et al. (2004c). The constant k_{2a} and k_{2b} represent the contribution of mixture-noise interactions and the mixture-process-noise interactions, respectively. The resulting prediction variance equation is

$$\begin{aligned}\underset{\mathbf{z},\varepsilon}{\mathrm{Var}}\left[\hat{y}(\mathbf{x},\mathbf{w},\mathbf{z})\right] = \left(\sigma_\varepsilon^2 + \sigma_\delta^2\right)\left[\mathbf{x}'\mathbf{C}^{11}\mathbf{x} + \left(\mathbf{xw}\right)'\mathbf{C}^{22}\left(\mathbf{xw}\right)\right] \\ +\sigma_\varepsilon^2\left(nk_{2a}^2\mathbf{x}'\mathbf{1}_m\mathbf{1}_m'\mathbf{x} + 2nk_{2a}k_{2b}\mathbf{x}'\mathbf{1}_m\mathbf{1}_n'\boldsymbol{\Xi}'\mathbf{1}_{cn}\mathbf{1}_m'\mathbf{x} + nk_{2b}^2\mathbf{x}'\mathbf{1}_m\mathbf{1}_{cn}'\boldsymbol{\Xi}\boldsymbol{\Xi}'\mathbf{1}_{cn}\mathbf{1}_m'\mathbf{x}\right)\end{aligned} , \quad (16)$$

where $\mathbf{1}_i$ (i=m, n, and cn) is the vector of 1s with length i.

In the design comparison, it is convenient to scale the prediction variance. The division by $\left(\sigma_\varepsilon^2 + \sigma_\delta^2\right)$ provides a scale-free measure for design comparison and multiplication by N penalizes lager designs. Using the variance component ratio $d = \sigma_\delta^2/\sigma_\varepsilon^2$, the scaled prediction variance can be written as

$$\begin{aligned}\frac{N\underset{\mathbf{z},\varepsilon}{\mathrm{Var}}\left[\hat{y}(\mathbf{x},\mathbf{w},\mathbf{z})\right]}{\left(\sigma_\varepsilon^2 + \sigma_\delta^2\right)} = N\left[\mathbf{x}'\mathbf{C}^{11}\mathbf{x} + \left(\mathbf{xw}\right)'\mathbf{C}^{22}\left(\mathbf{xw}\right)\right] \\ +\frac{Nn}{1+d}\left(k_{2a}^2\mathbf{x}'\mathbf{1}_m\mathbf{1}_m'\mathbf{x} + 2k_{2a}k_{2b}\mathbf{x}'\mathbf{1}_m\mathbf{1}_n'\boldsymbol{\Xi}'\mathbf{1}_{cn}\mathbf{1}_m'\mathbf{x} + k_{2b}^2\mathbf{x}'\mathbf{1}_m\mathbf{1}_{cn}'\boldsymbol{\Xi}\boldsymbol{\Xi}'\mathbf{1}_{cn}\mathbf{1}_m'\mathbf{x}\right)\end{aligned} . \quad (17)$$

The scaled prediction variance is a function of a proposed model, design matrix, and the contribution of interactions containing noise variables. Furthermore, the prediction variance depends on the variance component ratio, *d*, in the split-plot design structure.

Variance for the Slope

Borror et al. (2002) note that the vector $[\,\boldsymbol{\Theta}'\mathbf{x} + \boldsymbol{\Xi}'\boldsymbol{\Lambda}'\mathbf{x}\,]$ is a vector of the partial derivatives of the response surface with respect to the noise variables and represents the slope of the response surface in the direction of the noise variables. In a precision of estimation associated with the variance model, the variance of slope provides a direct measurement with same unit as the variance for the mean model. Murty and Studden (1972), Myers and Lahoda (1975), and Mukurjee and Huda (1985) give more detailed results focusing on the importance of the slope of response surface.

A general form for the variance of the slope in direction z_i (i = 1, 2, … , n) is developed by Goldfarb et al. (2004c). We rewrite the variance models using matrix notation. This matrix notation is simple and easy to be used in the computer program coding. The matrix form for the variance of the slope in each noise variable direction is as follows:

$$\mathrm{Var}_{z_i}(\text{slope}) = \left(\sigma_\varepsilon^2 + \sigma_\delta^2\right)\left\{\mathbf{x}'\mathbf{C}_i^{33}\mathbf{x} + (\mathbf{x}\otimes\mathbf{w})'\mathbf{C}_i^{44}(\mathbf{x}\otimes\mathbf{w}) + 2\mathbf{x}'\mathbf{C}_i^{34}(\mathbf{x}\otimes\mathbf{w})\right\},$$

where (i = 1, 2, … , n),

$$\mathbf{C}_i^{33} = \begin{bmatrix} C^{33}_{m(i-1)+1,m(i-1)+1} & \cdots & C^{33}_{m(i-1)+1,mi} \\ \vdots & \ddots & \vdots \\ C^{33}_{mi,m(i-1)+1} & \cdots & C^{33}_{mi,mi} \end{bmatrix}, \mathbf{C}_i^{34} = \begin{bmatrix} C^{34}_{m(i-1)+1,mc(i-1)+1} & \cdots & C^{34}_{m(i-1)+1,mci} \\ \vdots & \ddots & \vdots \\ C^{34}_{mi,mc(i-1)+1} & \cdots & C^{34}_{mi,mci} \end{bmatrix},$$

$$\text{and } \mathbf{C}_i^{44} = \begin{bmatrix} C^{44}_{mc(i-1)+1,mc(i-1)+1} & \cdots & C^{44}_{mc(i-1)+1,mci} \\ \vdots & \ddots & \vdots \\ C^{44}_{mci,mc(i-1)+1} & \cdots & C^{44}_{mci,mci} \end{bmatrix}.$$

As mentioned by Borror et al. (2002), the single subscript on the sub-matrix **C** is the noise variable for which the slope variance is computed. In design comparison for split-plot design, it is more convenient to make the quantity scale-free and penalize large design by dividing by $\left(\sigma_\varepsilon^2 + \sigma_\delta^2\right)$ and multiplying by *N*. Then, the scaled variance for the slope is given by

$$\frac{N\text{Var}_{z_i}(\text{slope})}{\left(\sigma_\varepsilon^2 + \sigma_\delta^2\right)} = N\left\{\mathbf{x}'\mathbf{C}_i^{33}\mathbf{x} + (\mathbf{x}\otimes\mathbf{w})'\mathbf{C}_i^{44}(\mathbf{x}\otimes\mathbf{w}) + 2\mathbf{x}'\mathbf{C}_i^{34}(\mathbf{x}\otimes\mathbf{w})\right\}.$$

Design Evaluation with Noise Variables Considering the Split-Plot Structure

As shown in Equations (13) to (17), the prediction variance for the mean model can be separated into the variance in estimating the mean model parameters and the variance due to the noise variables when the new observation, y, is observed. The variance associated with estimating the model parameters is a function of the proposed model and the design. However, the variance arising from the noise variables is a function of a proposed model and the coefficients of parameters containing noise variables. In other words, the design matrix does not affect the variance part from the noise variables. Therefore, the noise variables do not affect the design comparison with the mean model. Then, a simplified scaled

prediction variance, which only contains the variance in estimating the model parameters, is an alternative evaluation criterion for design comparison. The simplified prediction variance is given by

$$\text{Simplified SPV} = N\left[\mathbf{x}'\mathbf{C}^{11}\mathbf{x} + \left(\mathbf{x}\otimes\mathbf{w}\right)' \mathbf{C}^{22}\left(\mathbf{x}\otimes\mathbf{w}\right)\right].$$

This simplified SPV is not the same unit of prediction variance for the model only including mixture components and controllable process variables, but the value including noise variables in the design matrix **X**. Since it is free from the levels of the interaction including noise variables, we can reduce the terms for the contribution of mixture-noise interactions and the mixture-process-noise interactions, k_{2a} and k_{2b}. However, this simplified scaled prediction variance does not reflect the effect from noise variables such as transmitted variance due to the noise factors. When we consider variance from noise variables, the variance for the slope is a good measure, but it only provides the variability for the noise variable. Therefore, for combined comparison considering both the variance in estimating the mean model parameters and the variance due to the noise variables, we suggest the modified criterion of total prediction variance (TPV) given by

$$\begin{aligned}\text{TPV} = {} & \mathbf{x}'\mathbf{C}^{11}\mathbf{x} + \left(\mathbf{x}\otimes\mathbf{w}\right)' \mathbf{C}^{22}\left(\mathbf{x}\otimes\mathbf{w}\right) \\ & + \sum_{i=1}^{n} \rho_i \left[\mathbf{x}'\mathbf{C}_i^{33}\mathbf{x} + (\mathbf{x}\otimes\mathbf{w})'\mathbf{C}_i^{44}(\mathbf{x}\otimes\mathbf{w}) + 2\mathbf{x}'\mathbf{C}_i^{34}(\mathbf{x}\otimes\mathbf{w})\right]'\end{aligned}$$

where ρ_i is 0 if a noise variable is not considered or 1 if a noise variable is considered in comparing variance in estimating parameters. Another criterion for comparing designs is the ratio of the variance in estimating parameters and

variance for slope of noise variables. Let τ equal the variance of the slope divided by the variance in estimating parameters. The form of ratio is

$$\tau = \frac{\sum_{i=1}^{n} \rho_i \left[\mathbf{x}'\mathbf{C}_i^{33}\mathbf{x} + (\mathbf{x} \otimes \mathbf{w})'\mathbf{C}_i^{44}(\mathbf{x} \otimes \mathbf{w}) + 2\mathbf{x}'\mathbf{C}_i^{34}(\mathbf{x} \otimes \mathbf{w}) \right]}{\mathbf{x}'\mathbf{C}^{11}\mathbf{x} + (\mathbf{x} \otimes \mathbf{w})' \mathbf{C}^{22} (\mathbf{x} \otimes \mathbf{w})}. \quad (18)$$

This ratio indicates the magnitude of the variance from the noise variables relating to the variance from the mean model. In robust parameter design, it is usually preferred to have small values of this ratio because the goal of robust parameter design is to reduce the variation from the noise factors. We can graphically evaluate both criteria with the FDS plot.

Example 2: Design Comparison for Soap Manufacturing

Consider the soap manufacturing used in Example 1. Various designs could be used to estimate the model parameters. Goldfarb et al. (2004c) generate the three experimental designs shown in Table 4 for design evaluation.

TABLE 4. Three Experimental Designs for the Soap Manufacturing Experiment

Design Code	Description
A	A 20 run design using 5 run *D*-optimal design for mixture components generated by Design-Expert 6.0 at each design point of a 2^2 factorial design for the process and noise variables
B	A 20 run *D*-optimal design with 8 lack-of-fit points generated by Design-Expert 6.0
C	A 20 run *D*-optimal design with 4 lack-of-fit points and 4 replicates generated by Design-Expert 6.0

These were intended as completely randomized designs. We will evaluate them as if they were conducted as split-plots. The FDS plots over varying levels of the variance component ratio *d* for the total prediction variance and prediction variance ratio with these three designs are shown in Figure 11. The FDS plots for the total prediction variance show that when there is no WP error (variance component ratio d =0), design A has relatively superior prediction properties for the total prediction variance, as shown by the consistently lower and flatter slope when compared to other designs. As *d* increases, however, design B and C are preferred because they have lower total prediction variance for the entire design region. In the analysis of the total prediction variance, the FDS plots for design B and C do not show any distinguishable difference while they are noticeably different in the prediction variance ratio properties. Therefore we recommend using both graphs to compare design. For example, if the experimenters are interested in minimizing total variability for prediction in estimating parameters and transmitted from noise variables, total prediction variance properties should be considered for comparing designs. The FDS plots for prediction variance ratio are good alternatives when experimenters are interested in reducing variation transmitted from the noise variables over the variance in estimating parameters. For the prediction variance ratio, design A has the value unity for the entire design space for all levels of variance component ratio. The value of unity for this ratio means that the variance in estimating parameters and the variance transmitted from the noise variables are exactly the same, and not influenced by the levels of *d*. It is a very special condition that the ratio equals one.

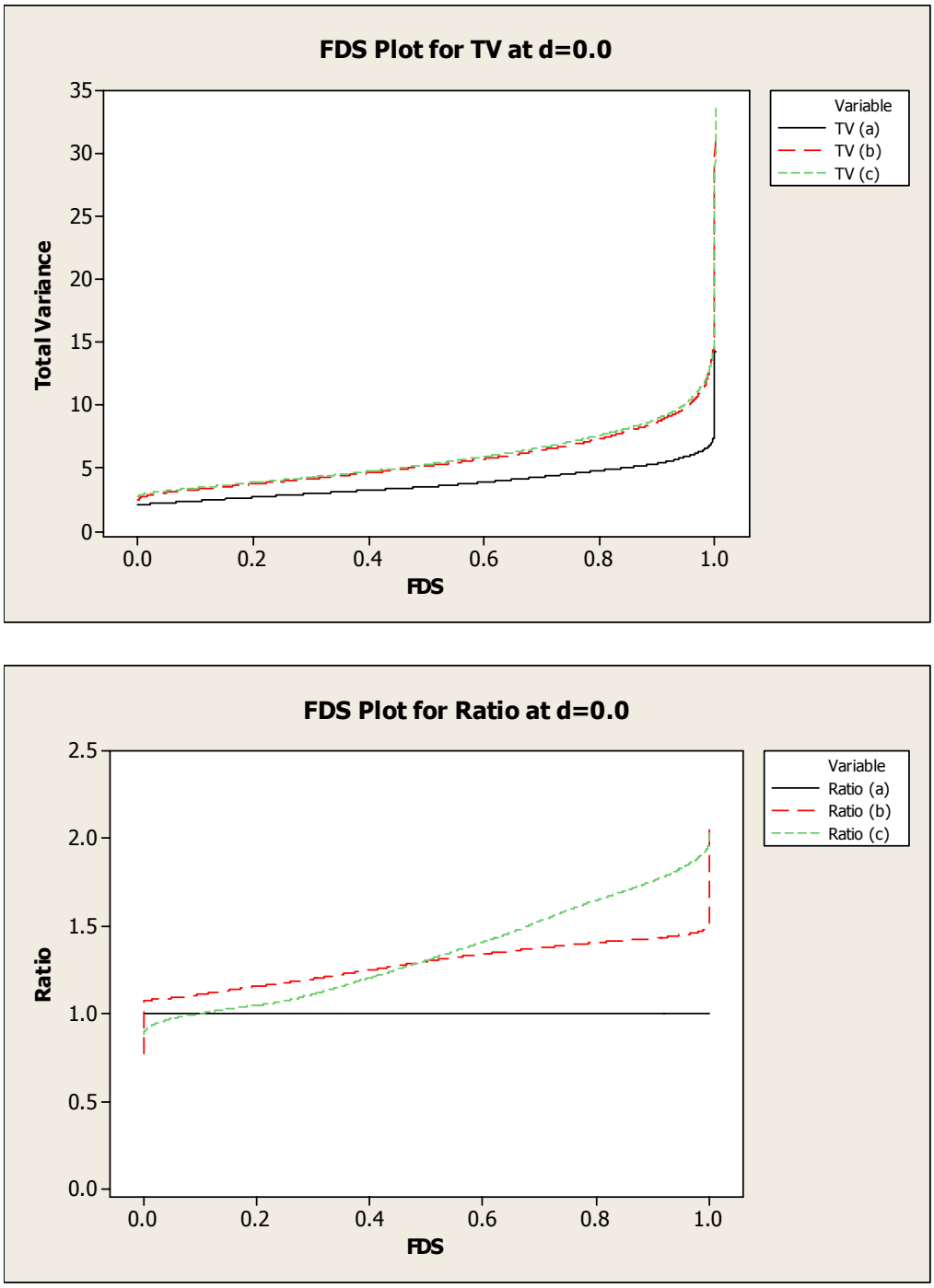

FIGURE 11. FDS Plot of Total Prediction Variance and Ratio for Example 2

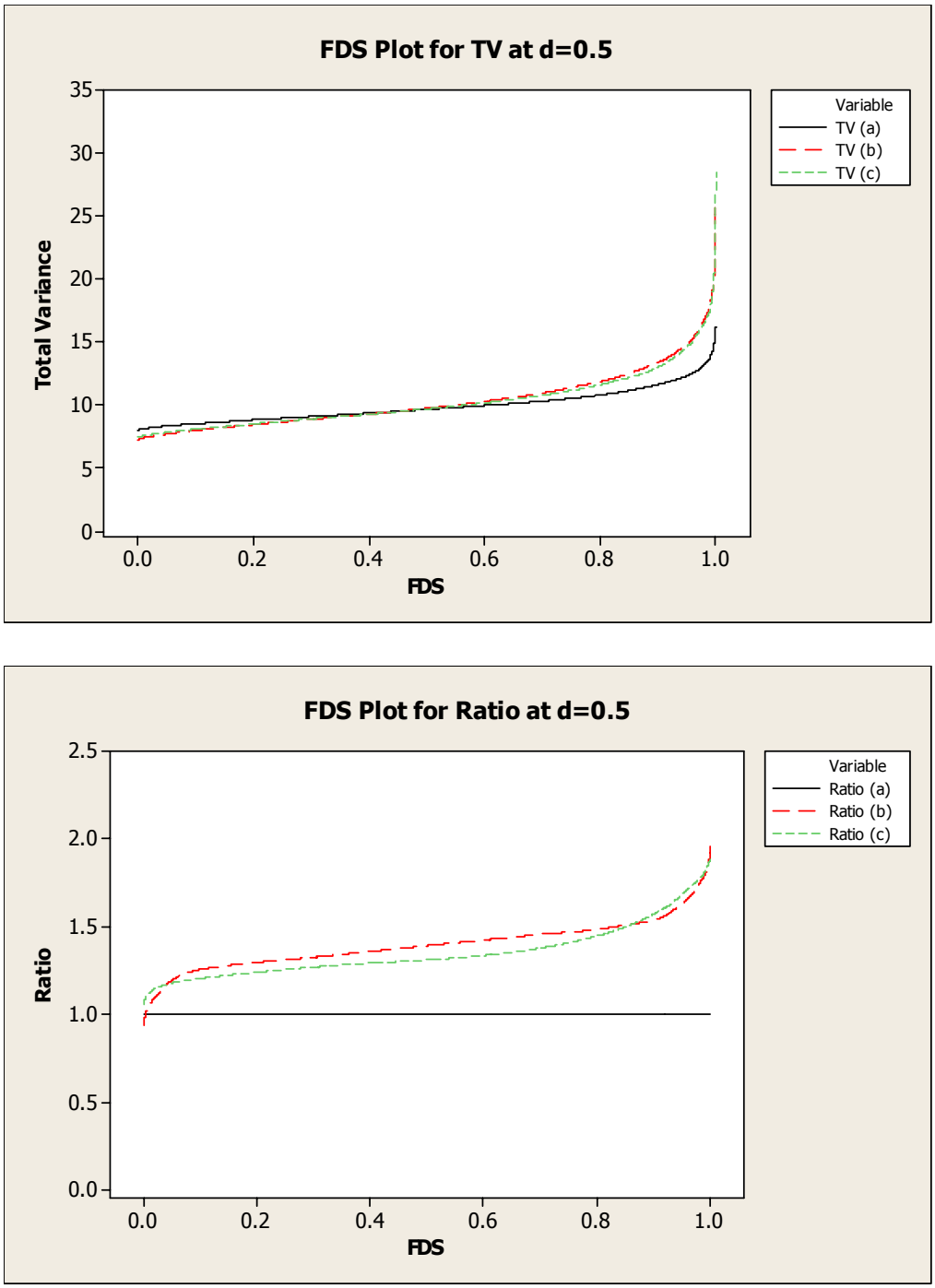

FIGURE 11. FDS Plot of Total Prediction Variance and Ratio for Example 2

(continued)

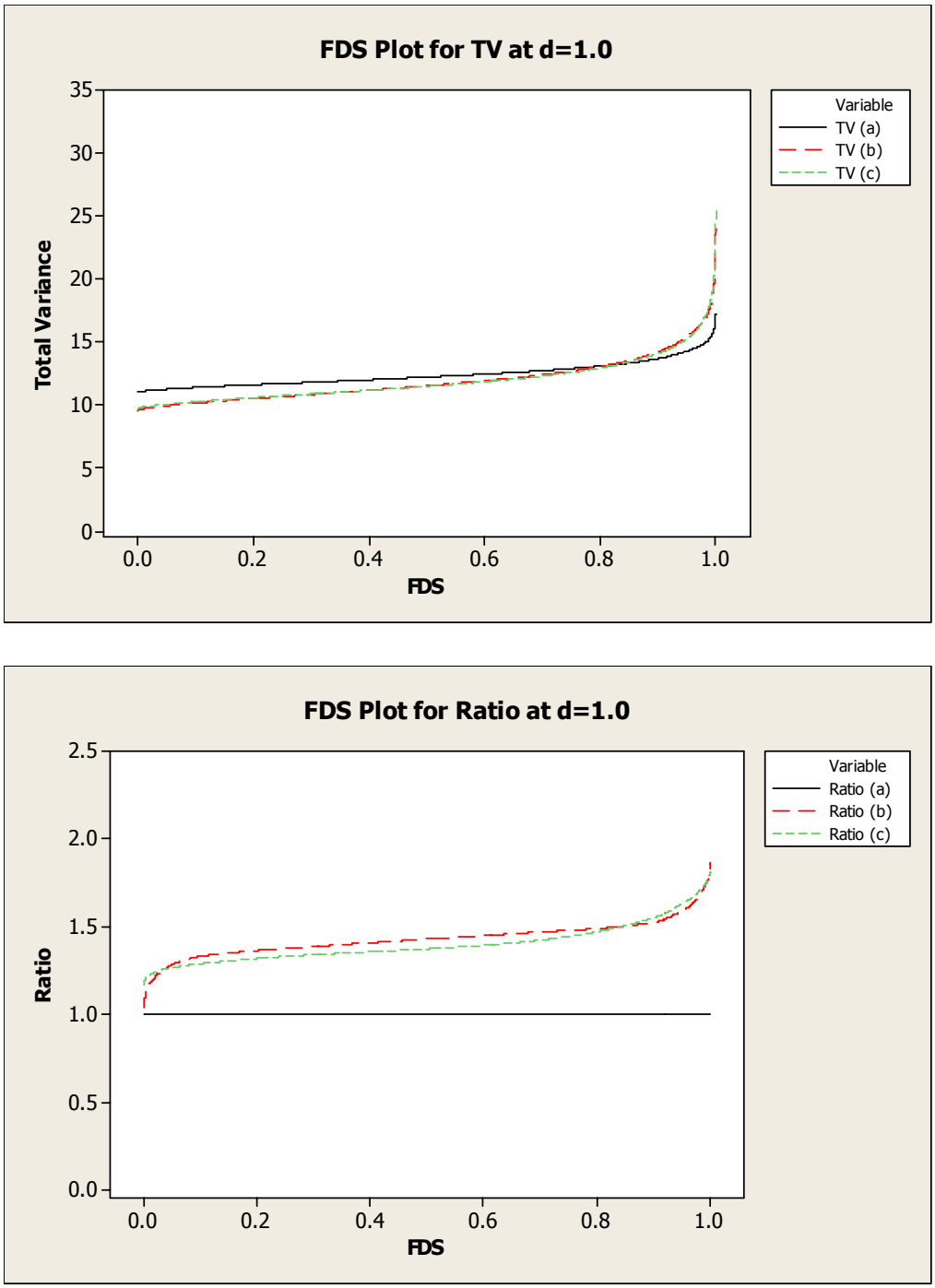

FIGURE 11. FDS Plot of Total Prediction Variance and Ratio for Example 2

(continued)

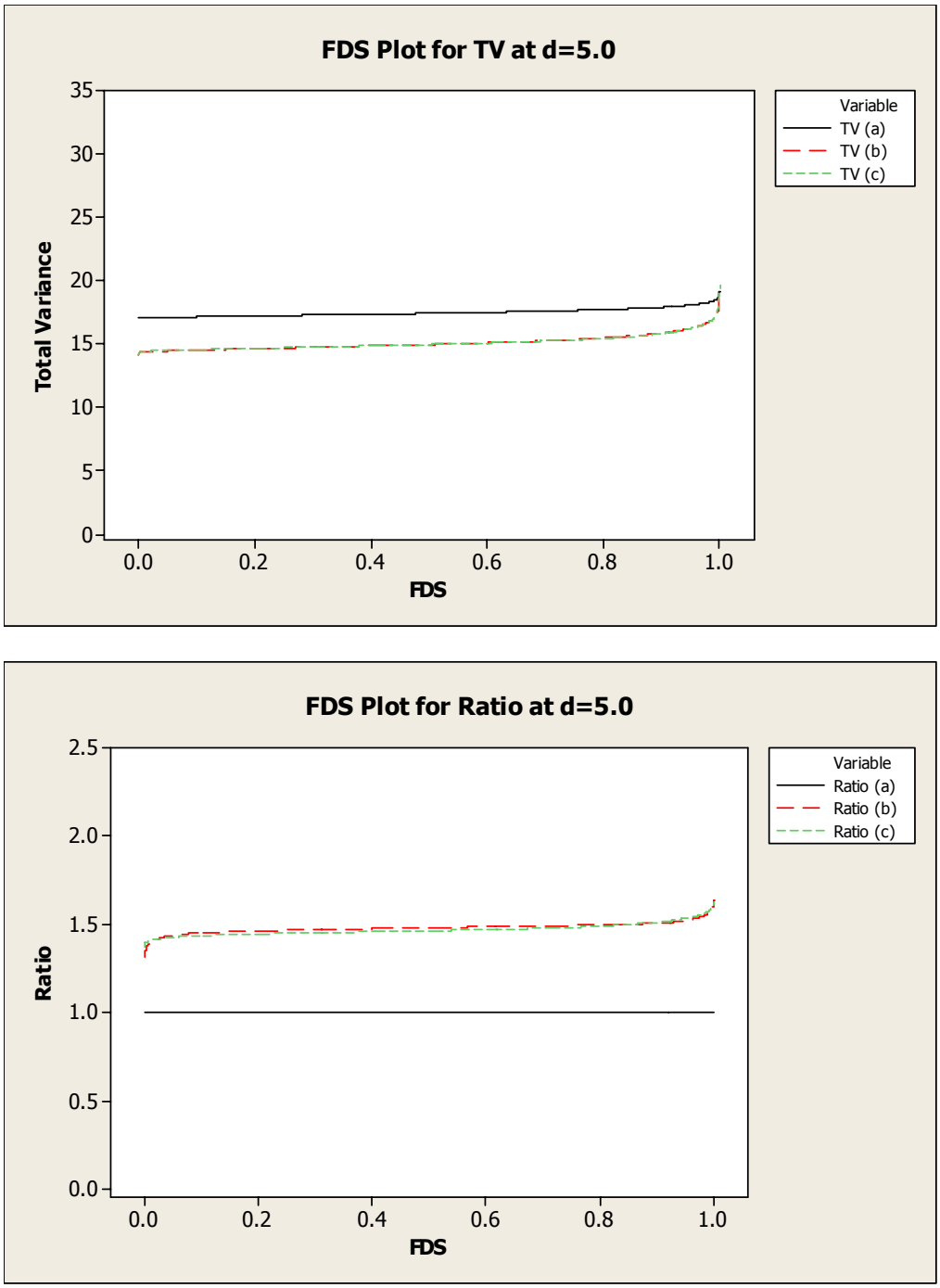

FIGURE 11. FDS Plot of Total Prediction Variance and Ratio for Example 2

(continued)

From Equation (18), we notice that if the covariance matrices for mixture terms and mixture-noise variable interaction terms at each noise variable direction are the same, the covariance matrices for mixture-process interaction terms and mixture-process-noise variable interaction terms at each noise variables direction are the same, and the covariance between mixture-process variables and mixture-variation transmitted from each noise variable are the same. In other words, if the proposed model for the mean model is the same as the slope of the response surface in the direction of the noise variables and the controllable variables are orthogonal in each SP, then the prediction variance ratio equals the number of noise variables in the proposed model.

G-Optimal Design using Genetic Algorithms

The most well known optimality criterion is *D*-optimality, which is based on the concept that the experimental design should be selected to maximize the determinant of the moment matrix. Design criteria which focus on the prediction variance include *G*-optimality, *V*-optimality, *I*-optimality. *G*-optimality focuses on the design which provides the *minimum* value from the *maximum* prediction variance $v(\mathbf{x})$ in the design space, given by

$$\underset{\zeta}{\text{Min}}\left[\underset{\mathbf{x}\in R}{\text{Max}}\, v(x)\right].$$

If the variance is scaled by N, 100% G-efficiency is equal to the number of parameters in the model. Another prediction variance-oriented optimality is *V*-optimality which considers the average prediction variance over the specific set of

points of interest in the design space. Another important design optimality criterion is *I*-optimality, for which prediction variance $v(\mathbf{x})$ is averaged over the design region of interest *R*, given by

$$\underset{\zeta}{\text{Min}} \frac{1}{K} \int_R v(\mathbf{x}) d\mathbf{x}$$

where *K* is the volume of design region *R*.

To generate the optimal design, we use a genetic algorithm (GA) combined with a desirability function, as suggest by Heredia-Langner et al. (2004). It considers the *G*-optimality criteria to minimize the maximum SPV as an individual desirability function given by

$$d_i = \begin{cases} 1, & SPV_i < L \\ \left(\dfrac{U - SPV_i}{U - L} \right)^t, & L < SPV_i < U \\ 0, & SPV_i > U \end{cases},$$

where SPV_i is the maximum SPV for the mean model and slope model, L and U are the minimum and maximum value for SPV_i obtained from *D* and *I*-optimal designs generated by JMP 7.0, *t* is a weight that controls the shape of the desirability function. Using this individual desirability functions, an overall desirability function was suggested, given by

$$D = \left(\prod_{i=1}^{m} d_i \right)^{1/m} = \left(d_1 \cdot d_2 \cdots d_m \right)^{1/m},$$

where d_i is the individual desirability function. If we consider SPV for the mean and slope with two noise variables, then *m*=3. We use a GA written in JMP 7.0

script for this desirability function to produce a new design for the robust design problem considering the split-plot structure.

Example 3: *G*-optimal design for Soap Manufacturing

Recalling the soap manufacturing from example 1, Goldfarb et al. (2005) considered a model with quadratic mixture terms, a quadratic mixing time effect, and a linear effect of plodder temperature, shown by

$$\begin{aligned} y(\mathbf{x},\mathbf{w},\mathbf{z}) = & \sum_i \beta_i x_i + \sum_{i<j}\sum \beta_{ij} x_i x_j \\ & + \sum_i \sum_p \alpha_{ip} x_i w_p^2 + \sum_{i<j}\sum_p \alpha_{ijp} x_i x_j w_p^2 \\ & + \sum_i \sum_t \theta_{it} x_i z_t + \sum_{i<j}\sum_t \theta_{ijt} x_i x_j z_t \\ & + \sum_i \sum_p \sum_t \lambda_{ipt} x_i w_p^2 z_t + \sum_{i<j}\sum_p \sum_t \lambda_{ijpt} x_i x_j w_p^2 z_t + \delta + \varepsilon \end{aligned},$$

where q=3, c=1, and n=1, using the same notation previously introduced for mixture variables, process variables and noise variables, respectively. This is slightly different from the original soap manufacturing example in that this model uses quadratic mixture terms and a quadratic process variable effect. Goldfarb et al. (2005) shows that the *G*-optimal design with N=30 has the largest improvement compared to the *D*-optimal design constructed from Design-Expert. We used the optimal design provided by Design -Expert, and the *I*-optimal design and the *D*-optimal design from JMP 7.0 as baseline designs to compare to the new *G*-optimal design. These designs are shown in Table 5 to 9. Since Goldfarb et al. (2005) did not consider the split-plot structure, these designs are only compared when the variance component ratio d=0.

TABLE 5. GA Mean Model Optimized 30-Run Design by Goldfarb et al. (2005)

X1	X2	X3	W1	Z1
0.2	0.5	0.3	-1	-1
0.2	0.5	0.3	-1	1
0.2	0.5	0.3	0	-1
0.2	0.5	0.3	0	1
0.33	0.5	0.18	-1	-1
0.38	0.33	0.3	-1	1
0.38	0.33	0.3	0	1
0.45	0.5	0.05	-1	-1
0.45	0.5	0.05	-1	1
0.45	0.5	0.05	0	-1
0.45	0.5	0.05	0	1
0.5	0.33	0.18	-1	-1
0.5	0.33	0.18	-1	1
0.5	0.33	0.18	0	-1
0.5	0.33	0.18	0	1
0.55	0.15	0.3	-1	-1
0.55	0.15	0.3	-1	1
0.55	0.15	0.3	0	-1
0.55	0.15	0.3	0	1
0.63	0.33	0.05	-1	-1
0.68	0.15	0.18	-1	1
0.68	0.15	0.18	0	-1
0.68	0.15	0.18	0	1
0.8	0.15	0.05	-1	-1
0.8	0.15	0.05	-1	1
0.8	0.15	0.05	0	-1
0.8	0.15	0.05	0	1
0.63	0.33	0.05	0	1
0.68	0.15	0.18	0	-1
0.68	0.15	0.18	0	1

TABLE 6. GA Slope Model Optimized 30-Run Design by Goldfarb et al. (2005)

X1	X2	X3	W1	Z1
0.2	0.5	0.3	-1	-1
0.2	0.5	0.3	-1	1
0.2	0.5	0.3	0	-1
0.2	0.5	0.3	0	1
0.33	0.5	0.18	-1	-1
0.38	0.33	0.3	-1	1
0.38	0.33	0.3	0	1
0.45	0.5	0.05	-1	-1
0.45	0.5	0.05	-1	1
0.45	0.5	0.05	0	-1
0.45	0.5	0.05	0	1
0.5	0.33	0.18	-1	-1
0.5	0.33	0.18	-1	1
0.5	0.33	0.18	0	-1
0.5	0.33	0.18	0	1
0.55	0.15	0.3	-1	-1
0.55	0.15	0.3	-1	1
0.55	0.15	0.3	0	-1
0.55	0.15	0.3	0	1
0.63	0.33	0.05	-1	-1
0.68	0.15	0.18	-1	1
0.68	0.15	0.18	0	-1
0.68	0.15	0.18	0	1
0.8	0.15	0.05	-1	-1
0.8	0.15	0.05	-1	1
0.8	0.15	0.05	0	-1
0.8	0.15	0.05	0	1
0.63	0.33	0.05	0	1
0.68	0.15	0.18	0	-1
0.68	0.15	0.18	0	1

TABLE 7. *D*-optimal Split-Plot Design generated by JMP 7.0

WP	X1	X2	X3	W1	Z1
1	0.45	0.5	0.05	-1	-1
1	0.325	0.5	0.175	-1	-1
1	0.8	0.15	0.05	-1	-1
1	0.62181	0.32819	0.05	0	-1
1	0.2	0.5	0.3	0	-1
1	0.55	0.15	0.3	0	-1
1	0.8	0.15	0.05	0	-1
1	0.2	0.5	0.3	-1	-1
1	0.625	0.325	0.05	-1	-1
1	0.55	0.15	0.3	-1	-1
1	0.535	0.29	0.175	-1	-1
1	0.45	0.5	0.05	0	-1
1	0.525	0.3	0.175	0	-1
1	0.375	0.325	0.3	-1	-1
1	0.325	0.5	0.175	0	-1
2	0.45	0.5	0.05	-1	1
2	0.625	0.325	0.05	-1	1
2	0.525	0.3	0.175	-1	1
2	0.55	0.15	0.3	0	1
2	0.2	0.5	0.3	0	1
2	0.325	0.5	0.175	-1	1
2	0.68231	0.15	0.16769	0	1
2	0.325	0.5	0.175	0	1
2	0.2	0.5	0.3	-1	1
2	0.55	0.15	0.3	-1	1
2	0.8	0.15	0.05	0	1
2	0.625	0.325	0.05	0	1
2	0.8	0.15	0.05	-1	1
2	0.45	0.5	0.05	0	1
2	0.475	0.325	0.2	0	1

TABLE 8. *I*-optimal Split-Plot Design generated by JMP 7.0

WP	X1	X2	X3	W1	Z1
1	0.325	0.5	0.175	-1	1
1	0.675	0.15	0.175	-1	1
1	0.525	0.3	0.175	0	1
1	0.525	0.325	0.15	-1	1
1	0.45	0.5	0.05	0	1
1	0.8	0.15	0.05	-1	1
1	0.55	0.15	0.3	-1	1
1	0.2	0.5	0.3	-1	1
1	0.325	0.5	0.175	0	1
1	0.2	0.5	0.3	0	1
1	0.8	0.15	0.05	0	1
1	0.607717	0.342283	0.05	0	1
1	0.55	0.15	0.3	0	1
1	0.375	0.325	0.3	-1	1
1	0.45	0.5	0.05	-1	1
2	0.675	0.15	0.175	0	-1
2	0.55	0.15	0.3	-1	-1
2	0.8	0.15	0.05	-1	-1
2	0.382644	0.317356	0.3	-1	-1
2	0.675	0.15	0.175	-1	-1
2	0.461296	0.363704	0.175	-1	-1
2	0.2	0.5	0.3	-1	-1
2	0.55	0.15	0.3	0	-1
2	0.2	0.5	0.3	0	-1
2	0.45	0.5	0.05	-1	-1
2	0.625	0.325	0.05	-1	-1
2	0.633452	0.316548	0.05	0	-1
2	0.45	0.5	0.05	0	-1
2	0.8	0.15	0.05	0	-1
2	0.475	0.35	0.175	0	-1

TABLE 9. *G*-optimal Split-Plot Design using GA (New Generated, *d*=0.0)

WP	X1	X2	X3	W1	Z1
1	0.4481	0.4994	0.0525	-0.9997	-1
1	0.3471	0.4763	0.1766	-1	-1
1	0.7797	0.1547	0.0656	-1	-1
1	0.6281	0.3219	0.05	0.0003	-1
1	0.2113	0.4887	0.3	0	-1
1	0.55	0.15	0.3	0	-1
1	0.7844	0.15	0.0656	0.0001	-1
1	0.2178	0.4991	0.2831	-1	-1
1	0.6282	0.3195	0.0523	-1	-1
1	0.5428	0.1596	0.2976	-1	-1
1	0.6001	0.2229	0.177	-1	-1
1	0.4504	0.4995	0.0501	0.0003	-1
1	0.5042	0.2792	0.2166	-0.0002	-1
1	0.3857	0.3263	0.288	-1	-1
1	0.3119	0.4988	0.1893	0	-1
2	0.4556	0.4943	0.0501	-1	1
2	0.6394	0.3059	0.0547	-1	1
2	0.5223	0.2446	0.2331	-1	1
2	0.55	0.15	0.3	0.0001	1
2	0.2111	0.4889	0.3	0	1
2	0.3141	0.499	0.1869	-1	1
2	0.6772	0.1504	0.1724	0	1
2	0.3075	0.5	0.1925	-0.0002	1
2	0.2268	0.4732	0.3	-0.9556	1
2	0.5591	0.15	0.2909	-0.999	1
2	0.7925	0.1512	0.0563	0.06	1
2	0.6236	0.3091	0.0673	0	1
2	0.7776	0.1517	0.0707	-1	1
2	0.4499	0.5	0.0501	0	1
2	0.4287	0.3073	0.264	0	1

To compare designs with restricted randomization constraints, we used different variance component ratios and compare our new design with the designs generated from JMP 7.0. In Table 10, we observe that the new *G*-optimal designs

significantly reduced the SPV values for the mean and slope model. In the dual optimization method for generating the optimal design we used the same weights on the mean and slope model. We can use different weights on the mean or slope model.

TABLE 10. Max. SPV for Mean and Slope Model in Example 3 (d=0)

Design	Criteria	Max. SPV for Mean	Max. SPV for Slope
Design-Expert	D-optimal	55.1831	20.6639
JMP 7.0	D-optimal	53.7757	18.2939
	I-optimal	52.2129	20.4888
Goldfarb et al. (2005)	G-optimal for Mean	55.2586	20.5250
	G-optimal for Slope	60.7178	21.7188
New	G-optimal (d=0.0)	42.9288	14.9036
	G-optimal (d=0.5)	42.6265	14.9725
	G-optimal (d=1.0)	42.8931	14.6936

To compare our new design with completely randomized designs by Goldfarb et al. (2005), we consider the variance component ration d=0 for other designs within a split-plot structure. For different component ratios, our new G-optimal design also reduced the SPV values. Table 11 and Table 12 show the maximum SPV for the mean and the slope model with d=0.5 and 1, respectively. We noticed that the maximum SPV values for the mean model decreases as d

increases. As the variance component ratio d increases, the whole-plot error due to the noise variables is increased and sub-plot error is decreased. We can get more precise parameter estimation with this decreased sub-plot error when the experiments are analyzed with the split-plot structure. As a result of precise parameter estimation, the prediction variance of the model decreases as d increases.

TABLE 11. Max. SPV for Mean and Slope Model for the Split-Plot (d=0.5)

Design	Criteria	Max. SPV for Mean	Max. SPV for Slope
JMP 7.0	*D*-optimal	40.8505	17.8816
	I-optimal	39.8086	19.0689
New	*G*-optimal (d=0.0)	33.7969	15.3380
	G-optimal (d=0.5)	33.3464	15.5785
	G-optimal (d=1.0)	32.5043	14.9047

TABLE 12. Max. SPV for Mean and Slope Model for the Split-Plot (d=1.0)

Design	Criteria	Max. SPV for Mean	Max. SPV for Slope
JMP 7.0	*D*-optimal	34.3879	16.6456
	I-optimal	33.6064	17.5928
New	*G*-optimal (d=0.0)	28.3876	15.0041
	G-optimal (d=0.5)	29.3889	15.3117
	G-optimal (d=1.0)	27.9869	14.8471

Table 10, 11, and 12 only show the values of the maximum SPV. This may not be enough information about the prediction capability of the designs. Rodriguez et al. (2010) suggested the variance ratio FDS (VRFDS) plot to compare all design of interest with respect to a reference design. This variance ratio FDS is

$$VR_i = \frac{SPV_i(\mathbf{x})}{SPV_{\text{Ref}}(\mathbf{x})},$$

where $SPV_i(x)$ is the scaled prediction variance for design *i* at a specific design point x and $SPV_{\text{Ref}}(\mathbf{x})$ is the SPV for the reference design at the design point x in the design region. After the variance ratio from random sample points over the design region are calculated, the values VR_i are sorted in ascending order. If VR_i is less than 1, it indicates that the reference design has bigger prediction variance than design *i*, so it has poorer prediction performance. If VR_i is greater than 1, it means that design *i* has poorer prediction performance than the reference design. From the VRFDS plot we can see the fraction of design space where the reference design predicts better or worse than design *i.* Figure 12 shows that the prediction capability of the reference design (new *G*-optimal design with *d*=0.0) is worse than *D*-optimal design and *G*-optimal design for the mean model over most of the design region, although the maximum prediction variance of the reference design was significantly reduced. The reference design is superior to the *I*-optimal design over at least 80% of the design region. Although the reference design has poor prediction variance over most of the design region compared to the *D*-optimal design and the *G*-optimal design for the mean model, the difference is less than

10% for the *D*-optimal design and 15% for the *G*-optimal design for the mean model. The new *G*-optimal design can be a good choice if the experimenter prefers the design which minimized the maximum prediction variance with stable prediction capability over the entire design region. The same graphical VRFDS plot can be used to compare the design for the predication variance for the slope model.

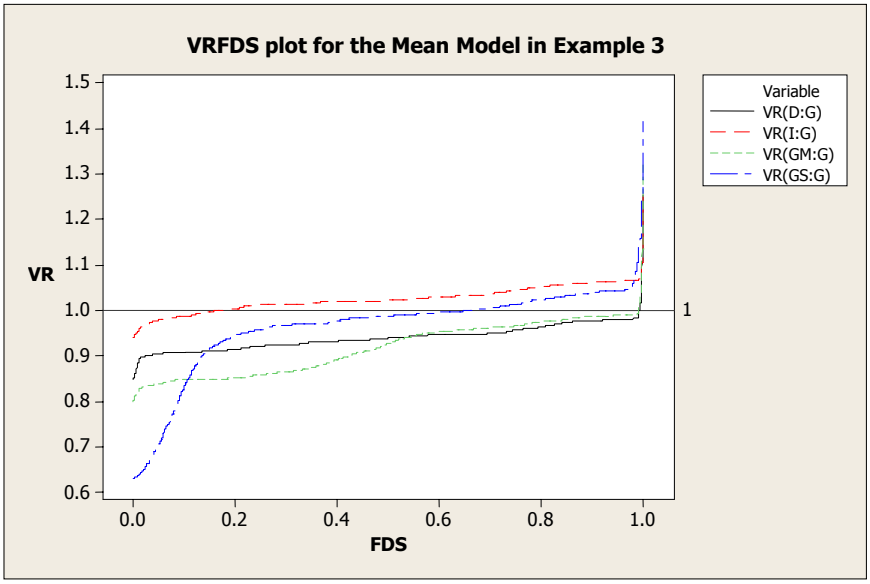

FIGURE 12. VRFDS Plot for the Mean Model in Example 3

As shown in Figure 13, the new design has poor prediction capability compared to all other designs over most of the design region, but it has dramatically superior prediction power to other designs over 5% of the design region, which will be the extreme boundary of the design region.

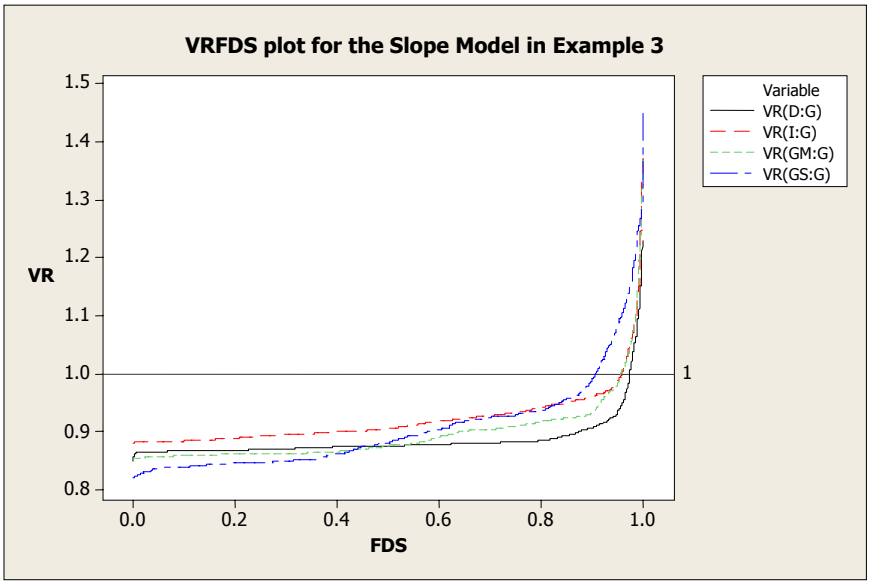

FIGURE 13. VRFDS Plot for the Slope Model in Example 3

Conclusion

In this chapter, we have discussed the appropriate analysis of mixture-process designs involving control and noise variables when complete randomization is not possible. In addition, the level of control by noise interactions can be ignored in the design comparison using the simplified SPV since the mean model is not directly affected by these interactions. The different levels of control by noise interactions do increase or decrease the amount of SPV, but we have shown that these interactions do not directly affect the resulting design matrix. Using TPV and the PV Ratio, FDS plots are constructed over various variance component ratio values for the split-plot structure. We have also generated *G*-optimal designs for the mixture-process problem considering restricted randomization with a split-plot structure. To create the optimal design, a genetic algorithm is used with a combined desirability function as the objective

function. This provides an optimal design with smaller maximum SPV values for both the mean and slope models when compared to other designs created with standard software.

CHAPTER 5

GRINDING WHEEL MANUFACTURING USING MIXTURE-PROCESS VARIABLE EXPERIMENTS WITHIN A SPLIT-PLOT STRUCTURE

A grinding wheel is a tool to grind, hone, and polish hard nonferrous materials such as ceramics, alumina, carbides, and glass. It is generally made from a mixture of coarse particles pressed and bonded to shape a solid circular disc. Various forms are available depending on the proposed usage for the wheel. There are many types of grinding wheels categorized by their main materials and the type of bond material. Diamond grinding wheel a logical choice to grind the hard objects because it is the hardest material known (around 8000 Knoop). In making the diamond grinding wheel, there are 4 mixture components and their following restrictions on these variables as shown in Table 13.

The process variables that influence on the grinding wheel are shown in Table 14. Among the process variables, the vibration is only controllable for purpose of an experiment. It is difficult to keep the same level of vibration on the wheel in the routine manufacturing process. Therefore, vibration is a noise variable.

In diamond grinding wheel manufacturing, the components of the wheel with the process variables are studied to improve the grinding wheel wear and life cycle. The wheel wear and life cycle can be improved by a reduction of the grinding force on the wheel by increasing the speed of the grinding wheel. We are

interested in studying the grinding force or grinding power to improve the wheel wear. The grinding wheel setup is shown in Figure 14.

TABLE 13. Mixture Components for Grinding Wheel Manufacturing

	Wheel Composition (4 components volume sum to 100%)			
	Copper *Conductor* (volume %)	**Resin** *Bond* (volume %)	**Diamond** *Concentration* (volume %)	**Beads** *Porosity* (volume %)
Max	34	35	31	12
Min	22	15	19	0

TABLE 14. Process Variables and Noise Variable (vibration) for Grinding Wheel Manufacturing.

	Wheel Process Parameters			
	Peripheral wheel speed V_s (m/s)	**Vibration** *Cycle* (Hz)	**Depth of cut** a_p (μm)	**Workpiece velocity** V_w (m/min)
Max	80	3	100	30
Min	30	1	10	10

The horizontal and vertical grinding forces, F_h and F_v, were measured using a force dynamometer. Aluminum oxide (Al_2O_3) with dimension of 23.6mm × 23.6mm × 10.00mm was used as the workpiece.

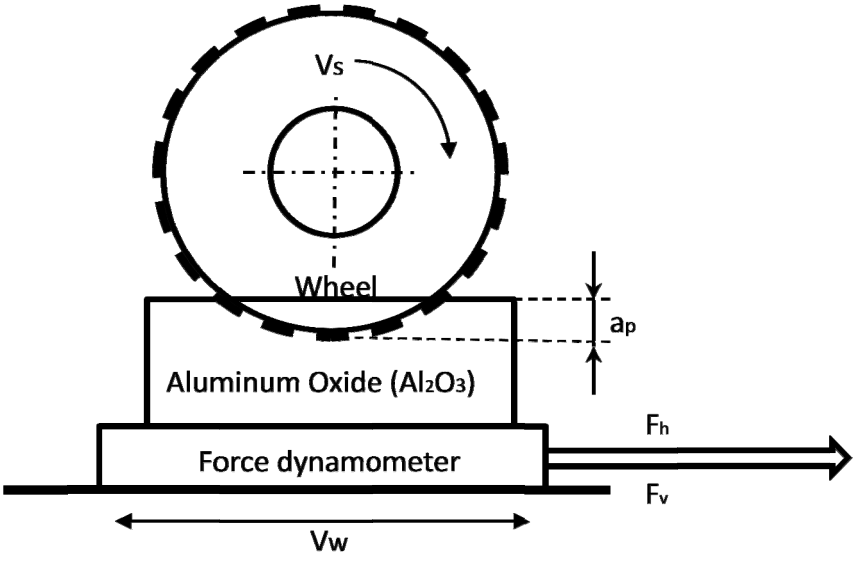

FIGURE 14. Grinding Wheel Setup Layout

In the evaluating of the grinding wheel manufacturing process, the mixture components interact with the process variables, resulting in a mixture-process variable experiment which requires a large number of runs to estimate the parameters. However, the order of experimental runs may not be completely randomized due to the difficulty of changing the level of the noise variable. Therefore, robust settings for the controllable process variable are required, which provide an acceptable mean response value and a minimum prediction error. Also, these constraints prohibit complete randomization of the experimental runs. If the experiments are not completely randomized and analyzed assuming a completely randomized design (CRD), it leads to an incorrect analysis. In the situation where complete randomization is unrealistic, all combinations of the easy-to-change factors are usually run at fixed levels of the hard-to-change factors, then a new

level of the hard-to-change factors is selected and the combinations of other factors are run at that level.

Notation and Model

Assume that the mixture components x_i and the controllable process variables w_p are the SP factors. The noise variables z_t are the WP factors. Furthermore, we suppose that there are p mixture components (x_i, i = 1, 2, … , q), c controllable variables (w_j, j = 1, 2, … , c), and q noise variables (z_t, t = 1, 2, … , n). Also suppose that there are m mixture terms, where m is a function of the number of the mixture components and the degree of the model. A response can be represented as a function of m mixture terms, q continuous noise variables, and c continuous controllable variables. The model can be written as

$$y = f(\mathbf{x}, \mathbf{w}, \mathbf{z}) = f_w(\mathbf{z})'\beta_{wp} + \delta + f_s(\mathbf{x}, \mathbf{w}, \mathbf{z})'\beta_{sp} + \varepsilon, \tag{19}$$

where β_{wp} is a vector of coefficients from the WP variables, β_{sp} is a vector of coefficients from the SP variables. $\delta \sim N(0, \sigma_\delta^2)$ comes from the WP randomization level and represents the random error term of the WP factors alone, and $\varepsilon \sim N(0, \sigma^2)$ comes from the SP randomization level and represents the random error term from the SP. The random components δ and ε are assumed to be independent. However, the WP terms $f_w(\mathbf{z}_t)'\beta_{wp}$, can be removed since the noise variables only affect the response through interacting with the mixture components. Then, this model has two different sources of error, WP and SP

errors and we assume that all noise variables are in the WP. Equation (19) without $f_w(\mathbf{z}_t)'\beta_{wp}$ can be expressed in matrix form as

$$y = f(\mathbf{x}, \mathbf{w}, \mathbf{z}) = \mathbf{x}'\boldsymbol{\beta} + \mathbf{x}'\mathbf{A}\mathbf{w} + \mathbf{x}'\boldsymbol{\Theta}\mathbf{z} + \mathbf{x}'\boldsymbol{\Lambda}\boldsymbol{\Xi}\mathbf{z} + \delta + \varepsilon \tag{20}$$

where

$$\mathbf{x}_{m\times 1} = \begin{bmatrix} x_1 \\ \vdots \\ x_m \end{bmatrix},\ \mathbf{w}_{c\times 1} = \begin{bmatrix} w_1 \\ \vdots \\ w_c \end{bmatrix},\ \mathbf{z}_{q\times 1} = \begin{bmatrix} z_1 \\ \vdots \\ z_n \end{bmatrix},\ ,\boldsymbol{\beta}_{m\times 1} = \begin{bmatrix} \beta_1 \\ \vdots \\ \beta_m \end{bmatrix}, \mathbf{A}_{m\times c} = \begin{bmatrix} \alpha_{11} & \cdots & \alpha_{1c} \\ \vdots & \ddots & \vdots \\ \alpha_{m1} & \cdots & \alpha_{mc} \end{bmatrix},$$

$$\boldsymbol{\Theta}_{m\times n} = \begin{bmatrix} \theta_{11} & \cdots & \theta_{1q} \\ \vdots & \ddots & \vdots \\ \theta_{m1} & \cdots & \theta_{mq} \end{bmatrix},\ \boldsymbol{\Lambda}_{m\times cn} = \begin{bmatrix} \lambda_{111}\cdots\lambda_{1c1} & \cdots & \lambda_{11n}\cdots\lambda_{1cn} \\ \vdots & \ddots & \vdots \\ \lambda_{m11}\cdots\lambda_{mc1} & \cdots & \lambda_{m1n}\cdots\lambda_{mcn} \end{bmatrix}, \text{ and}$$

$$\boldsymbol{\Xi}_{cn\times n} = \begin{bmatrix} w_1 & 0 & & 0 \\ \vdots & \vdots & \cdots & \vdots \\ w_c & 0 & & 0 \\ 0 & & & 0 \\ \vdots & & \ddots & \vdots \\ 0 & & & 0 \\ 0 & & 0 & w_1 \\ \vdots & \cdots & \vdots & \vdots \\ 0 & & 0 & w_c \end{bmatrix}.$$

x is the $m \times 1$ vector, **w** is the $c \times 1$ vector of controllable variables, and **z** is the $n \times 1$ vector of noise variables. **β** is the $m \times 1$ vectors coefficient matrix for mixture model terms, **A** is the $m \times c$ coefficient matrix for the mixture by controllable variable interactions and **Θ** is the $m \times n$ coefficient matrix for the mixture by noise variable interactions. **Λ** is the $m \times cn$ coefficient matrix for interactions involving mixture components, controllable variables, and noise

variables. Finally, $\boldsymbol{\Xi}$ is a $cn \times n$ block-diagonal matrix whose columns contain the w elements and blocks of 0s. The covariance matrix of the response is given by

$$\mathbf{V} = \sigma_{\delta}^2 \mathbf{J} + \sigma_{\varepsilon}^2 \mathbf{I} = \sigma_{\varepsilon}^2 [d\mathbf{J} + \mathbf{I}], \tag{21}$$

where $\mathbf{J} = \begin{bmatrix} \mathbf{1}_{n_1}\mathbf{1}'_{n_1} & 0 & \cdots & 0 \\ 0 & \mathbf{1}_{n_2}\mathbf{1}'_{n_2} & \cdots & 0 \\ \vdots & \vdots & \ddots & \vdots \\ 0 & 0 & \cdots & \mathbf{1}_{n_{wp}}\mathbf{1}'_{n_{wp}} \end{bmatrix}$, $d = \dfrac{\sigma_{\delta}^2}{\sigma_{\varepsilon}^2}$ (the variance component ratio),

and $\mathbf{1}_{n_i}$ is the vector of 1s with length n_i (i=1, … ,wp), which is the number of SP runs within each WP. Cho et al. (2010b) shows the inverse matrix form of covariance matrix with a balanced split-plot design shown as

$$\mathbf{V}^{-1} = \sigma_{\varepsilon}^{-2} \left(\mathbf{I} - \frac{d}{1+dk} \mathbf{J} \right)$$

where k is the number of sub-plots in each whole-plot and $\mathbf{JJ}=k\mathbf{J}$. They prove this result by directly multiplying Equation (21) by this inverse matrix to obtain the identity matrix. Letsinger et al. (1996) shows the method for the analysis of split-plot design; ordinary least squares (OLS), restricted maximum likelihood (REML), and iteratively reweighted least squares (IRLS). Goos et al. (2007) shows that the REML approach is preferred in general cases. We used the REML method to estimate the variance components, δ and ε. In general, the response model in the general linear model form is

$$\mathbf{y} = \mathbf{X}^* \boldsymbol{\beta}^* + \boldsymbol{\varepsilon}^*,$$

where the matrix $\mathbf{X}^*$ contains all columns representing the proposed model and the vector $\boldsymbol{\beta}^*$ contains the parameters. The model parameters $\boldsymbol{\beta}^*$ are estimated via generalized least squares as

$$\hat{\boldsymbol{\beta}}^* = \left(\mathbf{X}^{*'} \mathbf{V}^{-1} \mathbf{X}^* \right)^{-1} \mathbf{X}^{*'} \mathbf{V}^{-1} \mathbf{y} .$$

Robust Parameter Design

The expected value and variance of y can be found using the delta method, which utilize a Taylor series expansion of the model around the mean of z. Assume that the noise variables are uncorrelated, the model errors (δ and ε) are uncorrelated and independent, and the noise variables and the mixture components are uncorrelated with each other. $E_z(\mathbf{y})$ and $\mathrm{Var}_z(\mathbf{y})$ are obtained by taking conditional expectation of y(**x,w,z**) with respect to the noise variables ***z*** and the random errors, δ and ε.

$$E_z(\mathbf{y}) = f_w(0) + f_s(\mathbf{x}, \mathbf{w}, 0) = \mathbf{x}'\boldsymbol{\beta} + \mathbf{x}'\mathbf{A}\mathbf{w} \tag{22}$$

$$\mathrm{Var}_z(\mathbf{y}) = \left[\boldsymbol{\Theta}'\mathbf{x} + \boldsymbol{\Xi}'\boldsymbol{\Lambda}'\mathbf{x}\right]' \sum_{\mathbf{z}} \left[\boldsymbol{\Theta}'\mathbf{x} + \boldsymbol{\Xi}'\boldsymbol{\Lambda}'\mathbf{x}\right] + \sigma_\delta^2 + \sigma_\varepsilon^2 , \tag{23}$$

where $\sum_{\mathbf{z}} = diag(\sigma_{z_1}^2, \sigma_{z_2}^2, \cdots, \sigma_{z_n}^2)$ is an $n \times n$ diagonal matrix with the variance of the noise variables on the diagonal and 0 elsewhere and

$\left.\dfrac{\partial f_s(\mathbf{x}, \mathbf{w}, \mathbf{z})}{\partial \mathbf{z}}\right|_{\mathbf{z}=\mathbf{0}} = \boldsymbol{\Theta}'\mathbf{x} + \boldsymbol{\Xi}'\boldsymbol{\Lambda}'\mathbf{x}$. Since the noise variables are coded by the low and high level at $\pm\sigma_{noise}$, we can obtain $\sigma_{z_i}^2 = 1$. Borror et al. (2002) and Meyer et al. (2009) showed this process model and variance model in detail. Goldfarb et al.

(2003) developed this robust parameter design for the MPD. See Cho et al. (2011) more about the MPD considering a SPD.

Numerical optimization methods can be used to minimize the response variance while keeping the mean on a desired target as follows:

$$\text{Minimize } \text{Var}_z(\mathbf{y})$$

$$\text{Subject to } E_z(\mathbf{y}) = m,$$

where the choice of m can be $-\infty$ or $+\infty$ to minimize or maximize the mean, respectively. This provides the levels for the mixture and process variables that are robust to the noise variables in the operational setting.

Design Evaluation

In design evaluation, it is common to select the appropriate design depending on the practical situation. Two main categories for design selection are the measure-theoretic approach and variance oriented criteria. The *D*-optimality from standard alphabetic optimal criteria is well known and most often used to minimize the confidence region of the coefficients for the model parameters. However, in the response surface experiment, the response prediction is more interest and the optimality criteria associated with prediction variance are suggested. Therefore, the optimal design associated with variance oriented criteria is a rational selection for MPD experiments because the MPD is a special type of response surface experiments. The popular optimal design to minimize the prediction variance is *V* or *I* optimal design which minimizes the average prediction variance over the design space and it is available on many commercial

statistics package. *G*-optimal design has a goal of minimizing the maximum prediction variance over the entire design region and it is not yet adopted into the commercial software due to the computing difficulty and time expense. Goldfarb et al. (2005), Chung et al. (2007), and Rodriquez et al. (2009) use a genetic algorithm to generate *G*-optimal designs. We use the genetic algorithm to generate *G*-optimal design and compare this design with *D*-optimal and *I*-optimal design produced by JMP 7.0.

The prediction variance is an appropriate measure for evaluating a design with respect to the prediction capability. This prediction variance contains the variance in estimating the model parameters and the variance due to the noise variables when new observation, y, is estimated. Borror et al. (2002) and Goldfarb et al. (2004c) present the prediction variance for the mean and slope model for the design with noise variables. Cho et al. (2011) suggest total prediction variance (TPV) for combined comparison considering both the variance for the mean model and the variance for slope model given by

$$\begin{aligned}\mathrm{TPV} = {} & \mathbf{x}'\mathbf{C}^{11}\mathbf{x} + (\mathbf{x}\otimes\mathbf{w})'\,\mathbf{C}^{22}(\mathbf{x}\otimes\mathbf{w}) \\ & + \sum_{i=1}^{n}\rho_i\left[\mathbf{x}'\mathbf{C}_i^{33}\mathbf{x} + (\mathbf{x}\otimes\mathbf{w})'\mathbf{C}_i^{44}(\mathbf{x}\otimes\mathbf{w}) + 2\mathbf{x}'\mathbf{C}_i^{34}(\mathbf{x}\otimes\mathbf{w})\right],\end{aligned}$$

where ρ_i is 0 if a noise variable is not considered or 1 if a noise variable is considered in comparing variance in estimating parameters. Using the TPV, we can draw the FDS plots to compare designs.

In the following section, we first present a grinding wheel manufacturing example in which the standard analysis makes a poor estimation for the model

and prediction. Next, we will demonstrate the proper method to estimate the model parameters with the graphical evaluation for the design comparison when the noise variables are combined into the model with a restricted randomization.

Example 1: Grinding Wheel Experiment and Model Fitting

Using the notation described in Equations (19) and (20), the grinding wheel example is developed. In making grind wheel, there are four mixture components in the process, copper(x_1), resin(x_2), diamond(x_3), and beads(x_4). The ingredients have the following constraints;

$$0.22 \le x_1 \le 0.34$$
$$0.15 \le x_2 \le 0.35$$
$$0.19 \le x_3 \le 0.31$$
$$0.00 \le x_4 \le 0.12$$
$$x_1 + x_2 + x_3 + x_4 = 1 .$$

Three process variables and one noise variable are also considered; peripheral speed (w_1), depth of cut (w_2), workpiece velocity (w_3), and vibration (z_1), respectively. The peripheral speed (w_1) ranges from 30 (m/s) to 80 (m/s) and depth of cut (w_2) rages from 10 (μm) to 100 (μm) while workpiece velocity (w_3) ranges from 10 (m/min) to 30 (m/min). The vibration (z_1) treated as a noise variable and also hard-to-change rages from 1 (Hz) to 3 (Hz). The process variables and noise variable are coded with low level and high level (-1, 1) in this example. Since the vibration (z_1) is the only hard-to-change factor, it is assigned to the whole-plot. The mixture variables and controllable variables are assigned to the subplot. In this example, we use two methods to analyze this experiment,

CRD and SPD, and compare these two results. From the previous notation, we have q=4, c=3 and n=1. We considered the model with only linear mixture components crossed with interactions for linear process variables and noise variable and it led to the mixture terms, m=4. This linear assumption reduces the number of parameters to be estimated. JMP was used to generate a 64 run *D*-optimal design with 4 whole plots for the linear mixture model and the design and response data are shown in Table 15.

As shown in Table 15, this *D*-optimal design is not balanced. In other words, it has a different set of experimental setting in each whole plot. It violates the condition that guarantee the equivalence of the OLS and GLS coefficient developed by Vining et al. (2005) and we can expect the coefficients from CRD and SPD will be different. First, we use the CRD approach to analyze the data and find the significant effects at the 0.05 level and the R^2 and adjusted R^2 values are greater than 0.99 while the lack-of-fit p-value is 0.4, indicating an adequate model. The final model with the CRD is

$$\hat{y}(\mathbf{x},\mathbf{w},\mathbf{z}) = 297.32x_1 + 408.76x_2 + 200.76x_3 + 424.53x_4 \\ -96.35x_1z_1 + 496.68x_2z_1 - 299.96x_3z_1 + 69.31x_4z_1 \text{ ,}$$

where the mean square error, $\hat{\sigma}^2$, for the fitted model is 9.29. However, the SPD analysis provides a different result, indicating different significant effects from the CRD analysis. The SPD analysis shows that the interactions crossed with mixture and process variables are statistically significant although they are not significant in the CRD analysis.

TABLE 15. Grinding Wheel Design and Data

(Note: The variables have been coded)

Whole plots	Copper (%)	Resin (%)	Diamond (%)	Beads (%)	Vs (m/s)	ap (μm)	Vw (m/min)	Vibration (Hz)	Grinding force (N)
1	0.34	0.35	0.19	0.12	1	1	-1	-1	242.4218
1	0.22	0.35	0.31	0.12	-1	-1	1	-1	249.3193
1	0.34	0.35	0.19	0.12	1	-1	-1	-1	235.3835
1	0.22	0.35	0.31	0.12	1	-1	-1	-1	250.2714
1	0.34	0.35	0.31	0.00	-1	-1	1	-1	254.2503
1	0.34	0.35	0.19	0.12	-1	1	1	-1	244.0228
1	0.34	0.35	0.31	0.00	-1	-1	-1	-1	258.4568
1	0.34	0.35	0.31	0.00	1	1	1	-1	258.0021
1	0.34	0.23	0.31	0.12	-1	-1	-1	-1	311.7484
1	0.34	0.35	0.19	0.12	-1	-1	1	-1	237.6280
1	0.34	0.35	0.31	0.00	-1	1	1	-1	261.8456
1	0.22	0.35	0.31	0.12	-1	1	-1	-1	261.6021
1	0.34	0.23	0.31	0.12	-1	-1	-1	-1	314.8734
1	0.34	0.23	0.31	0.12	1	1	-1	-1	315.1220
1	0.34	0.35	0.31	0.00	1	-1	-1	-1	252.3785
1	0.34	0.23	0.31	0.12	1	-1	1	-1	297.6680
2	0.34	0.23	0.31	0.12	-1	-1	-1	1	302.9204
2	0.34	0.35	0.19	0.12	1	-1	1	1	421.9154
2	0.34	0.35	0.19	0.12	1	-1	-1	1	419.9290
2	0.22	0.35	0.31	0.12	-1	1	-1	1	399.4768
2	0.34	0.23	0.31	0.12	-1	1	-1	1	317.7841
2	0.34	0.23	0.31	0.12	1	1	1	1	311.5370
2	0.34	0.35	0.31	0.00	1	-1	-1	1	350.1878
2	0.22	0.35	0.31	0.12	1	-1	-1	1	385.0826
2	0.34	0.35	0.31	0.00	1	1	1	1	363.3043
2	0.34	0.23	0.31	0.12	-1	-1	1	1	302.9622
2	0.34	0.35	0.19	0.12	1	1	-1	1	432.6711
2	0.22	0.35	0.31	0.12	1	1	1	1	397.9650
2	0.34	0.35	0.19	0.12	-1	1	1	1	435.6764
2	0.34	0.35	0.31	0.00	-1	1	-1	1	367.3495
2	0.22	0.35	0.31	0.12	-1	-1	1	1	388.1549
2	0.34	0.35	0.19	0.12	-1	-1	1	1	422.9209

TABLE 15. Grinding Wheel Design and Data (Continued)

3	0.34	0.23	0.31	0.12	1	-1	1	-1	301.9962
3	0.34	0.35	0.31	0.00	1	-1	1	-1	249.7570
3	0.34	0.35	0.31	0.00	-1	1	-1	-1	269.8396
3	0.34	0.35	0.19	0.12	-1	-1	-1	-1	241.9454
3	0.34	0.23	0.31	0.12	-1	1	1	-1	316.2553
3	0.22	0.35	0.31	0.12	1	1	1	-1	253.1573
3	0.34	0.35	0.19	0.12	1	-1	1	-1	233.5462
3	0.22	0.35	0.31	0.12	1	1	1	-1	253.6144
3	0.22	0.35	0.31	0.12	-1	-1	1	-1	252.0492
3	0.34	0.35	0.31	0.00	1	1	-1	-1	261.8674
3	0.34	0.23	0.31	0.12	1	1	-1	-1	316.8510
3	0.34	0.35	0.19	0.12	-1	1	-1	-1	251.1588
3	0.34	0.23	0.31	0.12	-1	1	1	-1	317.2910
3	0.22	0.35	0.31	0.12	1	-1	-1	-1	249.0715
3	0.22	0.35	0.31	0.12	-1	1	-1	-1	260.3908
3	0.34	0.35	0.19	0.12	1	1	1	-1	240.6059
4	0.34	0.35	0.19	0.12	-1	-1	-1	1	417.3643
4	0.22	0.35	0.31	0.12	1	1	1	1	391.5886
4	0.34	0.23	0.31	0.12	1	-1	-1	1	295.6606
4	0.34	0.23	0.31	0.12	-1	1	1	1	307.4096
4	0.34	0.35	0.31	0.00	-1	-1	1	1	346.0890
4	0.34	0.35	0.31	0.00	1	-1	-1	1	346.3908
4	0.34	0.23	0.31	0.12	1	1	-1	1	307.6689
4	0.34	0.35	0.19	0.12	-1	1	-1	1	427.3109
4	0.34	0.35	0.31	0.00	1	1	1	1	357.1469
4	0.34	0.35	0.31	0.00	-1	1	-1	1	359.1781
4	0.34	0.23	0.31	0.12	1	-1	1	1	294.7852
4	0.22	0.35	0.31	0.12	-1	-1	1	1	380.7835
4	0.34	0.35	0.19	0.12	1	1	1	1	427.3924
4	0.22	0.35	0.31	0.12	1	-1	-1	1	381.0493
4	0.22	0.35	0.31	0.12	-1	1	-1	1	392.9133
4	0.34	0.35	0.31	0.00	-1	-1	1	1	346.2198

This result illustrates the role of whole-plot error and subplot error in SPD. Two different types of errors are used to calculate the test statistics for different factors.

For example, the t-ratio for whole-plot factor (z_1) is calculated using the whole-plot error. Test statistics for other subplot factors and interactions with the subplot factors are calculated using the subplot error. As shown by Lucas and Ju (1992), the subplot factors are precisely analyzed and determined to be significant using SPD in the model. Therefore, the suggested model is

$$\begin{aligned}\hat{y}(\mathbf{x},\mathbf{w},\mathbf{z}) = {} & 297.37x_1 + 407.98x_2 + 203.12x_3 + 419.80x_4 \\ & -5.36x_1w_1 + 7.95x_1w_2 + 6.24x_3w_2 - 4.49x_1w_3 + 6.49x_2w_3 - 6.73x_3w_3 \\ & -97.58x_1z_1 + 496.26x_2z_1 - 297.24x_3z_1 + 66.58x_4z_1 \end{aligned}$$

,

where the mean square error for WP, $\hat{\sigma}_\delta^2$, is 9.78 and the SP error, $\hat{\sigma}_\varepsilon^2$ is 1.38, resulting the variance component ratio $d = 7.08$. Usually, the WP error variance is larger than the SP error variance as shown by Box and Jones (1992). Vining et al. (2005) studied a split-plot experiment and estimated the variances using pure error indicating larger whole plot error variance than subplot error variance ($d >$ 1). The coefficient estimates of model parameters are not equivalent for CRD using OLS estimates and SPD using GLS estimates, because the *D*-optimal design in this example is not balanced. This example illustrated the problem with analyzing a SPD as if it was a CRD. The estimates of the coefficients are similar, but the significance test can lead to erroneous results.

Example 2: Robust Parameter Design and Simulation Study

Recall example 1. The mean and variance response functions for the mixture-process variables with a noise variable (z_1) are estimated using Equations (22) and (23), given by

$$\widehat{E(Y)} = 297.37x_1 + 407.98x_2 + 203.12x_3 + 419.80x_4 \\ -5.36x_1w_1 + 7.95x_1w_2 + 6.24x_3w_2 - 4.49x_1w_3 + 6.49x_2w_3 - 6.73x_3w_3$$

and

$$\widehat{\mathrm{Var}(Y)} = \hat{\sigma}_{z_1}^2(-97.58x_1 + 496.26x_2 - 297.24x_3 + 66.58x_4)^2 + \hat{\sigma}_{\delta}^2 + \hat{\sigma}_{\varepsilon}^2,$$

where $\hat{\sigma}_{z_1}^2$ =1 since the noise variables are coded by the low and high level at $\pm\sigma_{noise}$, and the variance components, $\hat{\sigma}_{\delta}^2$ =9.78 and $\hat{\sigma}_{\varepsilon}^2$ =1.38, are estimated via the REML method. In this robust parameter study, we need to minimize the value for the variance while concurrently minimizing the response for the mean. This dual optimization problem can be solved using the desirability function approach over the ranges of response for mean and variance model within the design. The suggested optimal levels are copper(x_1)=0.34, resin(x_2)=0.28, diamond(x_3)=0.31, and beads(x_4)=0.07 with the process variables, peripheral speed (w_1)=+1, depth of cut (w_2)=−1, and workpiece velocity (w_3)=+1 yielding 299.95(N) grinding force. If we don't consider the robust parameter design and mainly expect to minimize the response, then the suggested optimal levels are copper(x_1)=0.34, resin(x_2)=0.35, diamond(x_3)=0.19, and beads(x_4)=0.12 with the process variables, peripheral speed (w_1)=+1, depth of cut (w_2)=−1, and workpiece velocity (w_3)=+1 at vibration (z_1)=−1 yielding 232.41(N) grinding force. The response with RPD is greater than the response without considering RPD because the predicted response without RPD is estimated at vibration (z_1)=−1 and the response with RPD is at vibration (z_1)=0. Considering a new optimal lever at vibration (z_1)=−1, we can estimate the predicted response with RPD as 276.94(N) using E(z_1))=−1 for

Equation (22). It still has a large value for the response. However, it is optimized to have a less variation value when we treat the noise variable as a random effect. To show the effect of a noise variable, we simulate the model by treating the noise variable as a fixed effect (Normal) and a random effect (RPD). For the simulation study, we used the model resulted from Example 1 to generate the data which contain whole-plot error and subplot error with noise variables. The result in Table 16 (b) shows that the model considering noise variables is valid with the result from Example 2. The simulation study provides the importance of robust parameter design when the noise variables are considered in the model. Table 16 (a) shows the normal predicted response has the mean of 231.40(N) with Standard deviation 93.14 when we set the levels as suggested without RPD. It ranges from -161.2 to 566.6, indicting a large variability when the noise variables are not controlled in the process. Compared to the normal simulation result, Table 16 (b) provides an enhanced result with minimized variation ranging from 199.46 to 359.46 although it has 276.50(N) as the mean with standard deviation 21.50. With the levels suggested from RPD, we can estimate the predicted mean responses which are robust to the noise variables while it satisfies the targeted response values.

Table 16. Predicted Response Simulation with a Noise Variable Effect

Normal simulation

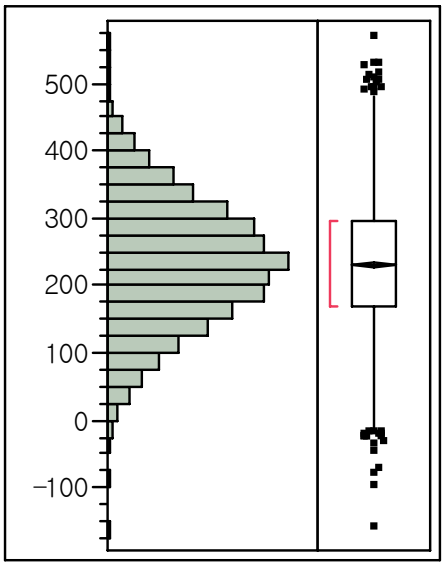

Quantiles

100.0%	maximum	566.6
99.5%		469.6
97.5%		411.9
90.0%		352.0
75.0%	quartile	294.4
50.0%	median	231.5
25.0%	quartile	169.4
10.0%		112.0
2.5%		45.0
0.5%		-5.3
0.0%	minimum	-161.2

Moments

Mean	231.40496
Std Dev	93.140348
Std Err Mean	1.3172034
upper 95% Mean	233.98725
lower 95% Mean	228.82266
N	5000

(a) Normal with Noise as Fixed Effect

RPD simulation

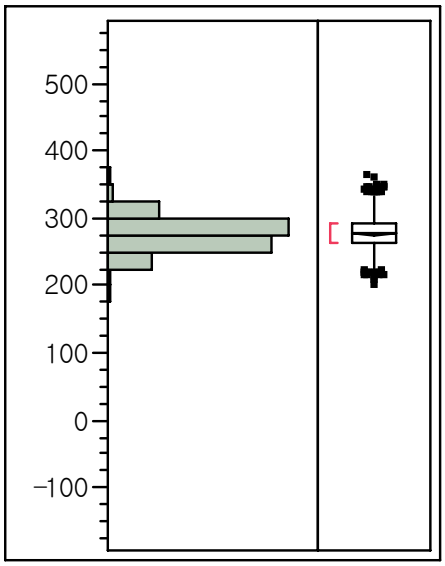

Quantiles

100.0%	maximum	359.46
99.5%		333.00
97.5%		318.93
90.0%		302.79
75.0%	quartile	290.70
50.0%	median	276.71
25.0%	quartile	262.29
10.0%		248.90
2.5%		232.76
0.5%		221.64
0.0%	minimum	199.46

Moments

Mean	276.50401
Std Dev	21.501201
Std Err Mean	0.3040729
upper 95% Mean	277.10012
lower 95% Mean	275.90789
N	5000

(b) RPD with Noise as Random Effect

Example 3: Design Comparison

Considering the grinding wheel experiments in Example 1, we now construct a *G*-optimal design using a genetic algorithm with a desirability function to select the dual optimal criteria for the mean and slope model. Using JMP7.0 script, we generate the *G*-optimal design for this grinding wheel experiment with the component variance ratio, d=7.0 as shown in Example 1 and notice that *D*-optimal design is also *G*-optimal with the 99.4% *G*-efficiency. In this grinding wheel experiment, the mixture region has very tight constraints on the mixture components using simple first-order linear model. This tight region of mixture components makes the prediction variances stable for the entire design space as shown in Figure 15.

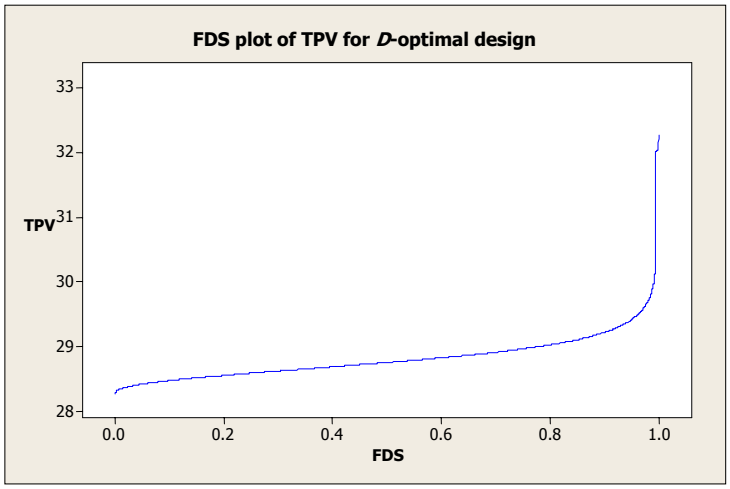

(a) FDS Plot of TPV for *D*-Optimal Design

FIGURE 15. FDS Plots of TPV in Example 3

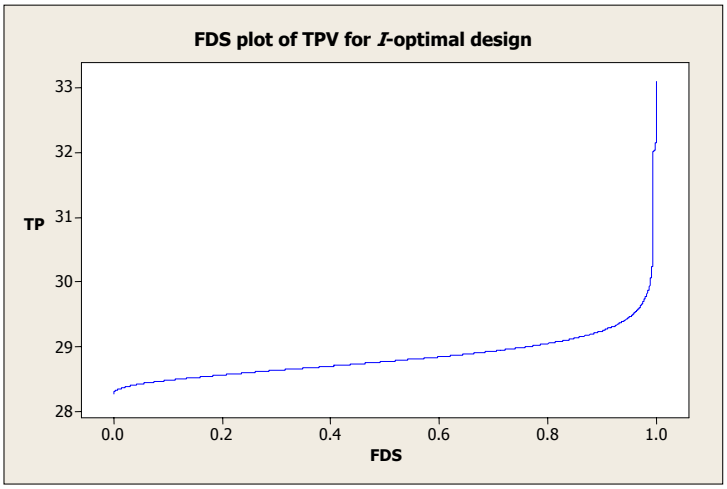

(b) FDS Plot of TPV for *I*-Optimal Design

FIGURE 15. FDS Plots of TPV in Example 3 (Continued)

The total prediction variances are between 28 and 29 over up to 90% design space for both the *D*- and *I*-optimal designs. The maximum total prediction variance is 32.2 and 33 for *D*- and *I*-optimal design, respectively. *D*-optimal design shows a slightly better performance in *G*-efficiency but the difference is not significant. Also no further improvement was achieved using GA algorithm for the G-optimal design.

Conclusion

In this chapter, we have showed the appropriate analysis of the grinding wheel manufacturing experiments when complete randomization is not possible. In addition, the robust parameter design analysis was demonstrated while the noise variables are considered in the experimental study. We have also generated *G*-optimal designs using a genetic algorithm for the grinding wheel experiments

considering restricted randomization with a split-plot structure and found the *D*-optimal design is also G-optimal when the mixture components are tightly constrained. These tight constraints produce the stable FDS plots when the mixture effects are mainly significant.

CHAPTER 6

CONCLUSION AND FUTURE RESEARCH

Conclusions

Chapter 3 considered the mixture-process variable design within a split-plot structure when the number of runs is dramatically increased when the mixture and process variables have a quadratic model with the interaction between mixture and process variables. We developed a graphical approach to evaluate designs using a variance component ratio when the complete randomization is restricted. It compares designs according to the prediction capability depending on the view of interest; minimizes the maximum of the prediction variance (*G*-optimality) or minimizes the average of the prediction variance (*I*-optimality).

In Chapter 4, new models were developed for experiments involving control and noise variables which are hard-to-change. This difficulty of level change for noise factor prohibits the complete randomization which is a basic assumption for the statistical analysis. We developed the simplified prediction variance model to compare and construct designs that are robust to the assumptions about the magnitude of interaction between control and noise variables and constructed designs that simultaneously optimize both the prediction variance for the mean model and the slope model. The traditional approach to evaluating or constructing optimal design for experiments with noise variables requires making assumptions about the magnitude of the contribution of the interactions involving noise variables. Furthermore, we obtained the designs

that are optimal for both the mean and slope model using desirability function with a genetic algorithm.

Chapter 5 used the model from Chapter 4 for a specific case study, the grinding wheel manufacturing experiment. This grinding wheel experiment has a tight mixture components region and extremely large parameters (4 mixture components, 3 process variables, 1 noise variable, and interactions between mixture, process, and noise variables). We demonstrated the robust parameter design analysis within split-plot structure and evaluated designs in prediction capability. Also, we showed that the tight mixture component constraints provide the stable FDS plots when the mixture effects are mainly significant.

Original Contributions

This research has developed new models to analyze the mixture-process experiments with control and noise variable within a split-plot structure by extending models developed by Goldfarb (2004c) that assume complete randomization. The new model considers a restricted randomization for the mixture-process variable experiments. Also, we develop a graphical tool using different variance component ratio for comparing various designs within a split-plot structure.

The second contribution is applying a simplified prediction variance to compare and construct designs for mixture-process variables design including control and noise variables under a split-plot scheme. This approach allows the robust comparisons not depending on the magnitude of interactions between

control and noise variables while the standard methods require the assumption about the magnitude of the contribution of the interactions involving noise variables.

The third original contribution is to apply a split-plot design with genetic algorithm to construct *G*-optimal mixture-process variable designs including noise variables when a complete randomization assumption is violated. It also provides a multiple optimization approach of desirability function for the mean and slope model. This approach to customize the objective function allows deciding the priority of design for the mean model and the slope model.

The statistical analysis is based on the randomization assumption. However, in practice, a complete randomization is not always guaranteed and the analysis based on a wrong assumption yields biased result. When a complete randomization assumption is inadequate, a split-plot structure can separate two types of error sources, whole-plot errors and subplot errors. It allows a precise estimation for the coefficients of the model parameters and provides an accurate prediction for the new observation, which is a main goal of response surface methodology. We provide an efficient and effective design generation strategy considering prediction properties within a split-plot structure.

Future Research

In this research, it was assumed that the noise variables were whole-plot factors (hard-to-change variables). The split-plot design could be extended for the situation where the mixture components are considered as hard-to-change factors.

Another extension would utilize the fractional factorial designs for the process variables. The model considered in this research were of full factorial forms for both mixture and process variables. It requires a large number of experimental runs as the number of variables increases. A fractional factorial approach can be studied with the alias patterns for the mixture-process variable designs.

For design generation, a genetic algorithm with a desirability function for *G*-optimality was used to select the dual optimal setting for the mean and slope model in this research. The desirability function can be extended to find the robust optimal design setting for the variance component ratio.

The current genetic algorithm requires a lot of computing time and it increases exponentially as more variables are added to the model. It would be valuable to develop an exchange algorithm to the update current design without evaluating all the points to minimize the maximum prediction variance. This type of algorithm could be much more computationally efficient.

REFERENCES

Borror; C. M.; Montgomery, D. C.; and Myers, R. H. (2002). "Evaluation of Statistical Designs for Experiments Involving Noise Variables." *Journal of Quality Technology* 34, pp. 54-70.

Box, G. E. P. and Hunter, J. S. (1957). "Multifactor Experimental Designs for Exploring Response Surfaces". *The Annals of Mathematical Statistics* 28, pp. 195-241.

Box, G. E. P. and Jones, S. (1992). "Split-Plot Designs for Robust Product Experimentation". *Journal of Applied Statistics* 19, pp. 3–26.

Cho, T-Y., Borror, C. M., and Montgomery, D. C. (2010) "Graphical Evaluation of Mixture-Process Variable Designs within a Split-Plot Structure", *Int. J. Quality Engineering and Technology* l, pp.2–26.

Cho, T-Y., Borror, C. M., and Montgomery, D. C. (2011) "Mixture-Process Variable Experiments Including Control and Noise Variables within a Split-Plot Structure", Approved to the *Int. J. Quality Engineering and Technology*

Chung, P. J.; Montgomery, D. C.; and Goldfarb, H. B. (2007). "Optimal Designs for Mixture-Process Experiments Involving Control and Noise Variables." *Journal of Quality Technology* 39, pp. 179-190.

Cornell, J. A. (2002). *Experiments with Mixtures: Designs, Models, and the Analysis of Mixture Data*, Third Edition. John Wiley & Sons, New York, NY.

Giovannitti-Jensen, A. and Myers, R. H. (1989). "Graphical Assessment of the Prediction Capability of Response Surface Designs". *Technometrics* 31, pp. 159-171.

Goldfarb, H. B.; Anderson-Cook, C. M.; Borror, C. M.; and Montgomery, D. C. (2004a). "Three-Dimensional Variance Dispersion Graphs for Mixture-Process Experiments." *Journal of Quality Technology* 36, pp.109-124.

Goldfarb, H. B.; Borror, C. M.; and Montgomery, D. C. (2003). "Mixture-Process Variable Experiments with Noise Variables." *Journal of Quality Technology* 35, pp.393-405.

Goldfarb, H. B.; Anderson-Cook, C. M.; Borror, C. M.; and Montgomery, D. C. (2004b). "Fraction of Design Space Plots for Assessing Mixture and Mixture-Process Designs." *Journal of Quality Technology* 36, pp.169-179.

Goldfarb, H. B.; Borror, C. M.; Montgomery, D. C.; and Anderson-Cook, C. M. (2004c). "Evaluating Mixture-Process Designs with Control and Noise Variables." *Journal of Quality Technology* 36, pp.245-262.

Goldfarb, H. B.; Borror, C. M.; Montgomery, D. C.; and Anderson-Cook, C. M. (2005). "Using Genetic Algorithms to Generate Mixture-Process Experimental Designs Involving Control and Noise Variables." *Journal of Quality Technology* 37, pp.60-74.

Goos, P. and Donev, A. N (2007). "Tailor-Made Split-Plot Designs for Mixture and Process Variables". *Journal of Quality Technology* 39, pp. 326-339.

Heredia-Langner, A., Montgomery, D. C., Carlyle, W. M.; and Borror, C. M. (2004). "Model-Robust Designs: A Genetic Algorithm Approach". *Journal of Quality Technology* 36, pp. 263-279.

Kowalski, S., Cornell, J.A., and Vining, G.G. (2002) "Split-plot designs and estimation methods for mixture experiments with process variables", *Technometrics*, Vol. 44, No. 1, pp.72–79.

Letsinger, J. D., Myers, R. H., and Lentner, M. (1996) "Response Surface Methods for Bi-Randomization Structures". *Journal of Quality Technology* 28, pp. 381-397.

Liang, L., Anderson-Cook, C. M., and Robinson, T. J. (2006). "Fraction of Design Space Plots for Split-plot Designs". *Quality and Reliability Engineering International* 22, pp. 275-289.

Lucas, J. M. and Ju, H. L. (1992). "Split Plotting and Randomization in Industrial Experiments". *ASQC Quality Congress Transactions.* American Society for Quality Control, Nashville, TN. pp. 374–382.

Mukerjee, R. and Huda, S. (1985). "Minimax Second and Third Order Designs to Estimate the Slope of a Response Surface". *Biometrika* 72, pp. 173-178.

Murty, V. N. and Studden, W. J. (1972). "Optimal Designs for Estimating the Slope of a Polynomial Regression". *Journal of the American Statistical Association* 67, pp. 869-873

Myers, R. H., Lahoda, S. J. (1975). "A Generalization of the Response Surface Mean Square Error Criterion with a Specific Application to the Slope". *Technometrics* 17, pp. 481-486.

Myers, R. H., Montgomery, D. C., and Anderson-Cook, C. M. (2009). Third Edition. *Response Surface Methodology*. John Wiley & Sons, New York, NY.

Piepel, G. and Anderson, C. M. (1992). "Variance Dispersion Graphs for Designs on Polyhedral Regions". *Proceedings of the Section on Physical and Engineering Sciences*, American Statistical Association, 111-117.

Rodriguez, M., Montgomery, D. C., and Borror, C. M. (2009). "Generating Experimental Designs Involving Control and Noise Variables Using Genetic Algorithms". *Quality and Reliability Engineering International* 25, pp. 1045-1065.

Rodriguez, M., Jones, B., Borror, C.M., and Montgomery, D.C. (2010). "Generating and Assessing Exact G-Optimal Designs". *Journal of Quality Technology* 42, pp. 3-20.

Rozum, M. A. and Myers, R. H. (1991). "Variance Dispersion Graphs for Cuboidal Regions". Paper Presented at Joint Statistical Meetings, American Statistical Association, Atlanta, GA.

SAS Institute Inc. (2007). JMP Version 7.0.1. Cary, NC.

State-Ease Inc. (2005). Design-Expert Version 7.0. Minneapolis, MN.

Steiner, S. H. and Hamada, M. (1997). "Making Mixtures Robust to Noise and Mixing Measurement Errors." *Journal of Quality Technology* 29, pp. 441-450.

Vining, G. G., Cornell, J. A., and Myers, R. H. (1993). "A Graphical Approach for Evaluating Mixture Designs". *Journal of the Royal Statistical Association Series C* 42, pp.127-138.

Vining, G. G., Kowalski, S. T., and Montgomery D. C. (2005). "Response Surface Designs Within a Split-Plot Structure". *Journal of Quality Technology* 37, pp. 115-129.

Zahran, A.; Anderson-Cook, C. M.; and Myers, R. H. (2003). "Fraction of Design Space to Assess Prediction Capability of Response Surface Designs." *Journal of Quality Technology* 35, pp.377-386.